

HOW SMALL BUGS TIE DOWN BIG ROCKS: MEASURING AND
MODELING THE FORCES ACTING BETWEEN NETS SPUN BY
CADDISFLY LARVAE (HYDROPSYCHIDAE) AND GRAVEL
PARTICLES AT THE ONSET OF MOTION

AS
36
2019
ERTH
.M35

A Thesis submitted to the faculty of
San Francisco State University
In partial fulfillment of
the requirements for
the Degree

Master of Science

In

Geoscience

by

Molly Katherine McLaughlin

San Francisco, California

Spring 2019

Copyright by
Molly Katherine Mclaughlin
2018

HOW SMALL BUGS TIE DOWN BIG ROCKS: MEASURING AND MODELING THE FORCES
ACTING BETWEEN NETS SPUN BY CADDISFLY LARVAE (HYDROPSYCHIDAE) AND GRAVEL
PARTICLES AT THE ONSET OF MOTION

Molly Katherine McLaughlin
San Francisco, California
2018

Many organisms, both plants and animals, influence geomorphic processes in rivers. Common aquatic insects, net-spinning caddisfly larvae (Tricoptera: Hydropsyche), build silk nets that can increase the threshold of sediment motion or critical shear stress τ^* by up to a factor of 2. Although previous research has shown nets increase τ^* , the magnitude of resisting force attributed to individual nets and the threshold of their effect as grain size increases is still unknown. To explore net strength, I conducted flume experiments at the Stroud Water Research Center in Avondale, Pennsylvania, where I made direct measurements of the forces acting between nets and individual sediment particles of various sizes using a strain gage during initial particle motion. I paired force readings with underwater video of each rock to make observations of the stretching, tearing and detachment of individual nets and measure the increase in force they contribute. Another way I detected the magnitude of force contributed by caddisfly nets is by comparing the measured peak forces to an abiotic model used to calculate the peak force without caddisflies to quantify the difference. Results from measurements made of the force contributed by individual nets and the difference of peak forces and an abiotic model for individual rock pulled from the bed suggest the threshold lies between 70 mm and 75 mm b-axis. Net measurements show larger rocks have nets that are contributing more force because larger rocks allow for larger nets to be built. The influence of caddisfly nets on bed stability has potentially significant implications for the timing and magnitude of bedload sediment transport in gravel-bedded rivers.

I certify that the Abstract is a correct representation of the content of this Thesis



Chair, Thesis Committee

April 17, 2019

Date

CERTIFICATION OF APPROVAL

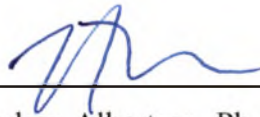
I certify that I have read **HOW SMALL BUGS TIE DOWN BIG ROCKS: MEASURING AND MODELING THE FORCES ACTING BETWEEN NETS SPUN BY CADDISFLY LARVAE (HYDROPSYCHIDAE) AND GRAVEL PARTICLES AT THE ONSET OF MOTION** by Molly Katherine Mclaughlin, and that in my opinion this work meets the criteria for approving a thesis submitted in partial fulfillment of the requirement for the degree Master of Science: Geoscience at San Francisco State University.



Leonard Sklar, Ph. D
Professor of Earth & Climate Sciences



Piero Mazzini, Ph. D
Professor of Earth & Climate Sciences



Lindsey Albertson, Ph. D
Professor of Ecology, Montana State
University

ACKNOWLEDGEMENTS

Special thanks to The National Science Foundation (DEB grant #1556684) for making this research possible, and The Stroud Water Research Center for allowing us to use their flumes and providing a place to stay at the center. Thanks to Ben Tumolo for helping to come up with the experimental design and setting up the experiment. Thanks to all the lab technicians who helped out with the experiment at Stroud. Thanks to Claire Masteller for helping me learn how to use Agisoft Photoscan and giving me pointers on how to best photograph the flumes. Thanks to Joey Verdian for his help in the field. Thanks to Celia LoBuono Gonzalez for her assistance with data processing and moral support. Thanks to my mom, Mariellen Mclaughlin and my dad Steve Mclaughlin for supporting me in my academic pursuits.

TABLE OF CONTENTS

List of Tables	vii
List of Figures	viii
List of Appendices.....	ix
1.0 Introduction.....	1
1.1 Hydropsychids and the Stabilizing Effect of Nets.....	3
2.0 Theoretical Framework.....	5
2.1 Net Characteristics and the Previous Model.....	6
3.0 Methods.....	9
3.1 Experimental Set-up.....	9
3.2 Synchronizing Force Readings and Video	12
3.3 Net Measurements.....	12
3.4 Pocket Geometry.....	12
3.5 Modeling Abiotic Pull Force	14
4.0 Results.....	16
4.1 Comparing Measured Peaks for Caddisfly and Control Pulls.....	16
4.2 Measured Versus Modeled Peak Force.....	17
4.3 Measurements of Forces Contributed by Individual Nets.....	21
4.4 Theoretical Abiotic Model	24
5.0 Discussion	27
6.0 Conclusion	32
7.0 References.....	35
8.0 Tables.....	38
9.0 Figures	41
10. Appendices.....	74

LIST OF TABLES

1. Metadata Table.....	38
2. Buoyant Weight T-Test.....	38
3. B-Axis T-Test	39
4. Normalized Difference (Measured-FP)/FP	39
5. Taustar crit (Measured-FP)	40
6. Taustar crit (Force Rise)	40

LIST OF FIGURES

1. Net-Spinning Caddisfly and Net with Scale	41
2. Force Balance Diagram for Albertson Model	42
3. Critical Shear Stress by Grain Size	43
4. Caddisfly Density with Depth into The Substrate.....	44
5. Comparisons of Measured τ^* To Model Predictions	45
6. The Stroud Water Research Center's Indoor River Laboratory	46
7. Schematic of Strain Gauge Apparatus	47
8. A Video-Force Gauge Match-Up	48
9. Example Photo of Pull Rock.....	49
10. Photo A Of 3-D Flume Model	50
11. Diagram of Structure from Motion Protocol for Flumes	51
12. Profile of a Pull Rock's Downstream Trajectory	52
13. Force Balance Diagram for Abiotic Model.....	53
14. T-Test of Raw Peak Forces for The Caddisfly and Control Pulls	54
15. Buoyant Weight And B-axis Diameter by Grain Size Treatment.....	55
16. Distribution of Normalized Difference Values for Control Pulls	56
17. T-test Of Normalized Difference Comparing Caddisfly and Control	57
18. T-test Of Normalized Difference For 30 mm Grain Size by Treatment.....	58
19. T-test Of Normalized Difference For 40 mm Grain Size by Treatment.....	59
20. T-test Of Normalized Difference For 50 mm Grain Size by Treatment.....	60
21. T-test Of Normalized Difference For 55 mm Grain Size by Treatment.....	61
22. T-test Of Normalized Difference For 60 mm Grain Size by Treatment.....	62
23. Normalized Difference for Caddisfly and Control Pulls by Grain Size	63
24. Net Measurement Diagram.....	64
25. Measured Crank Speeds from Demonstration Pull Video.....	65
26. Force Reading of A Caddisfly Rock Pull	66
27. Distribution Histogram of Force Rise During Stretching	67

28. Force Rise During Stretching by Buoyant Weight	68
29. Force Rise During Stretching by Distance Net Stretched.....	69
30. Force Rise During Stretching by Net Area	70
31. Force Rise During Stretching and Measured-Modeled Comparison	71
32. T-Test Of τ^* (Measured - Modeled) For All Rock Pulls.....	72
33. τ^* (Force Rise During Stretching) And Hypothetical Mean Comparison.....	73

LIST OF APPENDICES

1. Raw Peak Force Analysis	75
2. Table Measured Versus Modeled	94
3. Difference in Force	117
4. Net Measurements.....	118

1.0 INTRODUCTION

Rivers are essential contributors to the active processes shaping the landscape. Geomorphologists have learned a lot about the abiotic processes that govern river morphology, but very little is known about how plants and animals influence these processes. Organisms whose life cycles and habits alter their environment are known as ecosystem engineers (Jones et al., 1994). There has been an increase in research over the past few decades that illustrates how vegetation, aquatic mammals, and fish influence sediment transport regimes and channel morphology over time (Flecker, 1996; Moore et al., 2004; Braudrick et al., 2009; Curran and Cannatelli, 2014). Large scale laboratory flume experiments have successfully simulated and monitored the ways in which vegetation increases bank strength and supports meander formation (Braudrick et al., 2009). Fish also can influence transport processes in streams through diet. In the Orinoco river system of the Amazon, there is a species of fish that eats sand on the bed of streams and redistributes it in new locations throughout the river system (Flecker, 1996). The spawning practices of many types of fresh water fish influence sediment transport as they disturb sediment on river beds with their tails, to make structures known as redds, where they lay eggs (Moore et al., 2004). The dams built by beavers cause flooding and increase sediment retention upstream and are another excellent example of how organisms influence river morphology (Curran and Cannatelli, 2014). Even certain types of macroinvertebrates have been found to influence river morphodynamics (Rice et al., 2010; Johnson et al., 2009). While the influence of organisms on stream morphology has become more widely accepted, quantifying the effects that specific biological life habits have on geomorphic processes is still a major challenge.

Small aquatic insects can play a surprisingly big role in altering physical habitat features (Albertson and Allen, 2015; Romero, 2015). For example, multiple species of net-spinning caddisfly larvae, order Hydroptychidae, have been found to increase substrate stability in gravel-bedded rivers (Statzner et al., 1999; Cardinale

et al., 2004; Johnson et al., 2009; Albertson et al., 2014a; Albertson et al., 2014b) (Figure 1). The nets made by caddisfly larvae are built in the spaces between individual gravel particles on the beds of streams. The nets contribute a force in the opposite direction of flow, opposing hydraulic lift and drag forces, to create a frictional resistance, resulting in an increase in critical shear stress (Albertson et al., 2014a; Albertson et al., 2014b). The critical value of shear stress, is the force per unit area that water must overcome to transport sediment of a given size.

A theoretical model used to calculate critical shear stress in rivers has been modified to incorporate the effect of silk nets constructed by multiple species of caddisfly larvae hydroptychid (Albertson *et al.*, 2014a). Estimates made by the model are similar to measured values of critical shear stress in flume studies, where net-spinning caddisfly larvae have been found to increase the threshold of sediment motion by up to a factor of 2 (Albertson et al., 2014a). Although the Albertson et al. model has shown some success in predicting the increase in critical shear stress, the output values didn't always compare well to measured values of critical shear stress in an experiment with the same conditions. The model is built on assumptions that need to be tested, such as the binding force of the net always acts perpendicular the bed surface and nets are only built on the bottom half of particles.

To test these assumptions, we need to make direct measurements of the resisting forces of caddisfly nets. Therefore, I ask, how do caddisfly nets affect the physical mechanics of critical shear stress and the initiation of particle motion in gravel-bedded rivers? How do you directly measure the force of caddisfly nets? What is the magnitude of the force that nets can sustain? Over what range of grain sizes do nets significantly reduce mobility?

There is still a lot to learn about the detailed mechanics of the nets; the magnitude of the effect of caddisfly nets at larger scales in the natural world is still not fully understood. To help answer these questions, I participated in running flume experiments conducted the summer of 2016, at the Stroud Water Research Center in Avondale, Pennsylvania, where flumes were colonized with net-spinning

caddisfly larvae and given time to build nets. I then measured the forces needed to lift rocks of various sizes in flumes with and without caddisfly nets and derived a model from the abiotic forces acting on individual particles and compared its outputs with measurements to isolate the forces due to caddisfly nets.

1.1 Hydropsychids and the Stabilizing Effect of Nets

Net-spinning Caddisfly larvae (Trichoptera: Hydropsychidae) are about 1 cm in length and spend most of their life as larvae in benthic stream habitats (Figure 1). They are one of the most geographically wide-spread, diverse and abundant groups of insects seen throughout the world (Wiggins, 1977). The Wadable Stream Assessment (WSA) conducted in the United States by the Environmental Protection Agency (EPA) found that 56% of the 1,254 streams sampled contained hydropsychid caddisflies (USEPA, 2004). Net-spinning Caddisfly larvae densities range from hundreds to thousands per square meter with the highest densities exceeding 10,000 per square meter (Statzner, 1982; Miller, 1984; Albertson et al. 2018). Caddisfly larvae nets are remarkably strong. Measurements made of the tensile strength of silk thread range from 15.0 MPa for *Arctopsyche californica* with 16 load-bearing threads per net and 7.2 MPa for *Ceratopsyche oslari* with 37 load bearing threads per net (Albertson et al., 2014a).

Critical shear stress is the force per unit area that water must overcome to transport rocks of a given size. There have been multiple studies that have shown an increase in critical shear stress at the onset of sediment motion in the presence of nets spun by caddisflies. (Statzner et al., 1999; Cardinale et al., 2004; Johnson et al., 2009; Albertson et al., 2014a; Albertson et al., 2014b). Statzner and others published a paper in 1999 that tested the effect of caddisfly nets on 12 – 40 mm gravel that were colonized in streams at different insect densities and then installed in laboratory flumes (Statzner et al., 1999). This study measured shear stress with a hydrodynamic balance and saw an increase in critical shear stress by as much as a

factor of 2 when compared to a control (Statzner et al., 1999). Experiments conducted by Cardinale et al. (2004) used particle sizes of 2, 4 and 8 mm and measured an increase in flow velocity to transport sediment in the presence of caddisfly nets compared to a control (Cardinale et al., 2004). Another study by Johnson et al. (2009) looked at hydropsyches' effect on 4–6 and 6–8 mm gravel in naturally colonized baskets. Their results showed an increase in critical shear stress of 35% for 4–6 mm gravels compared to a control (Johnson et al., 2009). Despite the importance of these studies, they have several limitations, including small experimental flumes, elevated caddisfly density, and moving field-colonized baskets to the lab.

Albertson et al. (2014a) developed a theoretical model that accounts for the effect that caddisfly nets have on critical shear stress. The model accounts for mechanical properties of nets, geometry, and vertical distribution of insect silk threads from 2 different species. The model was parameterized by measuring the tensile strength, diameter, and number of silk threads in nets built by two common species of caddisfly, *Arctopsyche californica* and *Ceratopsyche oslari* (Albertson et al., 2014a). Predictions made by the model were compared to measurements made in lab experiments. The experiment was conducted in a 1.2 m long, 0.15 m wide and 0.20 m deep flume. They used four different caddisfly treatments: a control with no caddisflies, a monoculture of *Arctopsyche*, a monoculture of *Ceratopsyche*, and a 50:50 polyculture of *Arctopsyche* and *Ceratopsyche*. They used four different grain size treatments composed of uniform rounded grains with diameters of 10, 22, 45, and 65 mm. Caddisfly larvae were introduced to the sediment patches to colonize and build nets at a density of 2,000 m², they measured shear stress from vertical velocity profiles using an acoustic Doppler velocimeter. Results have shown that caddisfly larvae can increase critical shear stress by up to a factor of 2 in polyculture treatments. The effects of nets in monocultures and polycultures vary with grain size (Albertson et al., 2014a).

Although the model predictions were sometimes consistent with observed critical shear stress values, there were many assumptions built into the model that need to be tested to better understand the mechanics of the nets. None of the previous studies have ever been able to make direct measurements of the forces sustained by caddisfly nets. Quantifying the resisting forces of individual and multiple caddisfly nets on the transport of single gravel particles can tell us more about the mechanics. Making direct measurements of caddisfly nets would help to improve the accuracy of the model and its parameters.

2.0 THEORETICAL FRAMEWORK

A major process of fluvial geomorphology is the transport of bedload sediment. Sediment transport rates vary non-linearly with bed shear stress. Shear stress is a measure of force per unit area and is a friction induced by flowing water on the bed boundary from fluid drag due to turbulence (Dingman, 2009). The amount of shear stress necessary to initiate sediment motion dictates the magnitude and frequency of bedload transport, which has a major influence on channel morphology (Church, 2006; Parker et al., 2007). The critical value of a non-dimensionalized form of shear stress τ^* , can be calculated to determine the amount of stress water must overcome to transport a particle of a given grain size (Eq. 1).

$$(1) \quad \tau^* = \frac{\rho_f g h s}{(\rho_s - \rho_f) g D}$$

Calculating τ^* involves water density ρ_f , gravity g , water depth h , bed slope s , rock density ρ_s , and median grain size of bed material D . Values of τ^* are non-dimensional, and in gravel bedded rivers can vary between 0.02 and 0.06 for size classes with diameter greater than 2 mm (Buffington and Montgomery, 1997).

Theoretical models can be used to explain measured values of critical shear stress in natural rivers and laboratory flumes (Wiberg and Smith, 1987; Bridge and Bennett, 1992). Deriving critical shear stress consists of balancing the forces which act on a particle. The critical shear stress for a particle with a given size and density depends on the near-bed drag force, lift force to drag force ratio, and particle angle of repose (Wiberg and Smith, 1987). The forces acting on a sediment particle are gravity F'_g , buoyancy F_a , lift force F_L , and drag force F_D , due to the flow over the bed, and a resisting force F_R . The lift and drag forces are dependent on an undisturbed flow velocity surrounding the grain (Wiberg and Smith, 1987). A grain at the bed surface will begin to move when the resisting forces, against downstream motion, are equal to the drag forces directed downstream plus gravitational forces that are related to the bed slope (Wiberg and Smith, 1987).

Grain mobilizing shear stress for any grain size is a function of submerged (buoyant) grain weight, particle protrusion in the flow and inter-granular friction angle, as well as sediment sorting and size relative to neighbors (Buffington and Montgomery, 1999). Variability of critical shear stress in river beds with mixed grain sizes is caused by the distribution of grain sizes and packing geometry (Kirchner et al., 1990; Komar and Carling, 1991; Wilcock, 1993), as well as slope and bed roughness (Mueller et al., 2005; Lamb et al., 2008).

2.1 Net Characteristics and the Albertson Model

Incorporating biologic parameters like caddisfly nets into theoretical models and in-situ experiments, which previously considered only abiotic influences, helps us estimate critical shear stress at a higher resolution than current methods used in fluvial geomorphology. Caddisfly nets inhibit motion by increasing the resisting forces acting on a particle (Albertson et al., 2014a). These forces are dependent on multiple factors that include the depth below the bed surface where caddisfly larvae build their nets and the angle of the net with respect to the bed surface plane (Figure 2). There are many factors that cause variation in the amount of force

sustained by nets, including the tensile strength of the net, net diameter, the number of threads per net, the density of nets, and net location. The force of a net is broken into two components. One of the components is parallel to the bed surface, which directly opposes fluid drag. The other component acts normal to the bed, opposing hydraulic lift and contributes to the frictional resistance to movement (Albertson et al., 2014a). The total force of an individual net is treated as the sum of the force of each individual thread in the net. The threads within a net will break at a tensile loading that is equal to the product of cross-sectional area and thread strength (Albertson et al., 2014a). Additionally, interspecies differences in tensile strength, preferred net location, and the number of nets add complexity to the model.

In the Albertson τ^* model with caddisfly nets (Eq. 2), the force of the nets is assumed to act normal to the surface of the rock.

$$(2) \quad \tau^* = \frac{2}{(C_D)\alpha_D} \frac{1}{\langle f^2(z/z_0) \rangle} \frac{(\tan\phi \cos\beta - \sin\beta + F_{C_{resisting}}/F'g)}{[1 + (F_L/F_D)\tan\phi]}$$

The gravel stabilizing effect of caddisflies varies by grain size (Albertson et al., 2014) (Figure 3). Parameters of net characteristics that were used to calculate $F_{C_{resisting}}$ include silk thread tensile strength σ_T , silk thread diameter d , number of load-bearing threads per silk net N_T , length of silk net L_N , spacing between silk threads s , force sustained by a silk net F_{C_i} , mean silk net depth below bed surface η , insect body length L_C , as well as parameters to represent the limits to caddisfly density for small particle sizes. These parameters were measured by Albertson et al. (2014). The Albertson et al. model is based on Wiberg and Smith's 1987 calculation for critical shear stress, which includes channel slope β , friction angle ϕ , drag coefficient C_D , ratio of lift to drag force, shape factor α_D , Von Karman's constant $\langle f^2(z/z_0) \rangle$, and has been modified to incorporate the resisting forces generated by hydropsychid silk nets $F_{C_{resisting}}$ (Albertson et al., 2014a).

Polycultures have a greater effect on critical shear stress than just adding the influence of two separate species together, but the model accuracy in estimating this effect could be improved (Figure 4). The behavior of niche partitioning is at play, with one species building nets closer to bed surface, while the other builds nets deeper in sediments (Albertson *et al.*, 2014a). The variation of where caddisflies build their nets could increase net density, which would also contribute to a non-additive increase in τ^* . Some other influences could be caused by interspecies competition and net architecture that can vary between species. The effect of the poly-culture was maximized for a uniform grain size of 22 and 45 mm (Figure 5) (Albertson *et al.*, 2014a). The model may have also under predicted the effects of both species in poly-culture because it does not include grain clustering, where hydropsychid nets attach multiple grains together (Albertson *et al.*, 2014a).

In the model, FC_i is calculated as the sum of the force capacity of each individual thread carrying the load, which may not always be true. The force sustained by a silk net FC_i , may vary based on preliminary data from rock force readings collected in a previous flume study (Albertson *et al.*, 2014a), which show that the maximum force of the nets is seen when they are pulled their tightest right before breaking. The model could also be improved by considering cumulative effects related to multiple net forces. Sequential loading of nets as they begin stretching is a factor that was not considered in the model. The Albertson model also makes the assumption in the model is that the effect of the number of threads in the net is additive, which may not be the case. Another assumption made is that net forces are only felt at the bottom half portion of a rock, but field observations show that nets also occur on the upper portion of the side and tops of rocks as well.

3.0 METHODS

The methods I used to research the effect of caddisfly silk net mechanics included newly-developed techniques, which coupled laboratory experiments with computer imaging and video technology. I investigated the interaction of forces during transport at the individual grain level with and without the presence of caddisfly nets. I was able to measure the effect of silk nets at different grain sizes, mimicking transport of individual particles by pulling rocks from the bed one at a time and measuring force overtime with a strain gauge apparatus. Detailed information about each rock's weight and dimensions were also collected. Videos were taken of each pull in real time to give insight into the effects of net location and multiple nets as well as pocket geometry.

To make observations of net mechanics, I conducted experiments with a team of researchers at the Stroud Water Research Center in Avonndale, Pennsylvania (Figure 6). Flumes were colonized with net spinning caddisfly larvae and compared to control flumes without caddisflies. I then used the strain gauge apparatus, which was a pulley instrument developed for the experiment that was hooked up to a strain gauge and used to pull individual rocks from the bed, while measuring the force it takes to lift them. Each rock pull was documented with under water GoPro video footage. I also made a digital 3-D replica of each flume gravel bed set-up using photos to allow for measurements of pocket geometry to be made after the experiment was complete. I matched up the force reading data and videos to make individual measurements of the nets. I then derived an abiotic model to determine the force contributed by caddisfly nets by calculating the difference between the abiotic model and both control and caddisfly pulls.

3.1 Experimental Set-up

The experiment was conducted in 10 flumes contained in a greenhouse at the research center. The flume experimental design involved making direct measurements of the force required to mobilize gravel particles. The size of the

flumes and the maximum flow capacity of the flumes and pumps were not sufficient to mobilize gravel within the size range used in the experiment. Instead, rocks were transported using the strain gauge apparatus. The operator pulls rocks individually from the bed while measuring voltage that is later converted into newtons (N), providing a force reading over time of the pull (Figure 7). The strain gauge apparatus (referred to here as 'the rover') was constructed for these experiments and is designed to allow the operator to pull rocks from the bed in a way that mimics the lift and drag forces a rock would experience during water-driven transport. The strain gauge that was incorporated into the apparatus was programmed to read out a one to one ratio of volts to newtons. The strain meter was a model S100 5N by Strain Measurement Devices Inc. I epoxied hooks on the top of rocks so that a wire from the rover could be attached. The operator then turned a handle, which rotated gears, pulling up the wire that was attached to the rock and strain gauge sensor, transporting the rock from its pocket at a 45° angle.

The experiments ran through 5 replication time blocks. Each flume was randomly assigned one of five grain size bins between 30, 40, 50, 55, and 60 mm (Table 1). There were two flumes per grain size per time block with one flume containing caddisfly larvae and the other serving as a control without caddisflies. The flumes have a length of 10 m and a width of 0.4 m. Their slope without gravel was 3%. We covered the bottom of the flumes with a uniform layer of pebbles ranging from 3-7 mm diameter. Gravels of a randomly selected size class were then placed in a closely packed layer on top of the pebbles. Caddisflies and larger gravel were constrained to an experimental patch 1.5 m in length within each flume. The patch area was 0.6 m² and located 0.2 m downstream from the pump. Areas downstream of the patch was just the uniform bottom layer of pebbles. Within the patch, 12 rocks were randomly selected, and hooks were attached using marine epoxy so they could be slowly pulled from the bed. Once flumes were set up with gravel and hooks, the water supply to the flumes was turned on and the caddisfly colonization began.

Caddisfly larvae were collected from White Clay Creek, a stream that flows just outside the research center. About 500 - 550 hydropsychids were placed in each flume to reach target densities of around 1,000 per m², which is well within the range of natural stream densities (Statzner et al., 1999). The flumes were left to colonize for 72 hours, so hydropsychids could build their nets. To maintain a proper habitat for the caddisfly larvae during colonization, water was continuously pumped through the flumes. To provide an optimum temperature, we used water from White Clay Creek located outside the center, which also provided a food source. Water was continually pumped through the flumes except during data collection when conducting rock pulls.

Before force measurements were made, each rock that had a hook epoxied onto it was given a number and photographed. To facilitate force measurements, flume gravel patches were dammed using planks of wood and were filled up to about 3 inches from the top of the flume walls before turning off the pump. Eight of the 12 rocks that had hooks epoxied to them were then randomly selected with a random number generator to determine which of those rocks would be used for a force measurement. To operate the strain gauge apparatus once installed above the selected pull rock, the operator turned a rotating crank handle tightening the wire attached to the rock causing it to slowly lift out of its pocket. The pull was finished when the rock was completely out of its pocket and resting on the top of the rock downstream. A typical rock pull took about 15 to 25 seconds. Due to the nature of operating the instrument by hand the crank speed was somewhat irregular, the operator did their best to maintain a steady crank speed. Video footage of each rock pull was recorded with an underwater GoPro camera. After each rock was pulled and the force readings and video footage were collected, each rock was weighed and the lengths of the three principal axes were measured using a caliper with precision to a tenth of a millimeter.

3.2 Synchronizing Force Readings and Video

To interpret the measurements of the force contributed by caddisfly nets, Matlab software was used to synchronize video of each rock pull with the corresponding force readings using a script developed by Christian Braudrick (Braudrick, personal communication). These match-ups of video and force in real time help to identify individual net activation and break events in the force reading.

Matching up the videos with the force data using Matlab software allowed me to better measure the magnitude of the change in force following each net break (Figure 8). With these match-ups, I created time lapse images for each rock pull. These force video match-ups make it possible to identify and isolate net break events, calculate the magnitude of their effects, and quantify other influences in the force reading such as pocket geometry.

3.3 Net Measurements

The photos taken of each rock were used to make multiple measurements digitally, after the experiment. Each rock was photographed with an identification number and the scale was calculated for each photo using a mm to pixel ratio calculated from the intermediate-axis measurement of each rock in ImageJ software. With these photos, I also measured the number of nets on each rock (Figure 9). The net location was categorized based on five general regions as seen in videos looking downstream, in the direction the rock is being pulled. Those regions include front of rock, back of rock, left side, right side and bottom. I calculated net area (mm^2) with ImageJ from measurements of two perpendicular directions of intermediate lengths through the center of each net.

3.4 Pocket Geometry

Just like in natural stream beds, each rock that was pulled in the experiment sat in a pocket or depression formed by the rocks around it. When the rock was lifted out of its pocket, it had to slide past and over the rocks downstream in the

direction of the pull. To characterize and make measurements of pocket geometry, photos were taken of each of the 10 flume bed set-ups for every time block, prior to turning on the pumps. These photos were then used to make 3-D digital elevation models (DEMs), which are a set of elevation points (z) for each x and y location (Figure 10). These models were made with structure from motion photogrammetry methods, which analyze multiple photos to digitally replicate three dimensional objects (Morgan et al., 2016) (Figure 11). To get an accurate depiction of the flume, I took photos along the centerline of the flume in evenly-spaced 0.25 m increments, looking upstream and downstream at a 45° angle from vertical. I also took photos from the left and right edges of the flume looking upstream and downstream. This allowed me to have enough overlapping photographs to make an accurate depiction of the flumes comprising a dense point cloud of known bed elevations. To create the point clouds from my photos, I used the program Agisoft Photoscan.

I processed the DEM's in Matlab to determine the rock being pulled and then collected points of the downstream profile to get the friction angle. The changes in slope along each rock pull trajectory were used to calculate the changing friction angle over time. Making individual measurements of each rock pulls peak friction angle is important because each rock and its geometry are so different that averaging over all the friction angles would introduce error, making the models prediction less accurate. The peak friction angle was calculated using the y and z values from the DEM profile and a scale conversion that converts pixels to meters (Figure 12). I used the conversion on the z and y values and then calculated the cumulative distance over the change in slope that is later converted to degrees. The DEM scale conversion is about 0.0007 m per pixel for each flume. The slope is calculated over 11 pixels, which means slope values were averaged over approximately 8 mm. This value is appropriate because it is less than half of the minimum average grain size bin based on b-axis.

Picking the right number of points to average over in the downstream profile is important for determining an accurate friction angle. The profile of the

downstream rock is similar in shape to a half-circle, therefore the slope has to be within that $\pi/4$ radius. I chose a friction angle past 1 cm cumulative distance so that I would not be picking an angle that is too low for the rock to move over. I collected three profiles in parallel and 10 cells apart, downstream from each rock pull to determine the peak friction angle. These three profiles were gathered along a line perpendicular to the downstream profile. This helped to ensure we correctly estimated the peak friction angle. Often the profile taken directly from the center of the rock is not the highest angle the whole area of the rock traversed.

3.5 Modeling Abiotic Pull Force

To compare the force measurements made with the strain gauge with what might have occurred in the absence of caddisfly nets, I created a quasi-static equilibrium model for the force balance of a rock being pulled by a wire. The four main force terms are buoyant weight F'_g , frictional resistance μF_R , resisting force F_R , and the pull force F_p (Figure 13). Other variables include: the bed slope β , friction angle ϕ , and the angle of the net with respect to the bed θ . To create the equation, I began by adding up forces in the bed-normal (N) and bed-tangential (S) directions (Eqs. 2 and 3):

$$(2) \quad \sum F_N = F_p \sin \theta - F'_g \cos \beta - \mu F_R \cos(90^\circ - \phi) + F_R \sin(90^\circ - \phi),$$

$$(3) \quad \sum F_S = F_p \cos \theta + F'_g \sin \beta - \mu F_R \sin(90^\circ - \phi) - F_R \cos(90^\circ - \phi).$$

The next step was to solve for F_R in both the N and S directions (Eqs. 4 and 5).

$$(4) \text{ N:} \quad F_R = \frac{F_p \sin \theta - F'_g \cos \beta}{\mu \cos(90^\circ - \phi) - \sin(90^\circ - \phi)}$$

$$(5) \text{ S:} \quad F_R = \frac{F_p \cos \theta + F'_g \sin \beta}{\mu \sin(90^\circ - \phi) + \cos(90^\circ - \phi)}$$

The last step is to set the equations for F_R in the N and S directions equal to each

other and then solve for F_P (Eq. 6).

$$(6) \quad F_P = \frac{F'g \times (\cos\beta \times [\mu \sin(\frac{\pi}{2} - \phi) + \mu \cos(\frac{\pi}{2} - \phi)] + (\sin\beta \times [\mu \cos(\frac{\pi}{2} - \phi) - \mu \sin(\frac{\pi}{2} - \phi)])}{\sin\theta \times [\mu \sin(\frac{\pi}{2} - \phi) + \mu \cos(\frac{\pi}{2} - \phi)] - \cos\theta \times [\mu \cos(\frac{\pi}{2} - \phi) - \mu \sin(\frac{\pi}{2} - \phi)]}$$

The modeled F_P force was calculated for rock pulls in both the control and caddisfly treatments. The abiotic model helped me assess the precision of our measurements by calibrating it with rock pulls from the control flumes. The friction angle is determined from the flume's DEM. After calibrating the model with the control pulls by adjusting the friction coefficient to make it as accurate as possible. This model was used to quantify the total magnitude of force contributed by nets, separate from the abiotic forces of gravity and friction.

To analyze the force time series, I focused on the peak force. This is because the time of the force reading and the distance traveled within the abiotic model can't be synchronized due to irregular crank speed. The measured peak force was collected from each force time series and compared to the modeled peak force. Rock pull videos helped facilitate selection of an accurate measured peak force by making sure there are no influences of pocket geometry, for example; overlapping neighbor rocks or force spike anomalies. This is an issue because the abiotic force balance model doesn't account for these influences therefore, it is necessary to eliminate force peaks that don't have to do with what the model represents.

To collect representative peak force values, I used a protocol for determining the measured peak force from force readings for control and caddisfly treatments. First, I watched the rock pull video and looked at time series. While watching the video, I looked for any interference that might affect the measured peak force values. There were multiple types of interference to avoid. Pocket geometry was a major source of interference and would result when the rock being pulled also lifts neighboring rocks in front, back or on the sides. Another source of interference was from rocks downstream of the pull rock getting pushed out of the way. Another

common interference was when a pull rock was stuck then jolted out of its rest position in the pocket. These types of interference would cause spikes in the force readings. Some other more minor interferences came from the pull rock shuffling around in its pocket. Another issue I encountered came from the peak force happening too late in time series, after the rock has been lifted over the first downstream rock. Another interesting interference I encountered was pull rocks that were rotated to vertical before being lifted up over the downstream rock. When I did encounter interference, I would make a note of what kind and the time interference started and ended. When choosing a peak force, I made sure it was within the proper time and distance gap, before the pull rock was lifted up over the downstream rock. If interference occurred throughout the proper time gap, a measured peak force could not be used.

4.0 RESULTS

The statistical analysis for experimental results is broken into 3 sections: measured vs. modeled peak force, individual net measurements and applying the information to the Albertson et al. (2014a) model, which estimates the critical shear stress with the influence of caddisfly nets (Eq. 2).

4.1 Comparing Measured Peaks for Caddisfly and Control Pulls

After completing the experiment, I ran an analysis to see if I could detect whether caddisfly pulls had higher peak forces compared to the control pulls. To do this analysis, I used t-tests to compare the mean peak force between the caddisfly and control flumes for all time blocks. I also used t-tests to compare caddisfly and control pulls for each grain size bins. All tests showed no significant difference in mean peak force. I ran a one-tailed t-test assuming that nets don't make the rocks easier to move. The total number of rock pulls for the whole experiment was 423, 211 with the caddisfly treatment and 212 control rock pulls. The results show that caddisfly rock pulls on average are slightly higher for each grain size, except 60 mm,

where it is slightly lower, but these results are insignificant. Although there is a slight increase in the caddisfly pulls when compared to controls for all rocks, it is not a statistically significant difference ($p = 0.27$) (Figure 14).

The difference is statistically indistinguishable when comparing the raw peaks between the caddisfly and control pulls. There is a large amount of variability in both the caddisfly and control data sets. This is because each rock pull is unique. Every rock has an individual shape and weight and its own path as it traveled out of its pocket between rocks on the bed of the flume. The distributions of rock weights within each size class (Fig. 15) show that there is a lot of overlap which leads to an overlap in the peak forces as well. Since there are too many influences masking the effect of caddisfly nets in a simple peak force comparison, I needed to assess each rock pull individually.

4.2 Measured Versus Modeled Peak Force

To get a clearer understanding of how much force caddisfly nets actually contributed, I needed to identify force peaks from each force reading on a pull-by-pull basis. To do this I compared the measured peak forces to the predictions of the abiotic model for all pulls (Eq. 6). To calibrate the abiotic model (Eq. 6), I tested different friction coefficient (μ) values with peak forces from control pulls to see what best matched a hypothesized mean of zero (Figure 16). The reason I wanted the mean Measured – Modeled peak force to equal zero is because the modeled peak forces would then most closely match the measured peak forces from the experiment. I tried a range of values for μ in the abiotic model for all the control pulls. Although changing the friction coefficient showed little variation in the outcome of the modeled abiotic peak force values, I found that a coefficient of 0.6 aligns the control data best with a hypothesized mean of zero difference from measured.

To test the quality of the model calibration, I compared the modeled peak forces to the peak forces measured in the control pulls. I compared 101 modeled

peak forces (FP) with a mean of $(1.02 \pm 0.06 \text{ N})$ to all 99 measured peak forces from the rock pulls with a mean of $(1.04 \pm 0.06 \text{ N})$. This result shows that the theoretical model is sufficiently accurate in calculating the peak force. The difference between measured and modeled force is 0.02 N which means the model under-predicts by 2%. A t-test shows no significant difference between the modeled and measured mean peak forces ($p = 0.54$).

The quality of fit varies by grain size but not significantly. One way to see this is through normalizing the difference in peak forces as $(\text{measured} - \text{modeled})/\text{modeled}$. The main reason for normalizing by the modeled peak force is to compare results across grain sizes, because the magnitude of any difference would depend on grain size. A perfect fit would have a normalized difference of 0. Another way to compare the model with measurements is to simply take the difference between the measured and modeled with a perfect fit of 0. This is another more direct way to see whether the abiotic model is over or under predicting. After running the analysis, I found that the abiotic model either over or under predicts between 1 to 3 hundredths of a newton with standard errors between 4 to 5 hundredths of a newton. My analysis shows that the error in modeled vs. measured force does not systematically vary by grain size. The abiotic model is random in whether or not it over or under predicts.

After testing the accuracy of the abiotic model, I ran a t-test analysis by treatment (caddis or control) on all the pulls as a whole and by grain size treatment (30, 40, 50, 55, 60 mm) (Table 4). T-tests tell us whether or not there is a significant difference in mean force values between the caddis and control treatments. These are one tailed t-tests, assuming unequal variances. I assessed the difference between the caddisfly and control values, std. error of difference, degrees of freedom and P values. Knowing now that the abiotic model is an accurate fit for the control data, I can use it to see if it's possible to detect a significant increase in force for the caddisfly pulls.

I started by assessing all the rock pulls to see if I could detect a significant increase in normalized difference for caddisfly pulls compared to control pulls. I ran a t-test of normalized difference by treatment for all rocks (Figure 17). Since underwater video footage was not collected for time blocks 1 and 2, this analysis was only conducted for flumes from time blocks 3, 4 through time block 5, flume 5. There were a total of 93 Caddis pulls and 98 control pulls. This analysis showed a significant difference between control and caddisfly treatments. Caddisfly pulls had a mean normalized force difference of 0.25 ± 0.03 (mean \pm standard error), compared to 0.01 ± 0.02 for the control pulls. That is a difference of 0.24 ± 0.04 . This result is statistically significant ($p < 0.0001$). This result supports my hypothesis that nets increase the force it takes to transport a rock on average for the full grain size range used in the experiment. This shows that even when I combined all the grain sizes that there is still a significant increase in the peak force for caddisfly pulls when compared to controls. This also supports the need for a reference abiotic model because the difference between caddisfly and control pulls is much larger after assessing the peak force on a pull by pull basis.

Next, I used t-tests to compare the peak forces for separate grain size bins using the normalized difference calculation by treatment (Fig. 18) (Table 3). The first grain size bin I considered was 30 mm. I hypothesized that this grain size would have that largest difference between caddisfly and control pulls. It was actually the second largest difference. The caddisfly pulls had a normalized mean difference of 0.36 ± 0.09 , while the control pulls had a mean of 0.076 ± 0.04 . This results in a statistically significant difference ($p = 0.0041$) of 0.28 ± 0.10 . The difference is 0.04 larger than the difference for all the pulls.

The next size bin I ran a t-test for was the 40 mm bin with the normalized difference by treatment (Fig. 19). The caddisfly pulls have a mean of 0.25 ± 0.06 , and the control pulls have a mean of -0.11 ± 0.03 . This leaves a difference of 0.35 ± 0.07 . This result is statistically significant with a p value of <0.0001 . The

difference is 0.12 larger than the difference for all the pulls. This grain size treatment has the largest difference between caddisfly and control pulls.

The results for the t-test on the 50 mm grain size with the calculation normalized difference by treatment also showed a significant increase, but somewhat smaller than the previous size bins (Fig. 20). Although this is consistent with my hypothesis, I was surprised by how small of a difference there was for this grain size. The caddisfly pulls have a mean of 0.13 ± 0.04 and the control pulls have a mean of -0.04 ± 0.04 . This leaves a difference of 0.17 ± 0.06 . This result is statistically significant with a P value of 0.0024. The difference is 0.06 smaller than the difference for all the pulls. This grain size treatment has the smallest difference between caddis and control pulls.

The next t-test analysis is for normalized difference in force for the 55mm grain size bin by treatment (Fig. 21). Although this grain size bin contains larger sized particles, it has a significantly higher difference between caddisfly and control pulls when compared to the smaller 50 mm treatment. The caddisfly pulls have a mean of 0.26 ± 0.09 , and the control pulls have a mean of 0.07 ± 0.04 . This leaves a difference of 0.19 ± 0.09 . This result is statistically significant with a prob. > t of 0.0150. The difference is 0.04 smaller than the difference for all the pulls.

The last grain size bin is the 60mm treatment with the normalized difference by treatment (Fig. 22). This grain size treatment with has a higher difference than the smaller 55mm and 50mm treatments. The caddisfly pulls have a mean of 0.30 ± 0.08 and the control pulls have a mean of 0.09 ± 0.03 . This leaves a difference of 0.20 ± 0.08 . This result is statistically significant with a P value of 0.008. The difference is 0.03 smaller than the difference for all the pulls.

I also analyzed the individual rock pull data without the grainsize bins used in the experiments and used linear regression of the normalized difference by B-axis to compare treatments (Fig. 23). When both the control and caddisfly pulls are plotted together, the results show that the effect of the nets decreases with grain size. The mean for all the control pulls is 0.01 with a standard error of 0.02. The

caddisfly pulls mostly plot above this line and show a linear trend with the force of the nets increasing with a decrease in grain size. The equation for the best-fit line is: normalized difference = $0.22 - 0.0019 \cdot B$ axis (mm). The x intercept is 0.22; the line moves close to zero at 70 mm b-axis. The coefficient of determination for the regression (r^2) is 0.007 for the caddis treatment pulls. This is a significant fit with a p value of 0.02

4.3 Measurements of Forces Contributed by Individual Nets

Net force measurements are used to calculate force rise during stretching (N), which is the difference between the peak force, when the net breaks, and the force at the beginning of the rise in force leading to the peak. Another force measurement I made is the force decrease after net break (N), which is the difference between the peak force and the ending force after the net breaks (Fig. 24). The stretching time (s) is measured using the time between the beginning force and the peak force for each net break. Stretching distance (mm) is measured using the stretching time, average pull velocity (mm/s), and the net length in direction of pull (mm). The individual measurements of each net break are also incorporated into the previous Albertson et al, 2014 model for calculating critical shear stress with caddisfly nets to see how it compares to previous results.

Calculating the average crank speed can also allow for the comparison of the measured force with the modeled force over time. This also involves the use of the change in friction angle over distance traveled that is then converted into time with the average crank speed. Only five measured vs. modeled over time comparisons were made since crank speed is not constant (Fig. 25). A total of 94 video and force reading match-ups were made for all caddisfly flumes from time block 3, flume 1 to time block 5, flume 4.

The video and force reading match-ups reveal valuable information about the mechanics of caddisfly nets. The match-up videos allowed me to watch the rock pull while seeing the measured force simultaneously. While watching the match-up

videos, I documented information about how the net broke. Making these observations helps to understand how the three-dimensional dynamics of net stretching, tearing, and detachment affect the magnitude of the increase in critical shear stress cause by the nets. Some of these observations included net orientation, the number of nets, and type of net deformation including stretching, tearing or detachment. Most of the observations with net break events occurred when nets were stretched over time. A total of 136 out of 188 net observations were net break events where stretching occurred. There were 33 observations of individual thread break events where stretching occurred. A total of 17 events were net tears or detachments where very little stretching occurred.

Crank speed was calculated in two ways. The first way was with an equation for rotational velocity. The calculation uses the radius of the large gear, which the handle is attached to, to calculate the circumference. It took four rotations of the handle to complete one rotation of the gear, covering the total circumference. The equation is as follows:

$$(7) \quad V_c = \frac{C_G/N_R}{S_C}$$

In equation 7, V_c is the crank speed, C_G is gear circumference, N_R is the number of handle rotations per circumference, S_C is the time it takes for the gear to move the full circumference.

Another way I calculated crank speed was with a video of a demonstration pull where I used ImageJ to determine the change in distance pulled over time. I made the video into single frames, 60 per second and used a known length of a piece of the hardware on the rover to add scale to the photo. I made measurements to the length of a vertical piece of PVC making up the frame of the rover. As the handle turns the crank, rotating the gear, a horizontal piece of PVC that the wire and sensor is attached to, is pulled up, changing the visible length of the vertical piece of PVC making up the frame. I measured the change in this visible PVC length in different frames throughout the duration of the demonstration pull video. This change in distance measured from the video frames can be used to calculate the change in

distance overtime to get an average pull rate. The graph in Figure 25 shows that the crank speed is not constant. The average crank speed measured in the video is consistent with measured crank speed.

The individual net measurements were assessed with a regression analysis. For this analysis, I was primarily looking at the force rise during stretching, and what parameters best explain the variability in the data. These include b-axis, buoyant weight, and net area. This analysis helped me to determine how much the rise in force from nets depends on each of these factors (Figure 26).

There is a large range in values for the distribution of force rise during stretching (Table 4). To determine the cause of such a large spread in values, I assessed the relationship of force rise during stretching with some of the independent variables. I collected a total of 186 measurements of force rise during stretching (Figure 27). The mean of force rise during stretching is 0.16 N with a standard error of 0.012 N. The median is 0.11 N. Values span over 2 orders of magnitude, from 0.01 to 1 N. Although there is a large range in values for the force rise during stretching, the expected value of a single net as predicted from the Albertson et al. (2014a) model is 0.12 N for *Arctopsyche* and 0.07 for *Ceratopsyche*, both values are close to the median I measured.

First, I assessed the relationship between force rise during stretching and buoyant weight (Figure 28). For this comparison, I ran an orthogonal regression. The y-axis and x-axis in the graph are natural log transformed. The linear trend of this graph shows an increase in force rise during stretching with an increase in buoyant weight. This trend is very significant with an orthogonal ratio of 1.71. This relationship suggests that larger rocks have nets that contribute more force than nets attached to smaller rocks.

There is also a significant relationship between force rise during stretching and distance nets stretched (Figure 29). The y-axis in the graph is log transformed. This correlation shows that the force of the net is higher with an increase in the distance

a net is stretched. This effect explains only about 8% of variation in force. But the trend is highly significant with a Prob. > F of <0.0001.

To determine whether bigger nets accommodate more force, I compared force rise during stretching with net area (Figure 30). I used another orthogonal regression for this analysis and both the y and x-axes in the graph are natural log transformed. This linear trend shows that the force rise during stretching increases with net area. This correlation shows that the force of the net is higher when the size of the net is larger. This positive correlation has an orthogonal ratio of 1.01.

Next, I wanted to assess how net area varies with rock size because net area influences the force that can be sustained by a net. Results from my net area measurements show that net area increases with B-axis. This correlation of net area and B-axis has an R squared of 0.03 and a Prob. > F of <0.005. This suggests that caddisflies build bigger nets on larger rocks, on average. The trend line has an equation of net area (mm^2) = $11.6 + 0.453 \cdot \text{B axis (mm)}$. The slope is 0.45. This is an important result because the previous model assumed nets are the same size no matter what size that rock is.

After I analyzed both measured versus modeled peak force and measurements of forces contributed by individual nets, I analyzed the relationship between them (Figure 31). The one to one line in red represents a perfect match in values between the force rise during stretching and measured - modeled peak force. The green line is the trend of the data. Since the data mostly plots below the one to one line, the measured - modeled is often larger than the force rise during stretching of individual nets for that rock pull. The slope of the line is 0.45 with an R^2 of 0.22 and a P value less than 0.0001.

4.4 Theoretical Abiotic Model

Having collected a significant data set of net measurements, I wanted to put them into the context of the previously published Albertson et al. (2014a) model by using it to calculate τ^* and comparing my measurements with the model's

previously published predictions. To do this, I first assessed what is already known about the species used in the experiment. *Hydropsyche betteni* is the dominant species found in White Clay Creek and used for the experiment. Previous research at the Stroud Water Research Center (Albertson and Daniels, 2016) included measurements of *H. bettini*'s thread spacing and diameter, but there are other net and silk characteristics that are still needed to use the model for this species. The other net characteristics needed are mean net depth and net strength.

The average body length of *H. bettini* is about 12 mm (Albertson and Daniels, 2016). The average size of *H. bettini* is in between the larger *Arctopsyche californica* and smaller *Ceratopsyche oslari*, making it a good candidate for comparisons to previous measurements made with the Albertson et al. (2014a) model. The thread count for *H. betteni* of 18.5 is closer in size to the larger *Arctopsyche*, 16.3 but the thread diameter for *H. betteni* of 10 microns is less than the smaller *Ceratopsyche* of 25 microns. Based on these net measurements the species used in the experiment should have a stabilizing effect that lies somewhere between the two species used in the experiments that defined the Albertson et al. (2014a) model.

Because there were no measurements made of $F_{c_resisting}$ for *H. bettini*, I used the model to calculate τ^* with my own data from the force rise during stretching measurements and the measured-modeled force values. Specifically, I used the difference of (measured - modeled) and (force rise during stretching) in place of $F_{c_resisting}$ in the model for caddisfly and control flumes.

By using my measurements of force rise during stretching to calculate τ^* , I can put my results into the context of the model and determine if the increase in τ^* calculated with my net measurements and measured - modeled values are comparable to values previously measured in the Albertson et al. (2014a) experiment. The Albertson et al. (2014a) experiment had a caddisfly density of 1,500 m⁻² while the flumes in my experiment had densities of 1,000 m⁻², making the two studies reasonable to compare.

For this analysis, I used t-tests to compare τ^* with measured – modeled in place of $F_{c_resisting}$ by treatment (caddisfly or control) with all the rock pulls together and by grain size bin (30, 40, 50, 55, 60). I hypothesize that using my measurements of the force sustained by nets in the Albertson et al. (2014a) model in place of $F_{c_resisting}$ would lead to higher τ^* values than previously reported. For the different grainsize bins, I hypothesized that Caddisfly pulls would have a statistically significant increase in τ^* compared to control pulls. I also hypothesized that the effect of nets would decrease systematically with an increase in grainsize, lowering the τ^* values.

The first comparison I ran was τ^* (measured – modeled) between caddisfly and control for all rocks. For this comparison, I wanted to see if there is a significant increase in τ^* even when combining all grain sizes from the caddisfly treatments (Figure 32) (Table 5). This was conducted for all the same rock pulls as the measured versus modeled analysis. Caddisfly pulls had a mean of 0.042 ± 0.0006 , and control pulls were, 0.04 ± 0.0004 . That is a difference of -0.004 ± 0.0007 . This result is statistically significant with a prob. > t of < 0.0001*. This is a positive result that supports my hypothesis that nets do increase the critical shields stress it takes to transport a rock on average for all the grain size range used in the experiment.

The next comparison I ran was τ^* (measured – modeled) between caddisfly and control for the separate size bins (Figure 33) (Table 6). Caddisfly pulls had a statistically significant increase in force for all grain size bins separately as seen in the highly significant values. The variation in the increase in τ^* does not vary systematically although that is a sporadic trend in a smaller increase in τ^* for the larger grain sizes. The 40 mm grain size bin had the largest increase in τ^* 0.007 ± 0.001 N. The 30 mm size bin had an increase in τ^* of 0.005 ± 0.002 N. The 50, 55, and 60 mm grain size bins had increases in τ^* that were more closely aligned with the average increase in τ^* for all the rocks collectively.

In the 2014 Albertson et al. paper, the model calculated a τ^* value of 0.064 for 22 mm grains and measured 0.072 for polycultures of the same grainsize

(Albertson et al. 2014a). The control τ^* measured 0.04 N. That is an increase in force of 0.032 N in the presence of caddisfly nets based on the model. This increase is much higher than the highest detected increase seen in the 40 mm size bin. The Albertson et al. model calculated a τ^* value of 0.042 for 45 mm grains and measured 0.06 for polycultures in the same grain size in the 2014 experiment. The control had a measured τ^* of 0.037 N. That is an increase of 0.005 N, which is much closer in size to the increase in τ^* I calculated in this experiment. In the 2014 Albertson et al., paper, the theoretical model calculated a τ^* value of 0.045 for 65 mm grains and measured 0.055 for polycultures in the same grain size. The control measured 0.041 N, which means the model calculated an increase in τ^* of 0.004 N.

Next, I calculated τ^* incorporating the force rise during stretching values in the place of $F_{c_resisting}$ in the Albertson et al. model. I used t-tests to compare the results to the τ^* calculated without the caddisfly parameter, $F_{c_resisting}$. The results from the t-test analysis show a significant increase in τ^* for all rocks and the different size bins separately. The largest difference was seen in the 30 mm size bin with 26% increase in τ^* . The 55 mm size bin had second largest increase in τ^* of 18%. The t-test comparing all rocks had increase in τ^* of 8%. The smallest increase seen was for the 50 mm size bin with a 5% increase.

Because the net characteristics for *H. bettini* fall in between the two species used to calibrate the model, I used insect size as a proxy to estimate $F_{c_resisting}$ to incorporate it into the Albertson model. To do this, I plotted the known average insect body lengths with the known net strength of the other two species to extrapolate an estimation of net strength for *H. bettini*. With this extrapolation I was able to extrapolate an $F_{c_resisting}$ estimate of 0.089.

5.0 DISCUSSION

Previous work has begun to understand the interactions of net spinning caddisflies with the geomorphic processes that shape their environment. The Albertson et al. (2014a) model that was created to predict the critical shear stress in

the presence caddisflies was built on many assumptions. Therefore, understanding the underlying mechanisms of caddisfly nets will help to test these assumptions and improve the accuracy of the model. In this study, I have coupled measurements of the force necessary to lift individual gravel particles with high-resolution video and images to quantify the three-dimensional dynamics of net stretching, tearing, and detachment that dictate the magnitude of the increase in critical shear stress.

Consistent with previous findings, my results confirm that hydropsyhid caddisfly nets significantly increase the force required to move particles (Statzner et al., 1999; Cardinale et al., 2004; Johnson et al., 2009; Albertson et al., 2014a; Albertson et al., 2014b). While many previous studies were able to detect the effects of nets, this research measured the absolute magnitude of the forces, giving better insight into the mechanics of the transport of individual rocks in the presence of caddisfly nets. Albertson et al. (2014a) reported an increase in t^* by 2-fold for a grain size of 22 mm in polyculture treatments. Here I was able to reach similar findings from individual rock pulls and individual net measurements for larger gravel sizes. Measurements made of the force of individual nets that were stretched to the point of breaking by Albertson et al., (2014a, b), reported the maximum force sustained by a silk net, F_{ci} for the 2 species are as follows, *Ceratopsyche* nets sustained a force of 0.066 ± 0.004 N, and *Arctopsyche* nets sustained a force of 0.12 ± 0.013 N. When compared to my measured versus modeled analysis, both species are below the mean difference between the measured and modeled force with a value of 0.266 N. The mean force rise during stretching also was a higher value of 0.16 ± 0.013 N.

I also found a significant effect of caddisfly nets for all gravel size treatments. I used gravel sizes in this experiment that were larger than previously tested, therefore it was unknown whether caddisfly nets would have a significant effect on τ^* for these larger sizes. Particle sizes used in the Albertson et al. (2014a) experiment were uniform in size for each treatment and ranged from 10 to 65mm. The grain size treatments in this experiment were non-uniform and had a large

range in grain sizes per bin with the smallest rock pulled being 27 mm and the largest was 91 mm b-axis. Although I pulled rocks up to 90 mm, the size where the effect of nets is no longer detectable is 70 to 75 mm. Albertson et al. in 2014 detected a significant difference in τ^* between the control and the polyculture for a grain size of 65 mm b-axis, but the two monocultures did not have a significant difference compared to the control (Albertson et al. 2014a).

Another significant result was the decreasing effect of nets with increasing particle size. While this is a similar result compared to the theoretical model predictions, this is the first substantial set of experimental data to confirm a significant effect of nets for such large grain sizes. The Albertson model predicted the threshold of the effect to lie between 45 mm and 65 mm (Albertson et al., 2014a). Finding the limit based on individual rock pull data by grain size gives a better sense of what the grain size limit of the net's effect is. These data suggest the threshold lies somewhere between 70 mm and 75 mm b-axis.

My analysis based on the individual net measurements shows that larger rocks have larger nets that are contributing a greater force. My results help to confirm what previous studies had only just begun to understand. Albertson et al. in 2014 made measurements of net characteristics which showed that the larger *Arctopsyche* species built larger nets and needed a larger area to build these nets, competing for the more optimal space. There is a positive correlation, signifying that net size increases with rock size. Perhaps this pattern appears because there is more room for caddisflies to build larger nets between larger rocks. This size relationship would cause an increase in the force contributed by nets. Or it could be that multiple nets are activated at the same time on smaller rocks, so that when one breaks, the force is distributed to the next net, reducing how much the force drops, while larger rocks have nets breaking one at a time.

Analyzing the relationship between measured versus modeled peak force and measurements of forces contributed by individual nets revealed that the measured - modeled is often larger than the force rise during stretching of

individual nets. This finding could be due to multiple nets contributing to the resisting force simultaneously, which was not captured in the individual net measurements of force rise during stretching.

The results of this study have implications for why ecological engineering by caddisflies should be considered when assessing river morphodynamics. Results suggest that at high densities, net-spinning caddisflies can have a significant effect on stream bed mobility. Previous studies have shown that caddisfly density is commonly very high in rivers and can exceed $10,000 \text{ m}^{-2}$ (Miller, 1984; Cardinale et al., 2004). This is about 10 times higher than flume densities for this experiment and previous flume experiments, which shows that they are capable of having an effect even larger in nature than measured in lab experiments. The presence of caddisflies could have a significant impact of the distribution of gravel sizes on the bed, causing it to be larger in spread, by holding down gravel particles beyond what abiotic forces alone can sustain.

There is potential for net-spinning caddisflies to have an ecological impact through their role as ecosystem engineers as well. The stabilization of sediment by nets could even have an influence on coarse gravel beds such as salmonid spawning beds. Salmon and other anadromous fish search out a specific grain size distribution to spawn in around 10 mm to 100 mm b-axis (Riebe et al., 2014). This is within the same size range that caddisfly nets have been found to have a significant stabilizing influence. The presence of caddisfly nets could also support the development of biofilms in gravel bedded rivers which play an important ecological role in stream habitats (citation needed to support this statement). Streams with more frequent bedload transport often support less biofilm. The stabilizing effect of caddisfly nets would therefore allow more time for biofilms to grow.

Incipient sediment motion of river bed gravel is a fundamental component of channel morphology (Buffington and Montgomery, 1997). Insight into the impact that organisms have on the size and timing of bedload transport is changing how geomorphologists think about the processes shaping the landscape. It's possible that

the impact of net spinning caddisflies could cause a delayed onset of particle motion within a given size range in snowmelt driven hydrological regimes. This would result in less total sediment transport over the annual hydrograph when nets are present (Albertson et al., 2014a).

There are many new questions that emerge from this research, as well as limits to the experimental design that should be considered. The experimental bed particle size distributions we created in our flumes were narrow and uni-modal, but natural beds have much wider distributions. Is it possible that net spinning caddisflies prefer certain sizes? Size preference would play a crucial role in determining how much of an effect caddisfly nets have in natural streams. If caddisflies prefer larger cobbles to gravel, then it is possible that the density of caddisflies on those larger rocks would be higher and that could increase the effect beyond what I measured in this study. Conversely, if caddisflies concentrate on relatively immobile particles, then the density would be reduced on the smaller particles where nets have the greatest potential effect on particle stability.

This study used only one species, but what if multiple species were present? Locations with larger species, like *Arctospyche* in western north America, could see an increase in the grain size where nets can have an effect. How does their effect vary in different hydrological regimes for example, temperate, tropical, or arid environments?

There are many aspects of the experiment that could be improved. One shortcoming of the experiment was the non-constant crank speed which prevented me from being able to properly align time and distance data. Future experiments could change the two-dimensional characterization of the bed topography and the abiotic model to incorporate 3 dimensions. Although maintaining a 2-dimensional analysis also kept results comparable to previously published theoretical model, assessing the effect of nets in 3-D could give even more accurate results.

This research contributes to the growing literature quantifying the influence of ecosystem engineers and their influence on abiotic processes. The use of

computational analysis in quantifying the life habits of organisms is increasing. One example is a study that used high speed video to map scorpion stinger trajectories (Coelho et al., 2017). Research has shown that ecosystem engineers cause changes to their physical environment but quantifying the physical changes themselves is often a confounding factor (Albertson and Daniels, 2016). There are a variety of organisms whose impacts on shaping the environments are clearly seen but ways to quantify their effects remain unknown. Laboratory methods that experiment with ways of quantifying life habits of organisms and their impact on physical mechanisms of geomorphic change help to isolate the variables and remove outside influences.

6.0 CONCLUSION

The habits of many living organisms can influence physical ecosystem processes, but little work has quantified these effects. Understanding the influence of biologic processes on landscape morphology involves making direct measurements of the forces acting between organisms and the earth materials they alter. For this research, I made measurements of the forces applied to individual riverbed sediment particles by the nets of hydropsychid caddisfly larvae. I conducted flume experiments to explore the physical mechanics of caddisfly nets using a strain gage to measure the forces acting between nets and sediment particles of various sizes during the process of initial particle motion. To better detect the magnitude of force contributed by caddisfly nets I compared the measured peak forces to an abiotic model used to calculate the peak force without caddisflies to test whether the measured force was different from the model prediction. The abiotic model was applied for all caddisfly and control rock pulls.

After the experiment, I identified force peaks from each force reading on a pull by pull basis, and assessed which peaks were influenced by pocket geometry and rock shape. The abiotic model included the peak friction angle for each pull which was estimated from bed elevation profiles taken from digital elevation

models of each flume. To test the quality of fit of the model, I compared the model predicted forces to the actual peak forces measured in the control pulls.

I found a significant difference between control and caddisfly forces, on average, for all pulls and for all grain size treatments ranging from 30 mm to 60 mm. I also analyzed all the data without the grain size bins used in the experiments and plotted the normalized difference by intermediate-axis for both treatments. This shows what the maximum size of grains where caddisfly pulls exceeded controls and reveals the threshold of caddisfly nets stabilizing effect. Results from net measurements of force rise during stretching have values that span over 2 magnitudes from 0.01 to 1 Newton. Force rise during stretching is positively correlated with an increase in buoyant weight. Force rise during stretching increases with net area and the size of nets increases with rock size.

My findings provide further evidence that caddisfly nets significantly increase the force required to move particles. I detected a significant increase in force contributed by nets for all gravel particle size treatments tested. My data show that the effect of Caddisfly nets becomes less significant with increasing particle size; my results suggest the threshold lies somewhere between 70 mm and 75 mm b-axis.

While this is a similar result compared to the theoretical model predictions, this is the first substantial set of experimental data to confirm a significant effect of nets for such large grain sizes. Net measurements show larger rocks have nets that contribute more force because larger rocks allow for larger nets to be built. These results have many implications for understanding the impact of ecological engineering by caddisflies, such as increasing the spread in the distribution of gravel sizes on the bed by holding down gravel particles beyond what abiotic forces alone can sustain. My results support previous findings that nets can increase the shear stress required to initiate particle motion by more than a factor of two. The influence of caddisfly nets on bed stability has potentially significant implications for the timing and magnitude of bedload sediment transport in gravel-bedded

rivers. Many new questions emerge including the role of rock size preference, which could play a crucial role in determining how much of an effect caddisfly nets have in natural streams.

7.0 REFERENCES

- Albertson, L. K., Sklar, L. S., Pontau, P., Dow, M., & Cardinale, B. J. (2014a). Journal of Geophysical Research: Earth Surface in gravel-bedded streams, (1), 1–20. <https://doi.org/10.1002/2013JF003024>. Received
- Albertson, L. K., Cardinale, B. J., & Sklar, L. S. (2014b). Non-additive increases in sediment stability are generated by macroinvertebrate species interactions in laboratory streams. *PLoS ONE*, 9(8). <https://doi.org/10.1371/journal.pone.0103417>
- Albertson, L. K., & Daniels, M. D. (2016a). Effects of invasive crayfish on fine sediment accumulation, gravel movement, and macroinvertebrate communities. *Freshwater Science*, 35(2), 644–653. <https://doi-org.jpallnet.sfsu.edu/10.1086/685860>
- Albertson, L., & Daniels, M. (2016b). Resilience of aquatic net-spinning caddisfly silk structures to common global stressors. *Freshwater Biology*, 61(5), 670–679.
- Alexander S. Flecker (2017). Ecosystem Engineering by a Dominant Detritivore in a Diverse Tropical Stream, *Ecology*, 77(6), 1845–1854.
- Braudrick, C. A., Dietrich, W. E., Leverich, G. T., & Sklar, L. S. (2009). Experimental evidence for the conditions necessary to sustain meandering in coarse-bedded rivers. *Proceedings of the National Academy of Sciences of the United States of America*, 106(40), 16936–16941. <https://doi.org/10.1073/pnas.0909417106>
- Buffington, J. M., and D. R. Montgomery (1997), A systematic analysis of eight decades of incipient motion studies, with special reference to gravel-bedded rivers, *Water Resources*, 33(8), 1993–2029, doi:10.1029/96WR03190.
- Cardinale, B. J., E. R. Gelmann, and M. A. Palmer. (2004). Net spinning caddisflies as stream ecosystem engineers: The influence of Hydropsyche on benthic substrate stability. *Functional Ecology* 18:381– 387.
- Church, M. (2006). Bed material transport and the morphology of alluvial river channels. *Annual Review of Earth and Planetary Science*, 34, 325–354.
- Dingman, S. L. (2009) *Fluvial Hydraulics*. New York: Oxford University Press, USA.
- Johnson, M. F., I. Reid, S. P. Rice, and P. J. Wood. (2009). Stabilization of fine gravels by net-spinning caddisfly larvae. *Earth Surface Processes and Landforms* 34:413–423.

- Kirchner, J. W., Dietrich, W. E., Iseya, F., & Ikeda, H. (1990). The variability of critical shear stress, friction angle, and grain protrusion in water-worked sediments. *Sedimentology*, 37(4), 647–672. <https://doi.org/10.1111/j.1365-3091.1990.tb00627.x>
- Komar, P. D., and P. A. Carling (1991), Grain sorting in gravel-bed streams and the choice of particle sizes for flow-competence evaluations, *Sedimentology*, 38(3), 489–502.
- Kondolf, G. M. (2000), Assessing Salmonid Spawning Gravel Quality. *Transactions of the American Fisheries Society*, 129: 262-281. doi:10.1577/1548-8659(2000)129<0262:ASSGQ>2.0.CO;2
- Lamb, M. P., Dietrich, W. E., & Venditti, J. G. (2008). Is the critical shields stress for incipient sediment motion dependent on channel-bed slope? *Journal of Geophysical Research: Earth Surface*, 113(2), 1–20. <https://doi.org/10.1029/2007JF000831>
- Miller, J. (1984), Competition, predation, and catchnet differentiation among net-spinning caddisflies (Trichoptera), *Oikos*, 43, 117–121.
- Montgomery, D. R., Buffington, J. M., Peterson, N. P., Schuett-Hames D., Quinn, T. P., *Canadian Journal of Fisheries and Aquatic Sciences*, 1996, 53:1061-1070, <https://doi.org/10.1139/f96-028>
- Moore, J. W., Schindler, D. E., & Scheuerell, M. D. (2004). Disturbance of freshwater habitats by anadromous salmon in Alaska, 298–308. <https://doi.org/10.1007/s00442-004-1509-3>
- Mueller, E. R., J. Pitlick, and J. M. Nelson (2005), Variation in the reference Shields stress for bed load transport in gravel-bed streams and rivers, *Water Resour. Res.*, 41, W04006, doi:10.1029/2004WR003692.
- Parker, G., Wilcock, P. , Paola, C. , Dietrich, W. , & Pitlick, J. (2007). Physical basis for quasi-universal relations describing bankfull hydraulic geometry of single-thread gravel bed rivers. *Journal of Geophysical Research: Earth Surface*, 112(F4), n/a.
- Rice, P., Lancaster, J., Kemp, P., (2010) Experimentation at the interface of fluvial geomorphology, stream ecology and hydraulic engineering and the development of an effective, interdisciplinary river science. *Earth Surf. Process. Landforms* 35, 64–77.

- Statzner, B. (2012). Geomorphology Geomorphological implications of engineering bed sediments by lotic animals. *Geomorphology*, 157–158, 49–65.
<https://doi.org/10.1016/j.geomorph.2011.03.022>
- Statzner, B., Arens, M. F., Champagne, J. Y., Morel, R., & Herouin, E. (1999). Silk-producing stream insects and gravel erosion: Significant biological effects on critical shear stress. *Water Resources Research*, 35(11), 3495–3506.
<https://doi.org/10.1029/1999WR900196>
- Statzner, B. (1982). Population dynamics of Hydropsychidae (Insecta; Trichoptera) in teh N’Zi River (Ivory Coast), a temporary stream partly treated with the insecticide Chlorphozim. *Revue d’Hydrobiologie Tropicale* 15:157–176.
- USEPA (United States Environmental Protection Agency). (2004). Wadable Stream Assessment
- Wiberg, P. L., and J. D. Smith (1987), Calculations of the critical shear stress for motion of uniform and heterogeneous sediments, *Water Resour. Res.*, 23(8), 1471–1480, doi:10.1029/WR023i008p01471.
- Wiggins, G. B. (1977) Larvae of the North American Caddisfly Genera. Toronto University Press. Wilcock, P. R. (1993), Critical shear stress of natural sediments, *J. Hydraul. Eng.*, 119(4), 491–505.

8.0 TABLES

Table 1. Experimental Design

Time blocks	5
Flumes	10
Treatments (Caddisfly or Control)	2
Grain size distributions (30-60 mm)	5
Flumes per grainsize	2
Rock pulls per flume	8
Total number of rock pulls	430
Number of rock pulls in raw bulk analysis	421
Number of net measurement observations	189
Number of rock pulls in measured versus modeled analysis	195

Table 2. Buoyant weight (g)

Grain Treatment	Control			Caddisfly			T-Test					
	#	Mean	Std Dev.	Std Error	#	Mean	Std Dev.	Std Error	Difference	Std Error of Difference	Degrees of Freedom	Prob > t
30	48	37.1	19.6	2.8	42	37.7	13.8	2.1	-0.6	3.6	88	0.873
40	42	85.7	26.6	4.1	41	73.4	30.4	4.7	12.2	6.3	81	0.055
50	42	121.9	53.5	8.3	44	109.5	58.8	8.9	12.4	12.1	84	0.310
55	41	149.3	53.2	8.3	42	146.6	48.1	7.4	2.7	11.1	81	0.810
60	43	204.2	59.0	9.0	44	194.2	70.5	10.6	10.0	14.0	85	0.476
All	216	117.6	72.9	5.0	213	113.2	73.4	5.0	4.4	7.1	427	0.536

Table 3. B-axis

Grain Treatment	Control				Caddisfly				T-Test			
	#	Mean	Std Dev.	Std Error	#	Mean	Std Dev.	Std Error	Difference	Std Error of Difference	Degrees of Freedom	Prob > t
30	41	38.8	5.5	0.9	41	36.3	9.7	1.5	-2.4	1.7	80	0.165
40	42	47.6	4.2	0.6	41	44.6	4.9	0.8	-2.9	1.0	81	0.004
50	39	54.2	4.9	0.8	40	53.3	6.3	1.0	-0.9	1.3	77	0.464
55	41	59.4	6.7	1.0	41	58.9	5.3	0.8	-0.6	1.3	80	0.672
60	43	64.7	7.8	1.2	42	65.0	5.5	0.8	0.3	1.5	83	0.823
All	206	53.0	10.9	0.8	205	51.7	12.1	0.8	-1.3	1.1	409	0.242

Table 4. Normalized Difference (Meas-FP)/FP

Grain Treatment	Control				Caddisfly				T-Test			
	#	Mean	Std Dev.	Std Error	#	Mean	Std Dev.	Std Error	Difference	Std Error of Difference	Degrees of Freedom	Prob > t
30	16	0.08	0.17	0.04	16	0.36	0.36	0.09	0.28	0.10	30	0.004
40	21	0.11	0.12	0.03	25	0.25	0.29	0.06	0.35	0.07	44	<.0001
50	21	0.04	0.20	0.04	21	0.13	0.17	0.04	0.17	0.06	40	0.0024
55	24	0.07	0.20	0.04	17	0.26	0.35	0.09	0.19	0.09	39	0.0150
60	16	0.09	0.13	0.03	14	0.29	0.28	0.08	0.20	0.08	28	0.0080
All	98	0.01	0.18	0.02	93	0.25	0.30	0.03	0.24	0.04	189	<.0001

Table 5. Taustar crit (Measured-FP)

Grain Treatment	Control				Caddisfly				T-Test			
	#	Mean	Std Dev.	Std Error	#	Mean	Std Dev.	Std Error	Difference	Std Error of Difference	Degrees of Freedom	Prob > t
30	16	0.039	0.003	0.001	16	0.045	0.007	0.002	0.005	0.002	30	0.0034
40	22	0.036	0.003	0.001	25	0.042	0.005	0.001	0.007	0.001	45	<.0001
50	24	0.038	0.005	0.001	21	0.040	0.003	0.001	0.003	0.001	43	0.0163
55	24	0.039	0.003	0.001	17	0.043	0.007	0.002	0.004	0.002	39	0.0094
60	16	0.039	0.002	0.001	14	0.042	0.004	0.001	0.003	0.001	28	0.0098
All	102	0.038	0.004	0.000	93	0.042	0.006	0.001	0.004	0.001	193	<.0001

Table 6. Taustar crit (Force rise during stretching)

Grain Treatment	t* without nets				Caddisfly				T-Test			
	Mean	Std Dev.	#	Std Error	Mean	Std Dev.	Std Error	Difference	Degrees of Freedom	Prob > t		
30	0.0379	0.008	39	0.048	0.048	0.008	0.001	0.010	38	<.0001		
40	0.0379	0.048	75	0.043	0.043	0.005	0.001	0.005	74	<.0001		
50	0.0379	0.003	61	0.040	0.040	0.003	0.000	0.002	61	<.0001		
55	0.0379	0.008	41	0.045	0.045	0.008	0.001	0.007	40	<.0001		
60	0.0379	0.042	26	0.042	0.042	0.004	0.001	0.004	25	<.0001		
All	0.0379	0.003	189	0.041	0.041	0.003	0.000	0.003	188	<.0001		

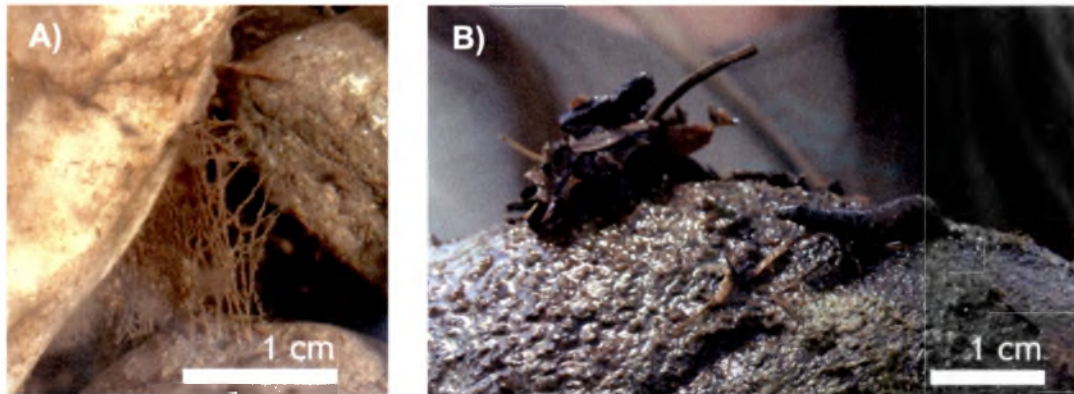
9.0 FIGURES

Figure 1) *Bettini* caddisfly net in one of the flume experiments with scalebar (A) and an *Arctopsyche* specimen from a river in Montana with scalebar (B). These nets are made up of many silk threads. The photo on the right is of an *Arctopsyche* caddisfly larvae, which is a relatively large species. The caddisfly's net dwells in the background. Net-spinning caddisflies are insects that live on the bed of streams. They build nets in between gravel particles that are used to filter food out of the water and as a place to live (Wiggins, 1977).

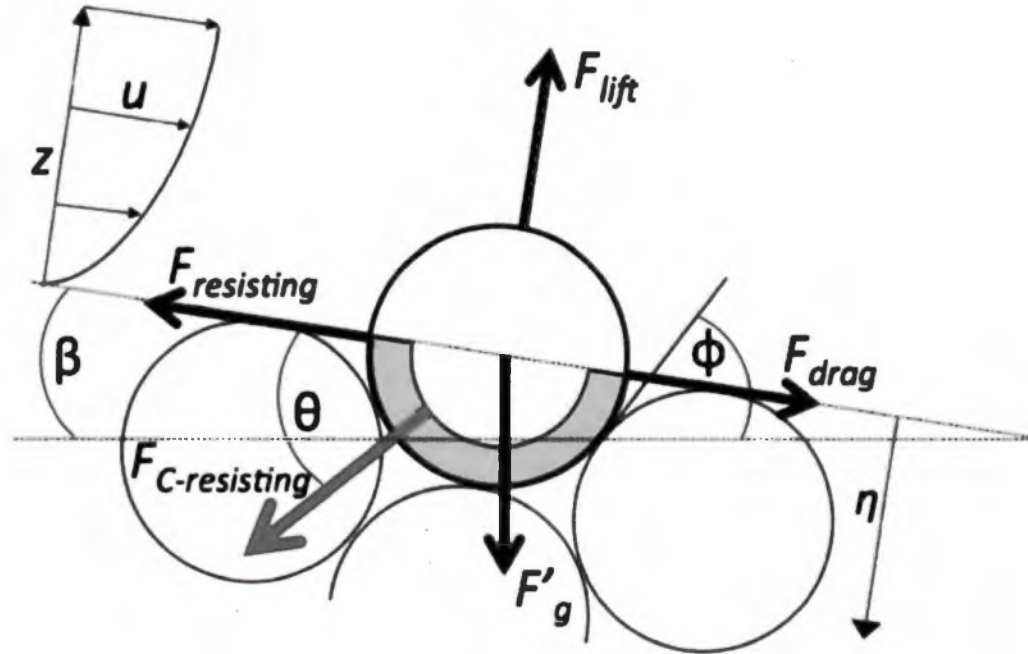


Figure 2) Force balance diagram of the forces acting on a particle at the onset of motion in the presence of caddisfly nets. The abiotic factors include drag force, F_{drag} , buoyant gravitational force, F'_g , lift force, F_{lift} , resisting forces, $F_{resisting}$, bed slope, β , grain friction angle, ϕ , velocity profile, u , and flow depth above the grain, z . The factors contributed by caddisfly nets include, resisting forces generated by nets, $F_{C-resisting}$, assuming that caddisflies build silk nets on the bottom half (gray shading) that contribute a binding force that resists down-stream motion, the depth below the bed surface where caddisfly nets are built, η , and the angle of the net with respect to the bed surface plane, θ (Albertson et al., 2014a).

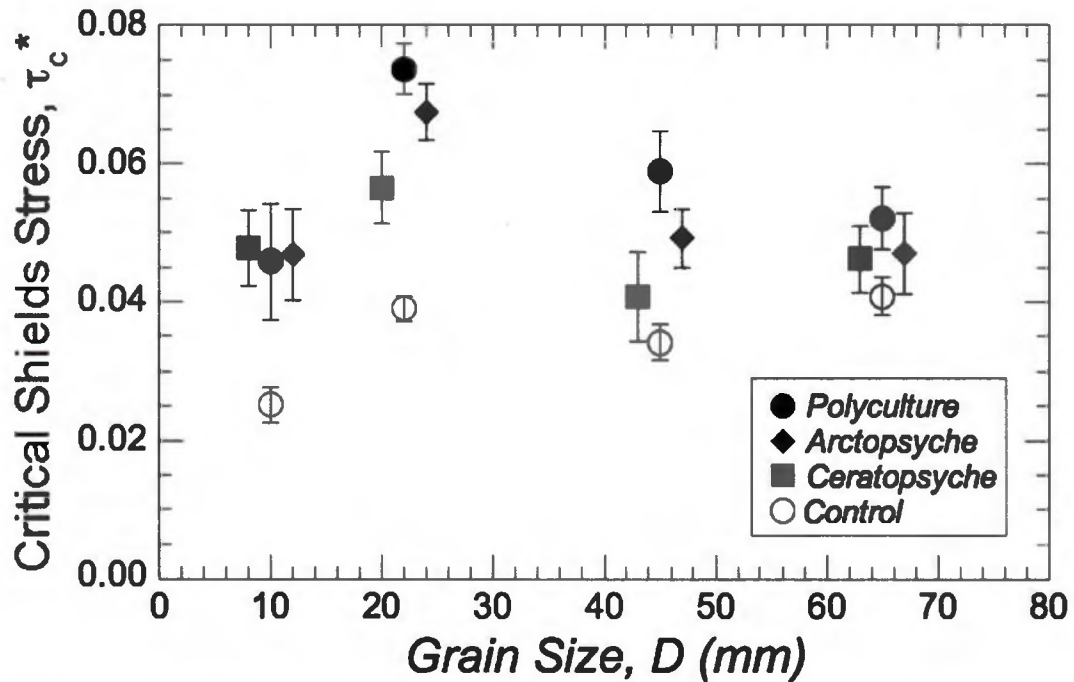


Figure 3) Measured critical shear stress values for 3 caddisfly cultures and a control by grain size. These are the results of an experiment measuring the critical shear stress, τ^* for a polyculture of two caddisfly species (black circle), the monocultures of the two species, *Arctopsyche* (black diamond), *Ceratopsyche* (grey square) and a control (white circle) as a function of grain size. The critical value of shear stress, τ^* is the force that water must overcome to transport sediment and can be calculated to determine the amount of force that it would take to transport a particle of a given grain size. These results show that caddisfly nets can increase critical shear stress by a factor of 2 (Albertson et al. 2014a).

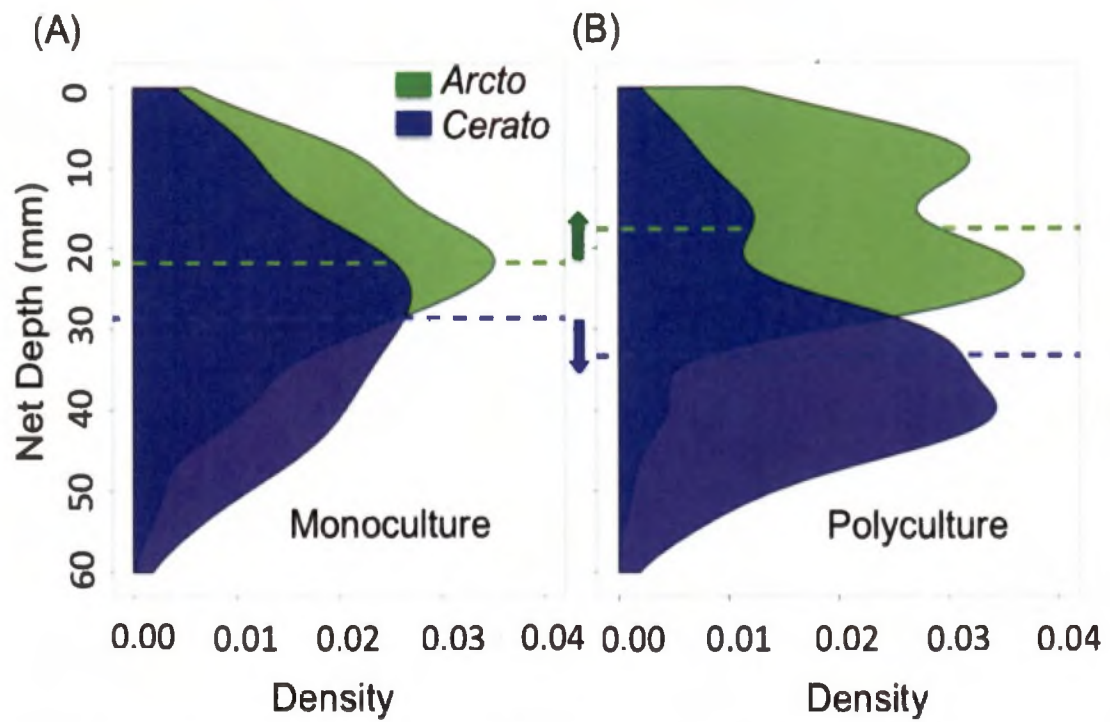


Figure 4) Caddisfly density with depth into the substrate and niche partitioning. These graphs show the variation in caddisfly density with depth into the substrate for monocultures of the two species (A) and the two species together in a polyculture (B). Niche partitioning and a vertical distribution of species allows for higher net densities over a larger distribution of net depth. (Albertson et al, 2014b)

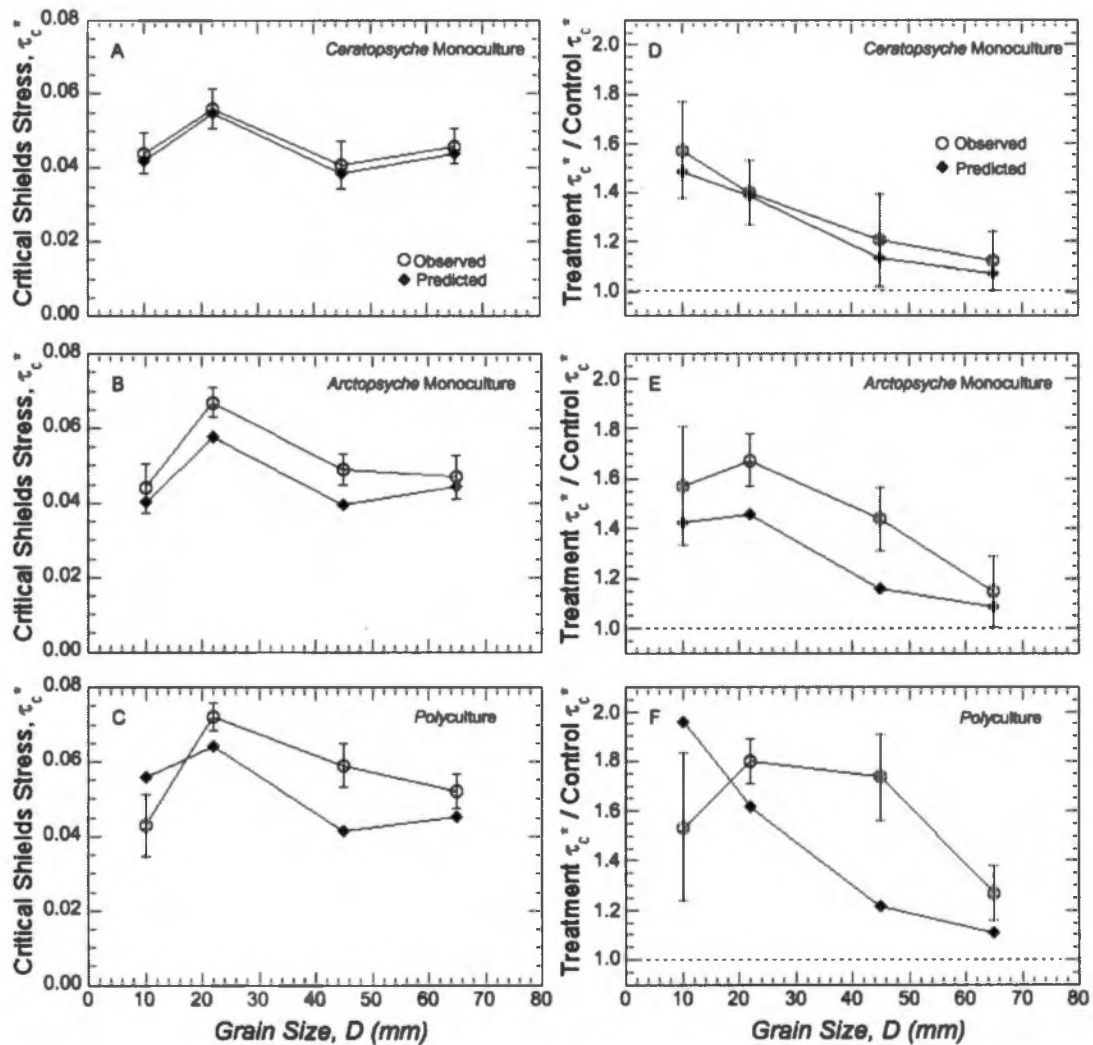


Figure 5) Comparisons of measured τ^* to model predictions for the control, the two monocultures and a polyculture of both species (A-B) and the ratio of treatment τ^* and control τ^* by grainsize (mm) (D-F). White circles are observed data points and black diamonds are model predictions for a given grain size. The similarities between measured and modeled values are variable, perhaps due to assumptions made that are built into the model (Albertson et al. 2014a).



Figure 6) The Stroud Water Research Center's indoor river laboratory in Avondale, Pennsylvania. The flumes provided caddisflies with habitat and water was sourced from nearby White Clay Creek, which also organic particulates which was a food source for the insects. The lab contains 10 flumes, 3.3 m long, 0.4 m wide and 0.3 m deep.

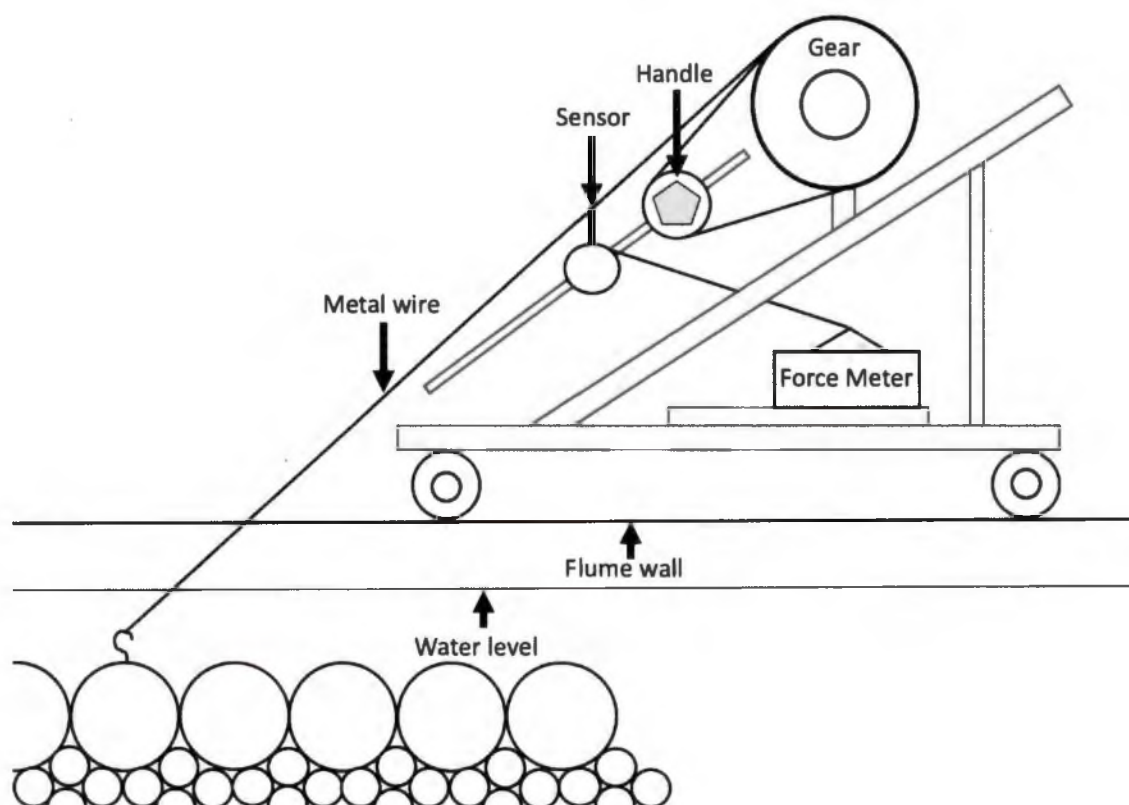


Figure 7) Schematic of the strain gauge apparatus used to mimic the transport of individual particles from the bed. This instrument was developed for the experiment and used a gear and pulley system controlled by the operator by a rotating the handle. This apparatus to pull individual rocks from the bed while measuring the force it takes to transport them.

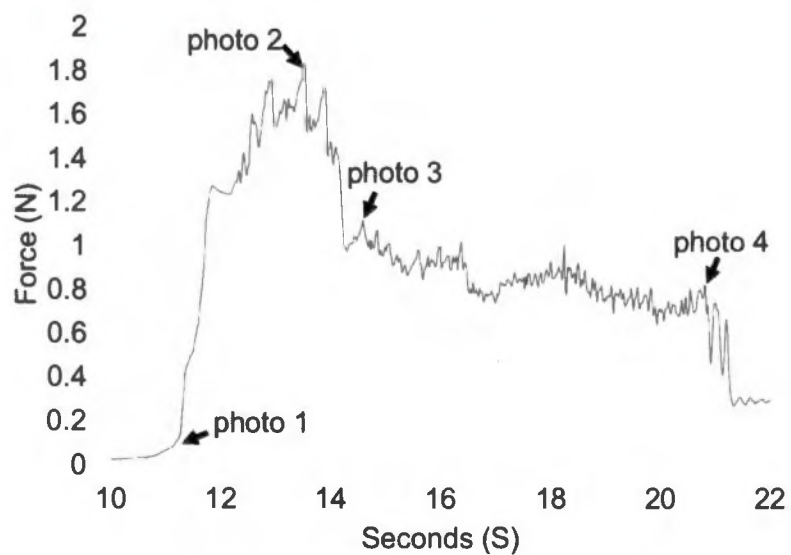
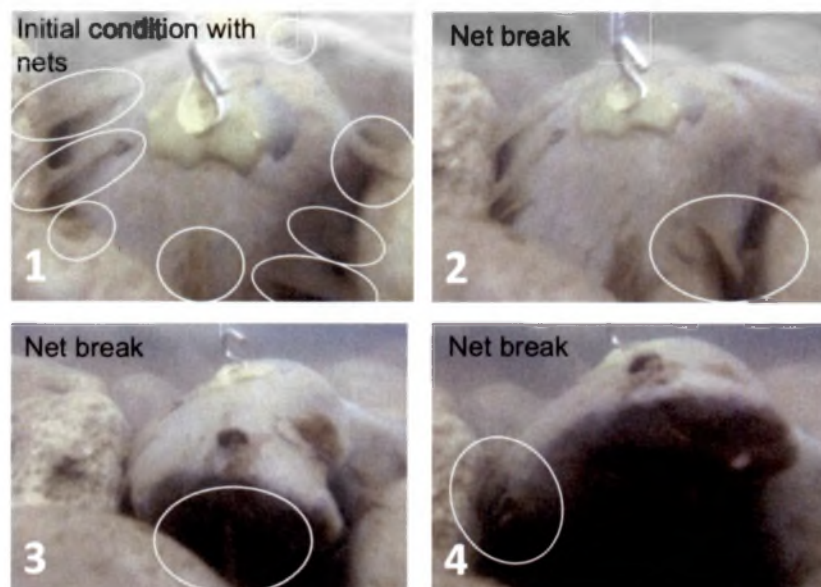


Figure 8) A Video-force gauge match-up. This diagram shows how I used synchronized force readings of rock pulls with video footage to identify net break events and the influence of pocket geometry on the force reading. The numbered photos above (1-4) are net break events and correspond to the locations labeled on the graph below.



Figure 9) Example photo of a pull rock with a rock number placard. The rock has a hook epoxied to the top, and has many nets attached. This rock is from time block 4, flume 7, rock pull 9. Scaled photos of rocks that were pulled were used to make measurements of net area and net location.



Figure 10) Photo of 3-D flume models created in Agisoft Photoscan with pull rocks highlighted in pink. The legend in the bottom right corner show the 3 principle axis dimensions. The Z-direction is vertical, the Y-direction is the length of the flume and the X-direction is the width of the flume.

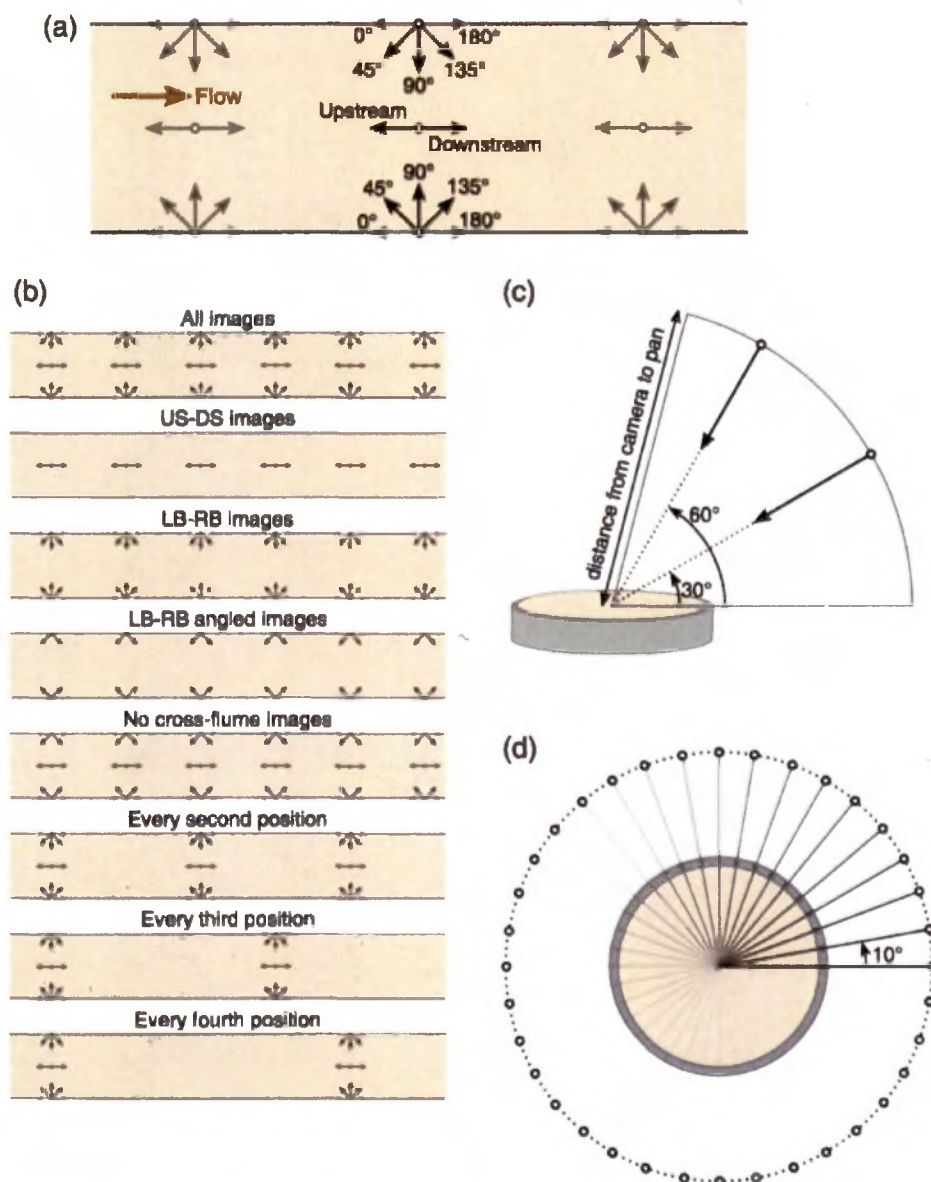


Figure 11) Diagram of structure from motion protocol for flumes. This illustration demonstrates camera angles in a flume (A), different photo position combinations for a flume(B), vertical angles for photographing pans (C), horizontal angles for photographing pans (D). Both (C) and (D) do not apply to this study (Morgan et al, 2016).

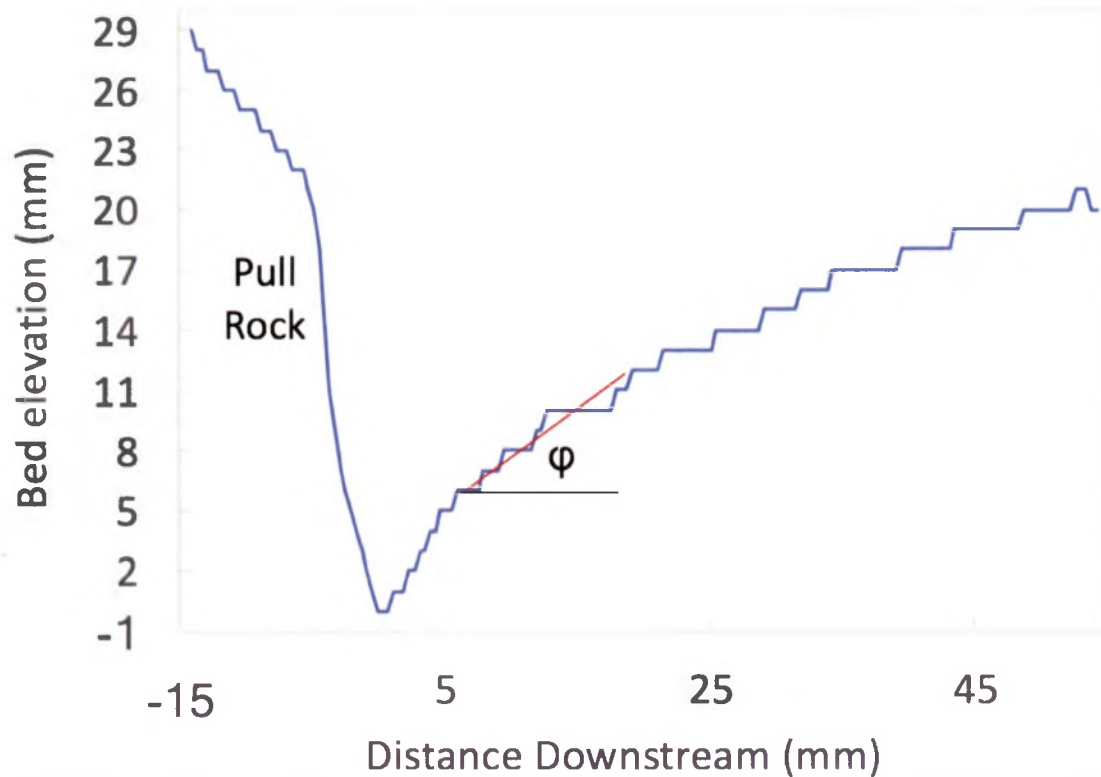


Figure 12) Example profile of a pull rock's downstream trajectory taken from a 3-D model of the flume set up. The Y-axis shows elevation above the bed. The X-axis shows the distance downstream with the origin being the downstream edge of the rock being pulled. Profiles of each rock's trajectory were used to calculate the peak friction angle that was then used in the abiotic model to calculate modeled peak force for each rock pull.

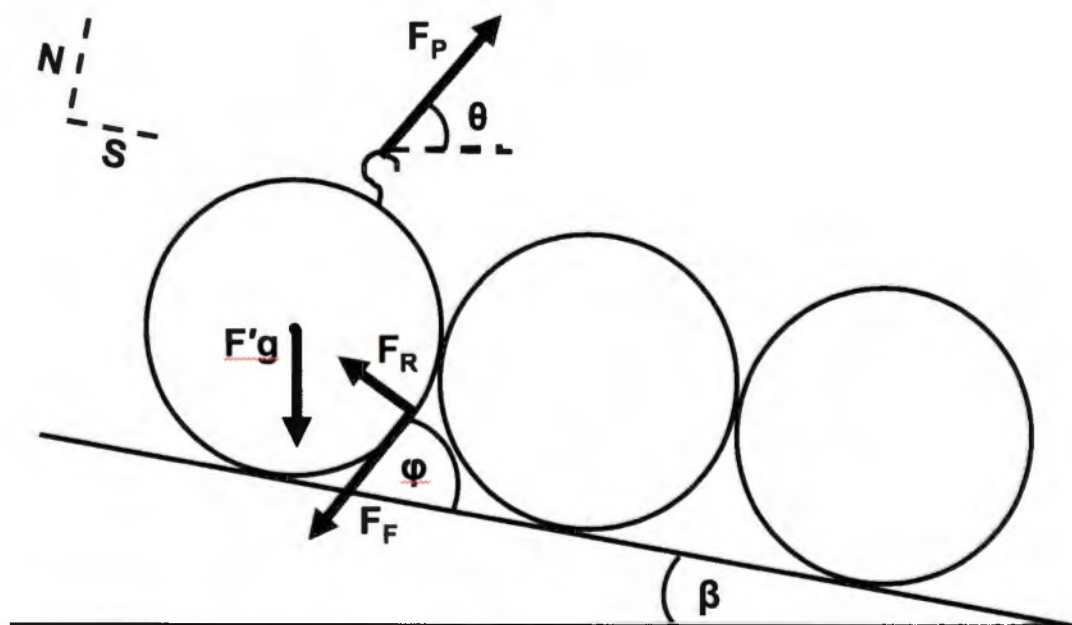


Figure 13) Force balance diagram showing the abiotic forces acting at the moment of transport of an individual particle by strain gauge apparatus. The variables include, pull force F_P , buoyant weight $F'g$, friction force F_F , friction coefficient μ , bed slope β , friction angle φ , resisting force F_R , and angle of the net with respect to the bed θ . This force balance sketch was used to create the quasi-static abiotic model used to calculate the force it would take to pull each rock without nets. The abiotic model used a friction coefficient and information of the buoyant weight of each rock as well as the friction angle the rock experienced while getting pulled downstream out of its pocket.

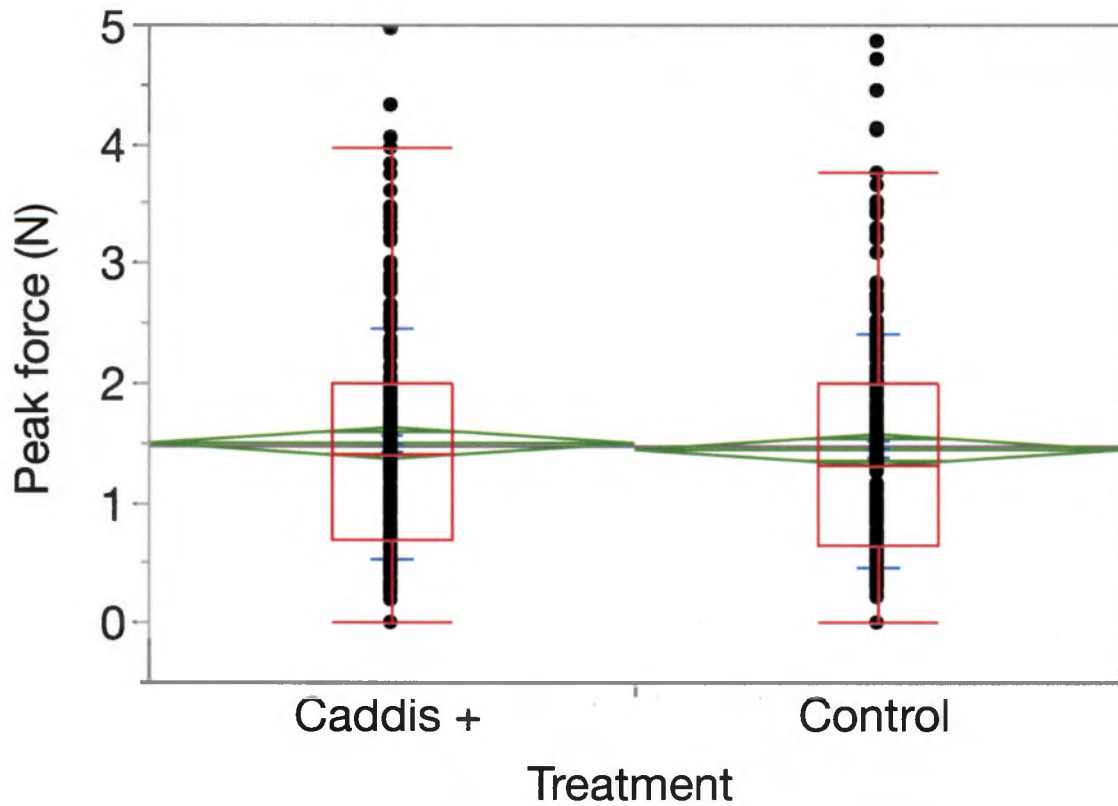


Figure 14) T-test of raw peak forces for the caddisfly and control pulls. Results show that the Caddisfly and Control peak forces are not statistically different ($p=0.277$). This is because each rock pull is unique, every rock has an individual shape and weight and its own different path it traveled out of its pocket between rocks on the bed of the flume.

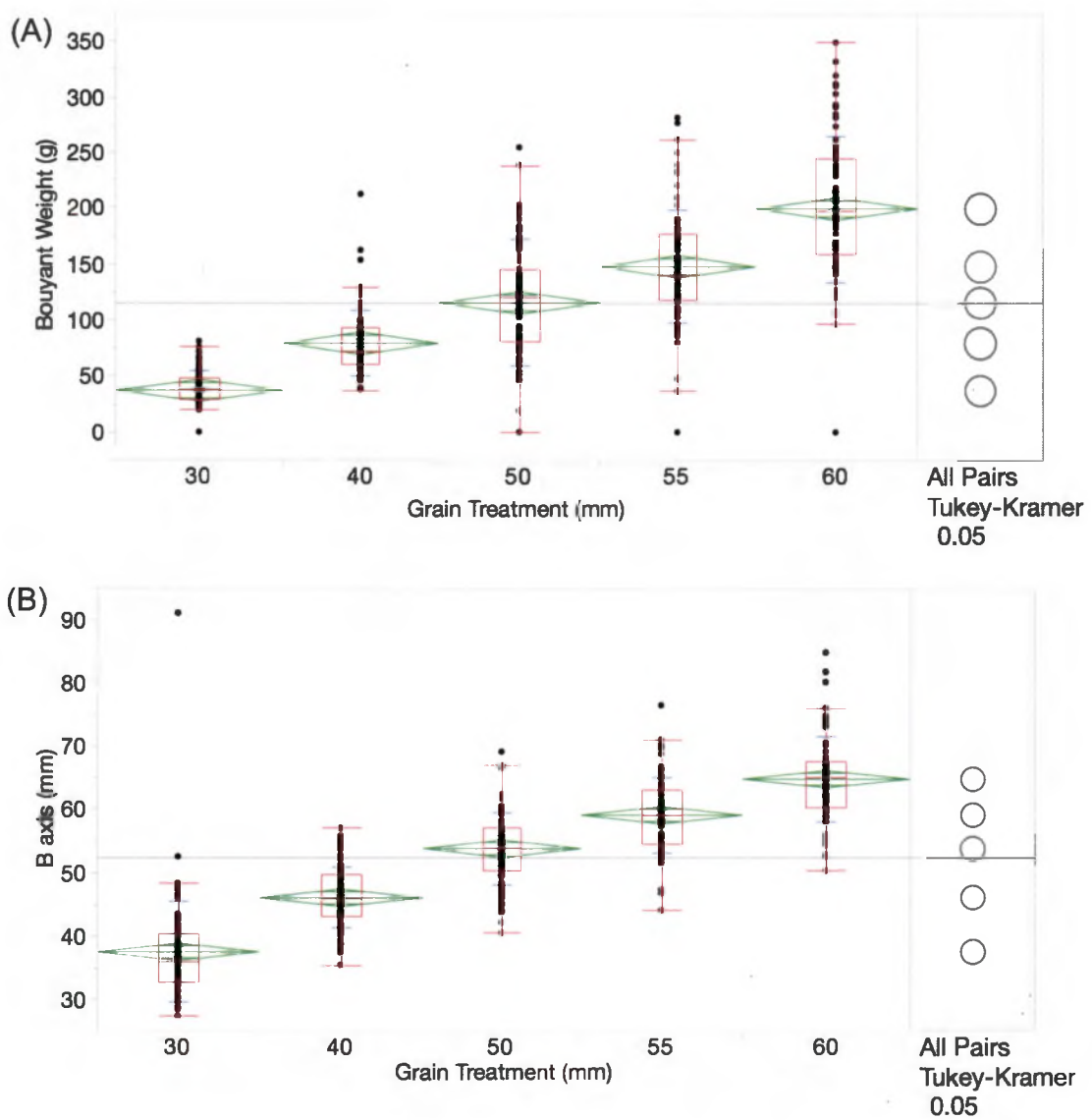


Figure 15) Buoyant weight (A) and B-axis grain diameter (B) across the different grain size treatments for both Caddisfly and Control pulls. While each grain size treatment has statistically different means for buoyant weight and B-axis, they all show a large distribution of values.

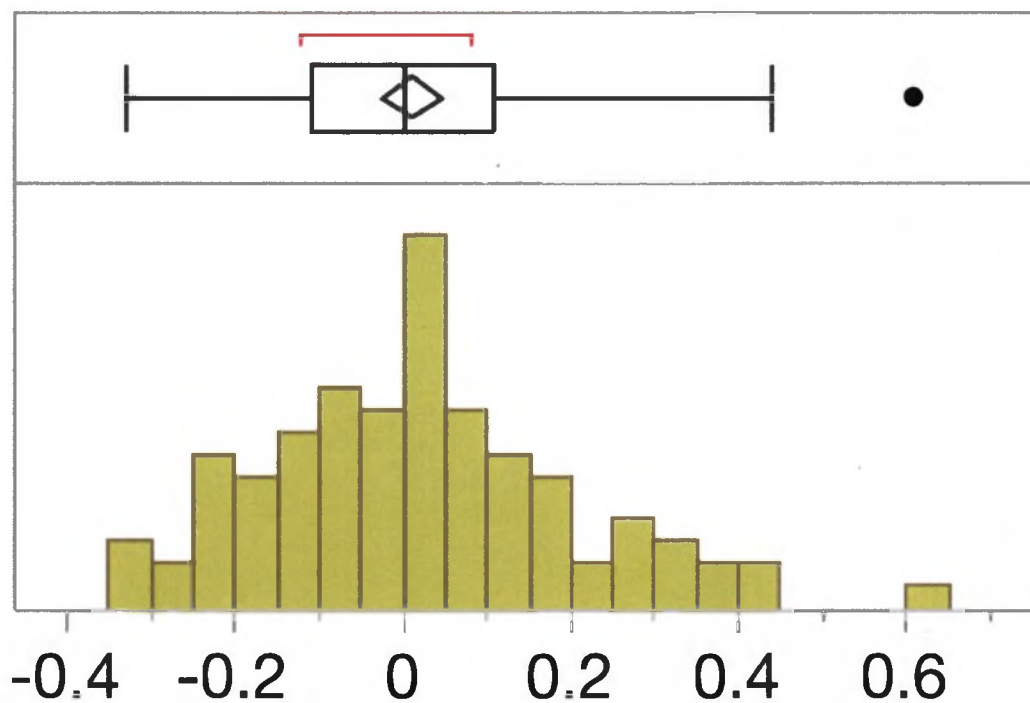
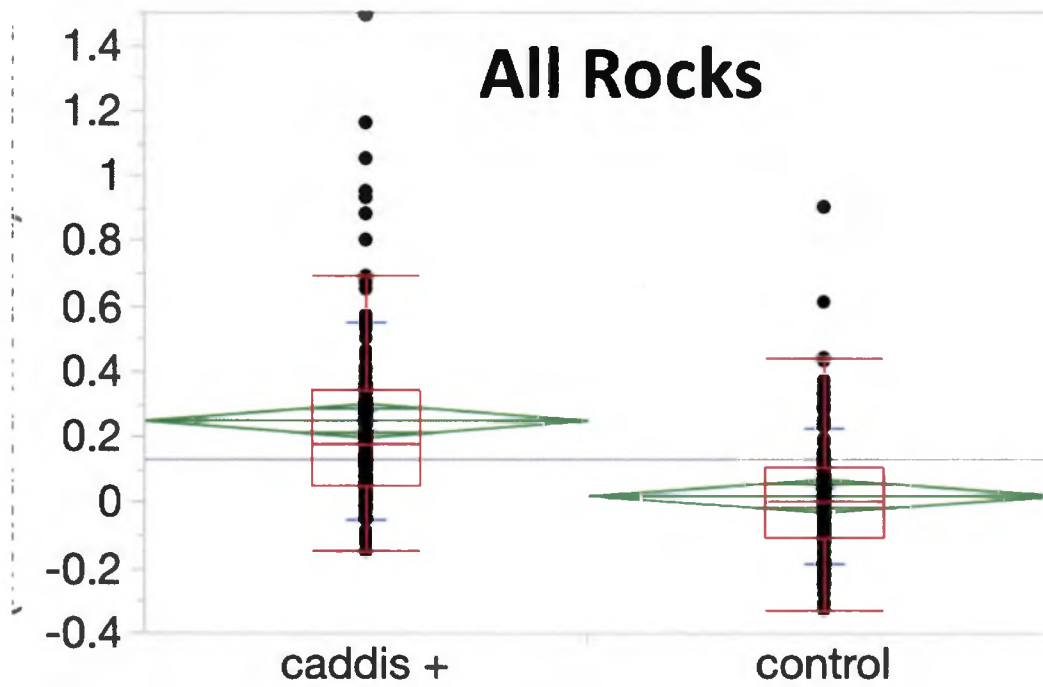


Figure 16) Distribution of normalized difference values for control pulls. To test the quality of fit of the abiotic model, I look at how closely the normalized difference for the controls compares to a hypothetical mean of zero. The results show that the mean of the data is not statistically different from zero ($p=0.539$).



Figü

t-

test analysis of the normalized difference for all rocks by treatment show that caddisfly pulls have a statistically significant increase in force (t-test: $p=0.0001$).

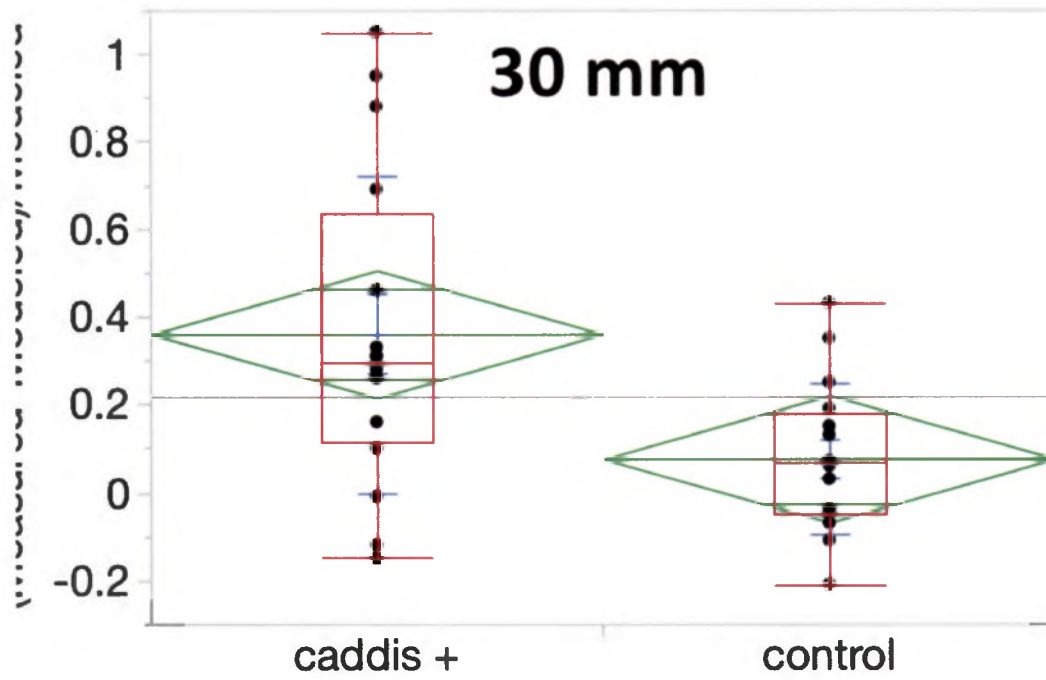


Figure 1. Results show that caddisfly pulls have a statistically significant increase in force (t-test: $p=0.0041$).

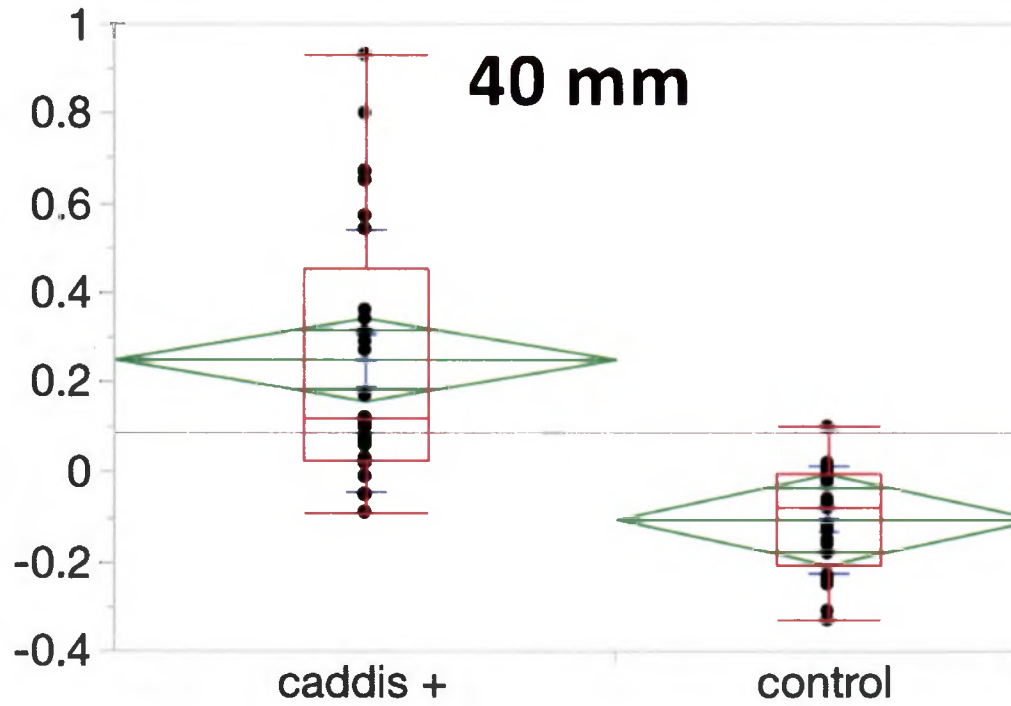


Fig. 1. Results show that caddisfly pulls have a statistically significant increase in force (t-test: $p=0.0001$).

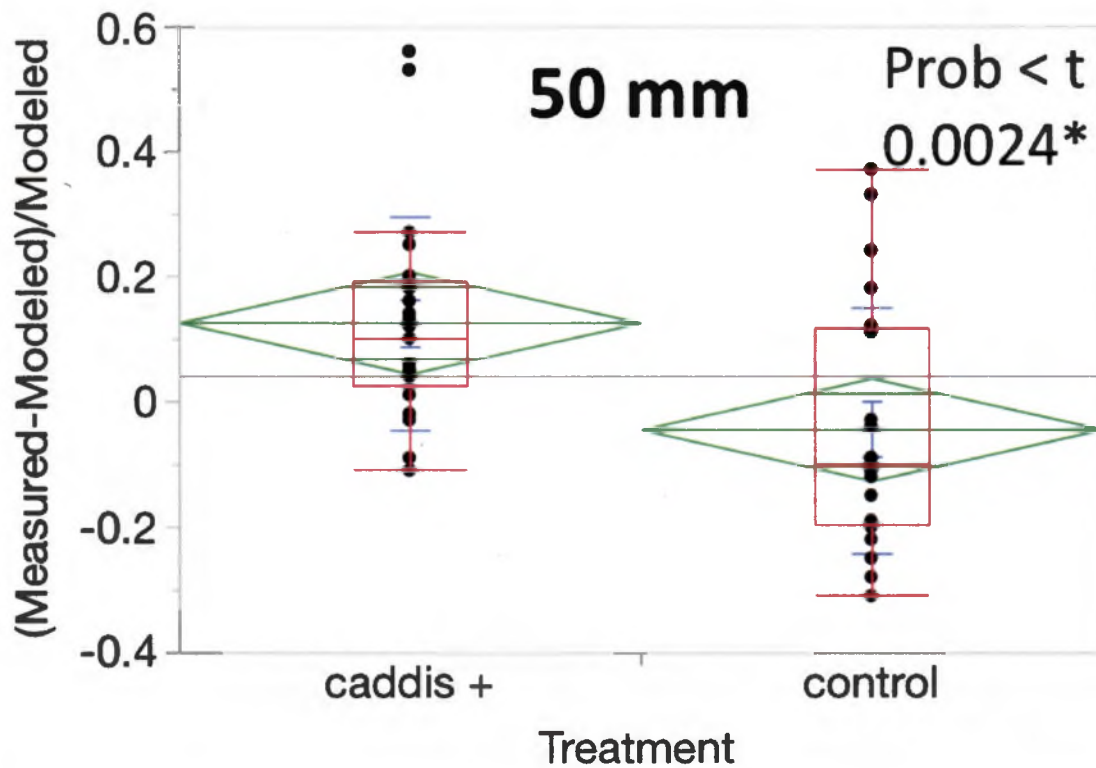


Figure 20) T-test analysis of normalized difference for 50 mm size pull by treatment. Results show that caddisfly pulls have a statistically significant increase in force (t-test: $p=0.0024$).

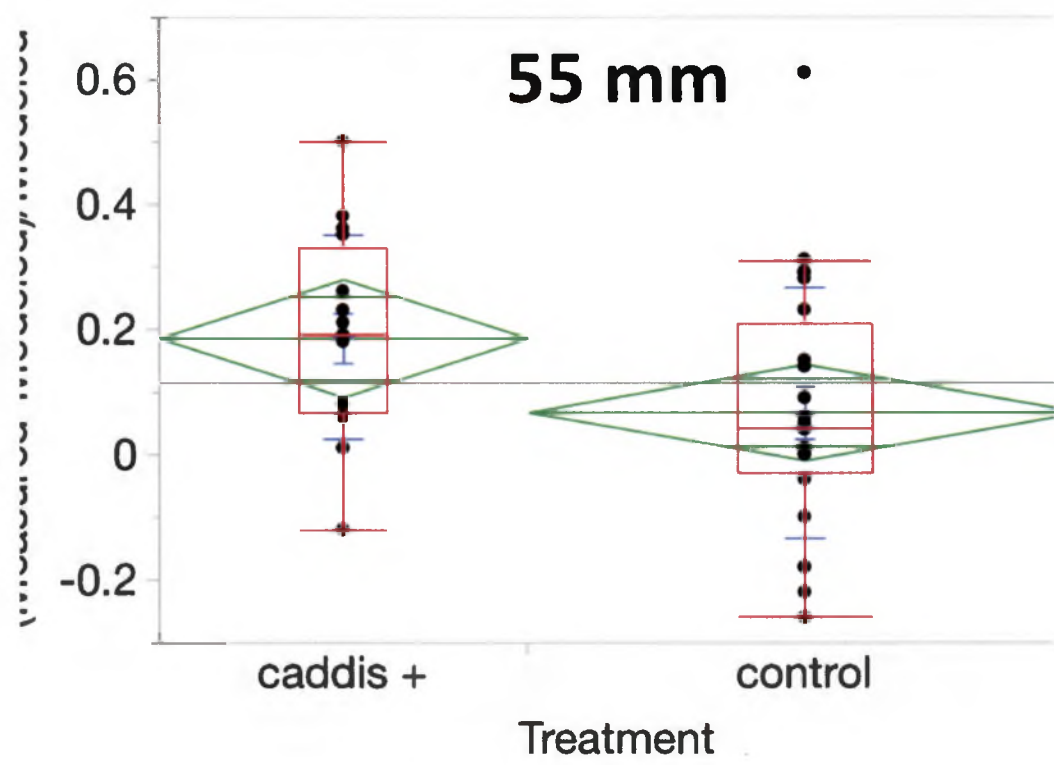


Figure 1. Results show that caddisfly pulls have a statistically significant increase in force (t-test: $p=0.0278$).

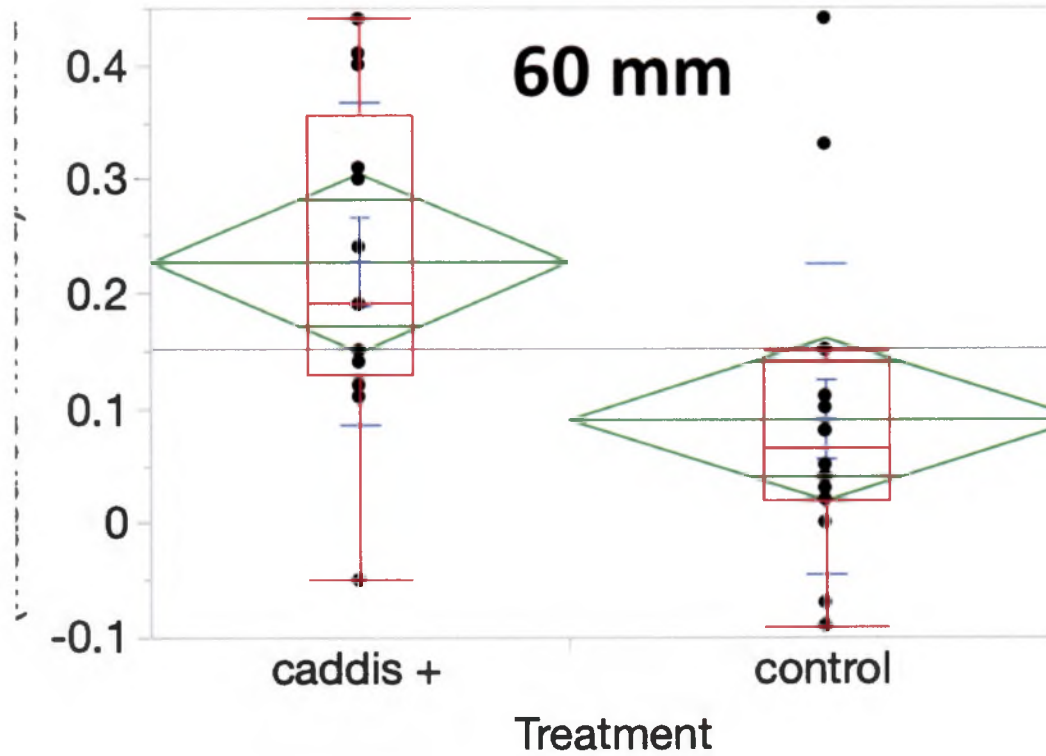


Figure 22) t-test analysis of normalized difference for 60 mm size pull by treatment. Results show that caddisfly pulls have a statistically significant increase in force (t-test: $p=0.0064$).

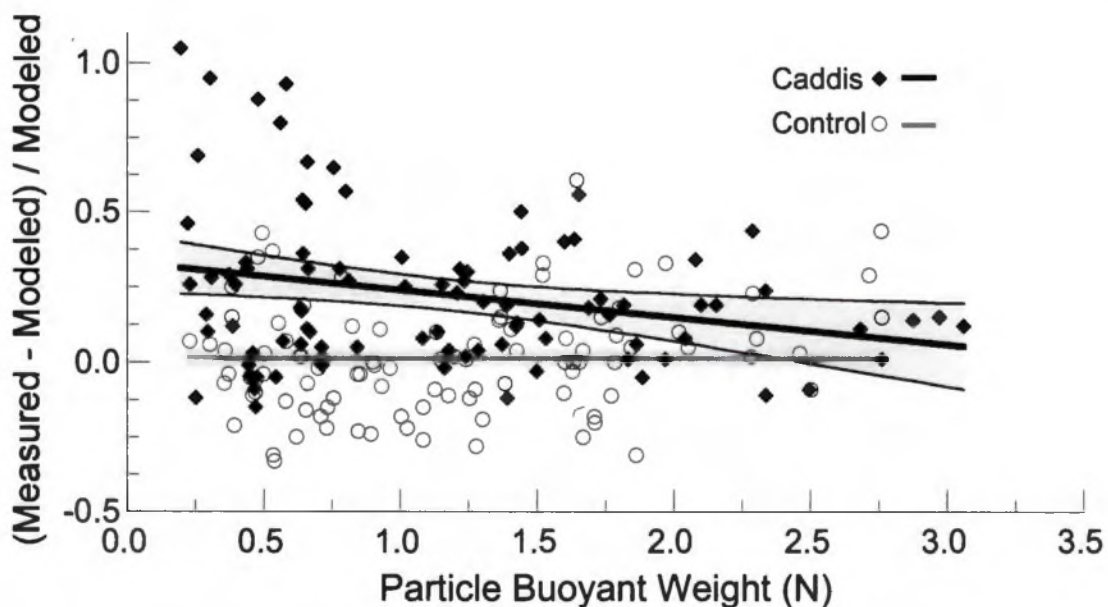


Figure 23) Normalized difference for both caddisfly (black diamond) and control (white circle) pulls by grain size. Normalized difference is on the y-axis and buoyant weight (N) on the x-axis. These results show how direct measurements of force help to determine at what grain size can you no longer detect the effect of the nets. Comparing control and caddisfly with buoyant weight shows very significant trend. The trend line for the caddisfly pulls and the mean for control pulls merge around 2.5 N or about 70 mm B-axis.

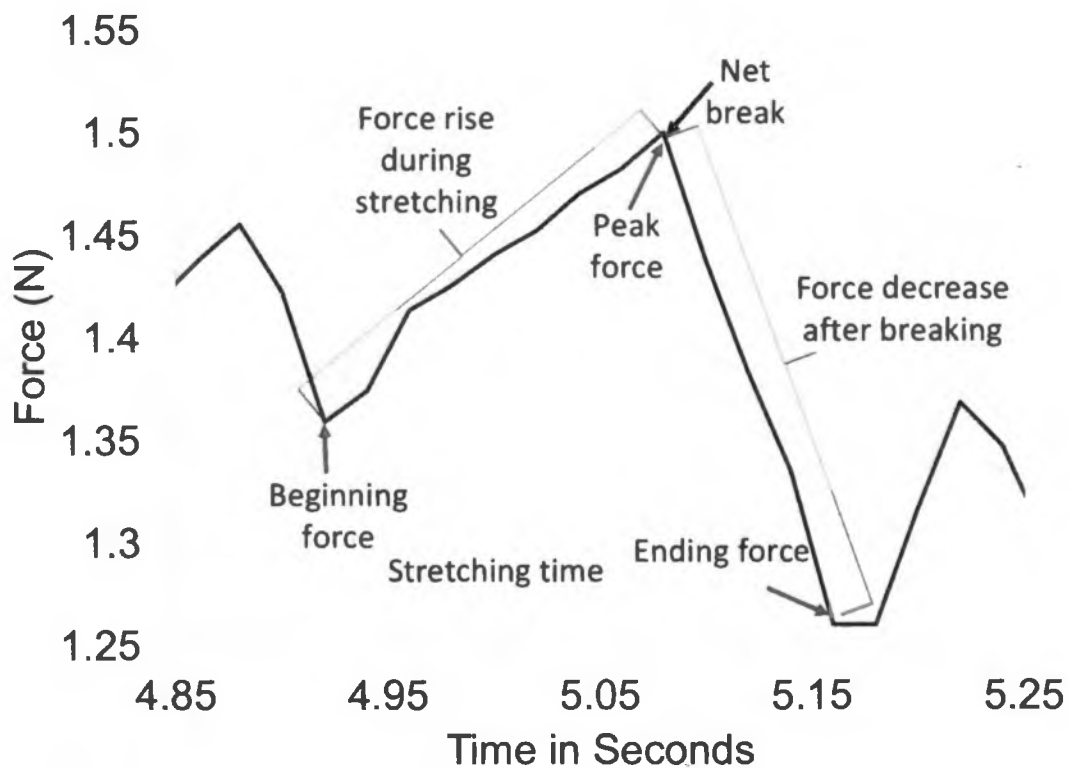


Figure 24) Diagram of the measurements made of the forces contributed by individual caddisfly larvae nets. This graph schematic shows Force (N) over time in seconds. The effect of the nets can be detected by looking at the total force contributed by caddisfly nets and comparing the force reading before nets are activated and after they've been stretched to their total load capacity. The beginning peak and ending force are used to calculate the force rise during stretching and force increase after breaking of nets.

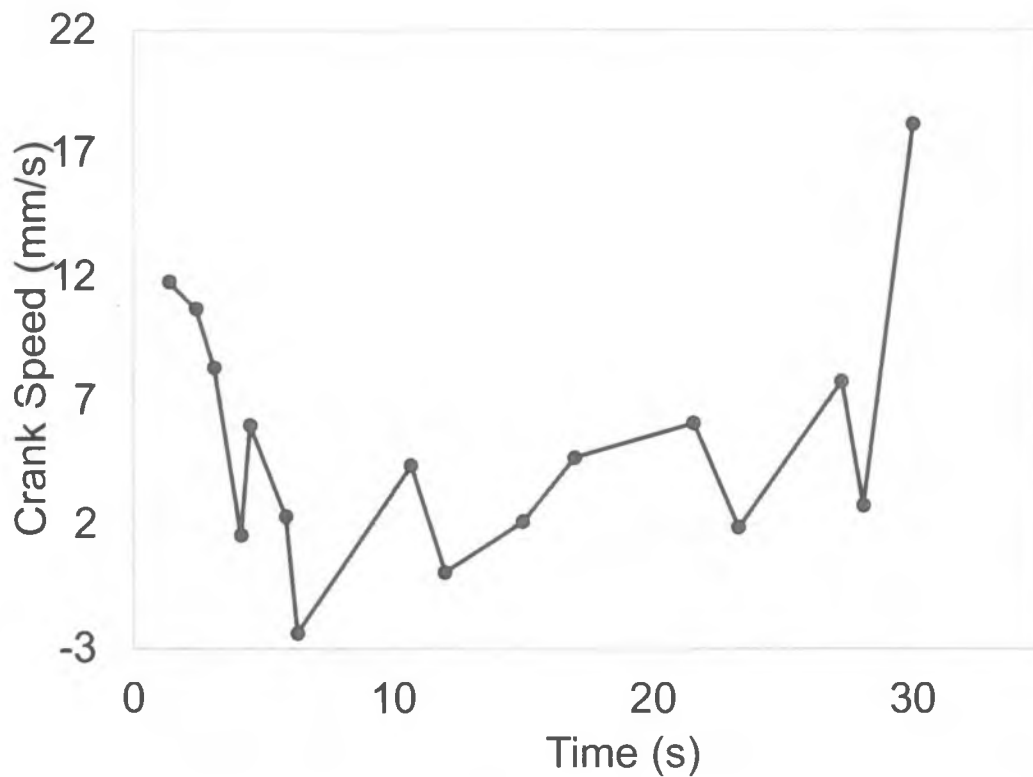


Figure 25) Measured crank speeds over time from demonstration pull video. This is a graph of the average crank speed calculated from scaled stills from a demonstration rock pull. This graph shows that there is a lot of variability in the average crank speed which makes accurately matching up the force and video for each pull unlikely.

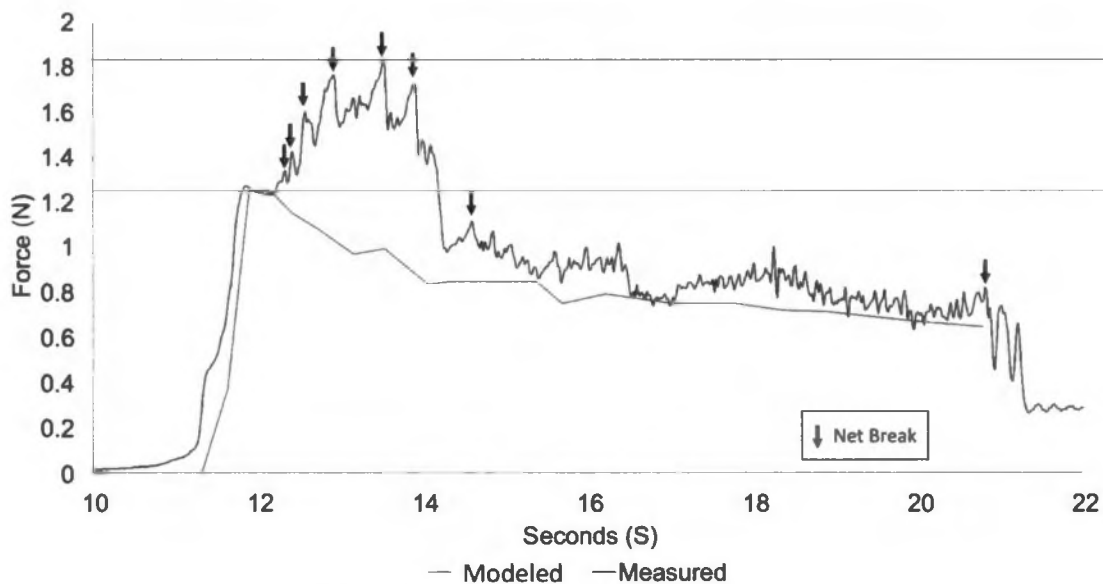


Figure 26) Force reading of a caddisfly rock pull. The net break events are indicated by an upside-down arrow. The blue line is the measured peak force and the red line is the modeled abiotic peak force. These are the two values that are used to calculate the normalized difference.

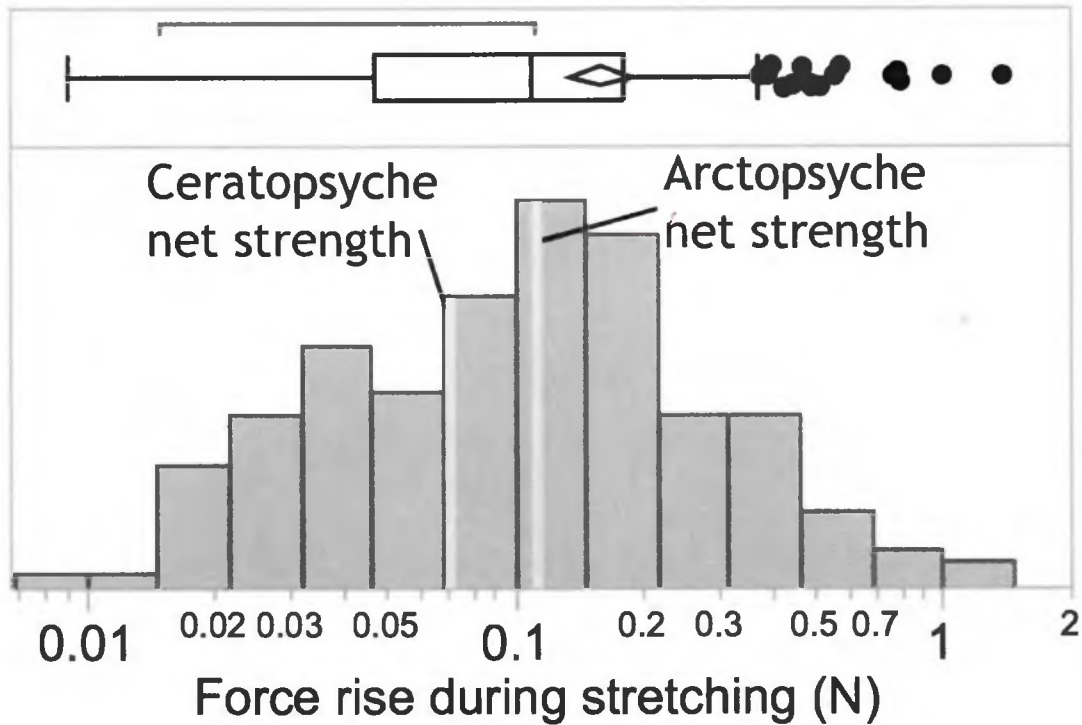


Figure 27) Distribution histogram of force rise during stretching. The range of values measured spans two orders of magnitude. The mean value from my measurements of 0.12 N aligns closely with previously measured *Arctopsyche* mean net strength of 0.16 N and *Ceratopsyche* mean net strength of 0.07 N which are both indicated by neon-yellow vertical stripes (Albertson et al. 2014).

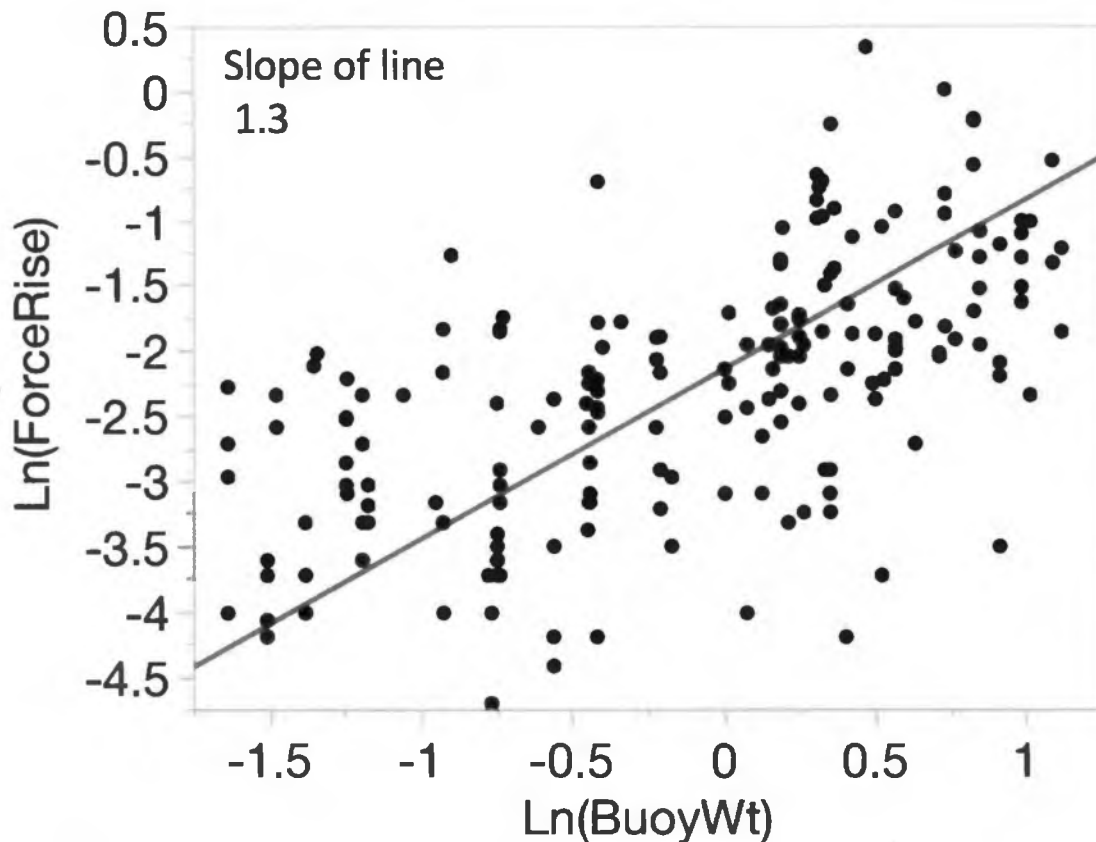


Figure 28) Orthogonal regression of force rise during stretching (N) and buoyant weight (N). The X and Y-axis are in natural log space. The green line indicates the trend of the data and has a slope of 1.3. These results show that force rise during stretching positively correlates with buoyant weight.

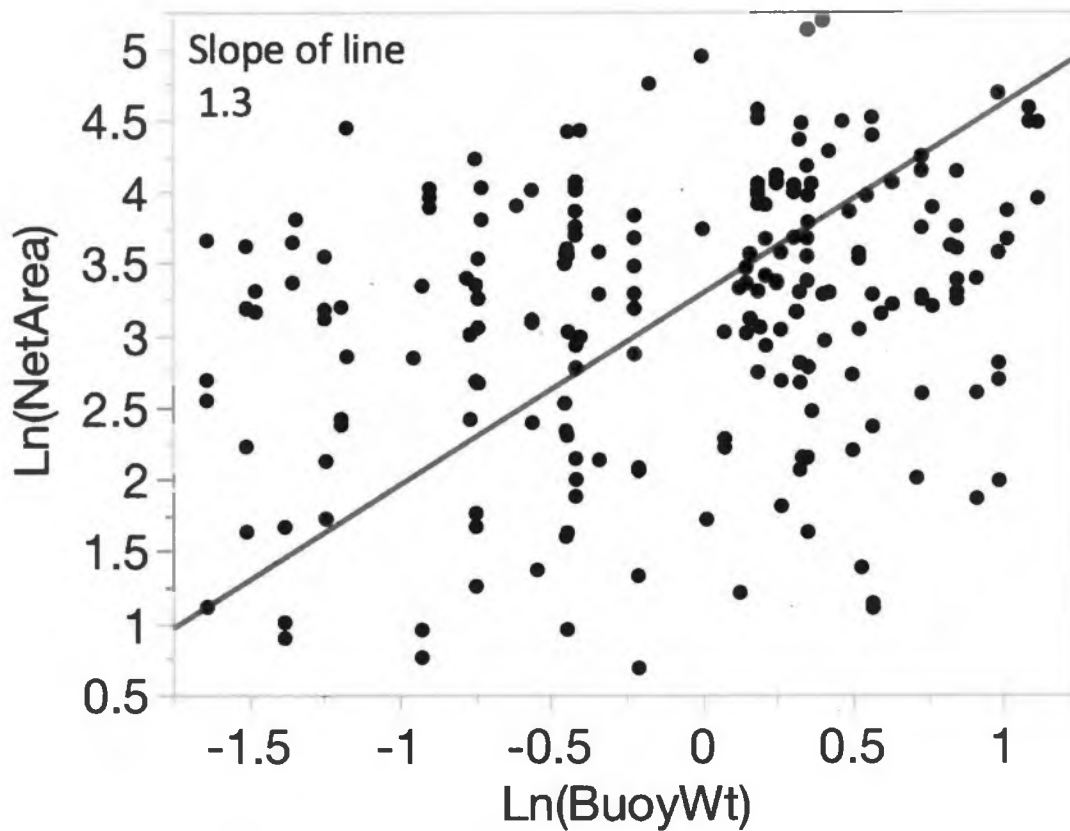


Figure 29) Orthogonal regression with the natural log of net area (mm^2) and the natural log of buoyant weight (N). The trend of the data is indicated by the red line and has a slope of 1.3. These results show that net area positively correlates with buoyant weight.

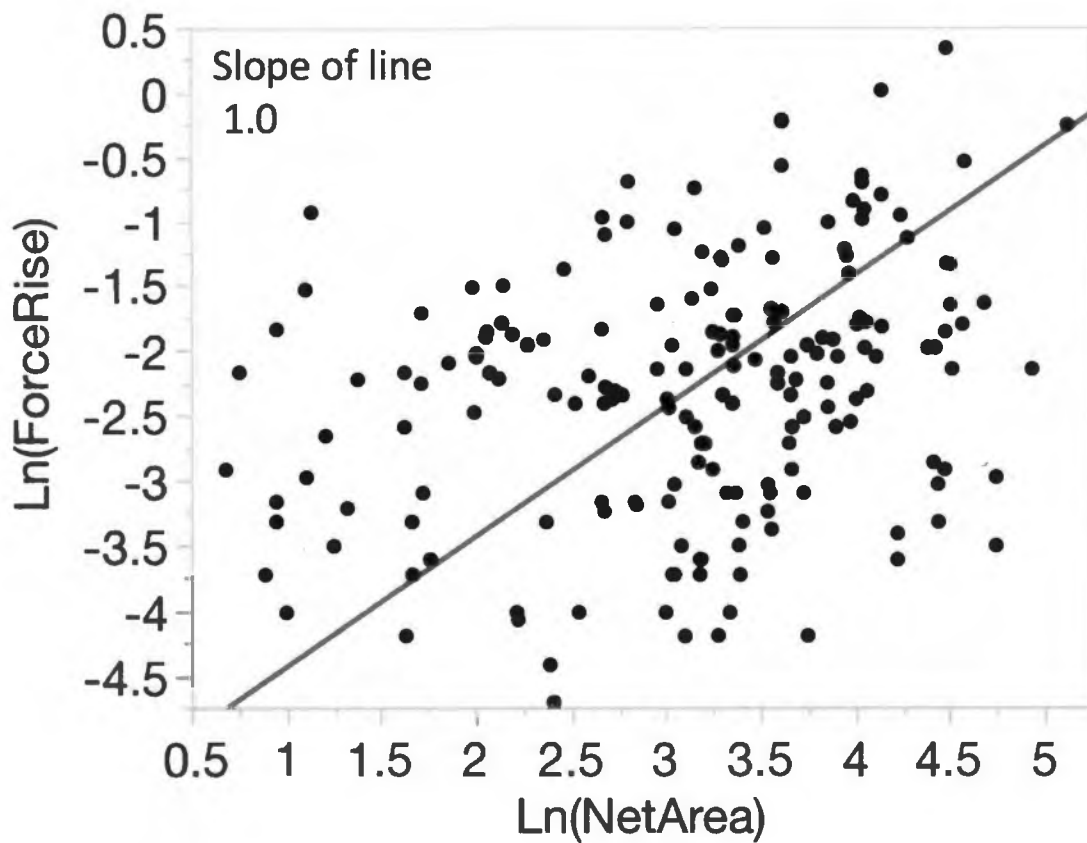


Figure 30) Orthogonal regression with force rise during stretching (N) and Net Area (mm^2). Both axes are log transformed. The red line represents the trend of the data and has a slope of 1. These results show that force rise during stretching positively correlates with buoyant weight.

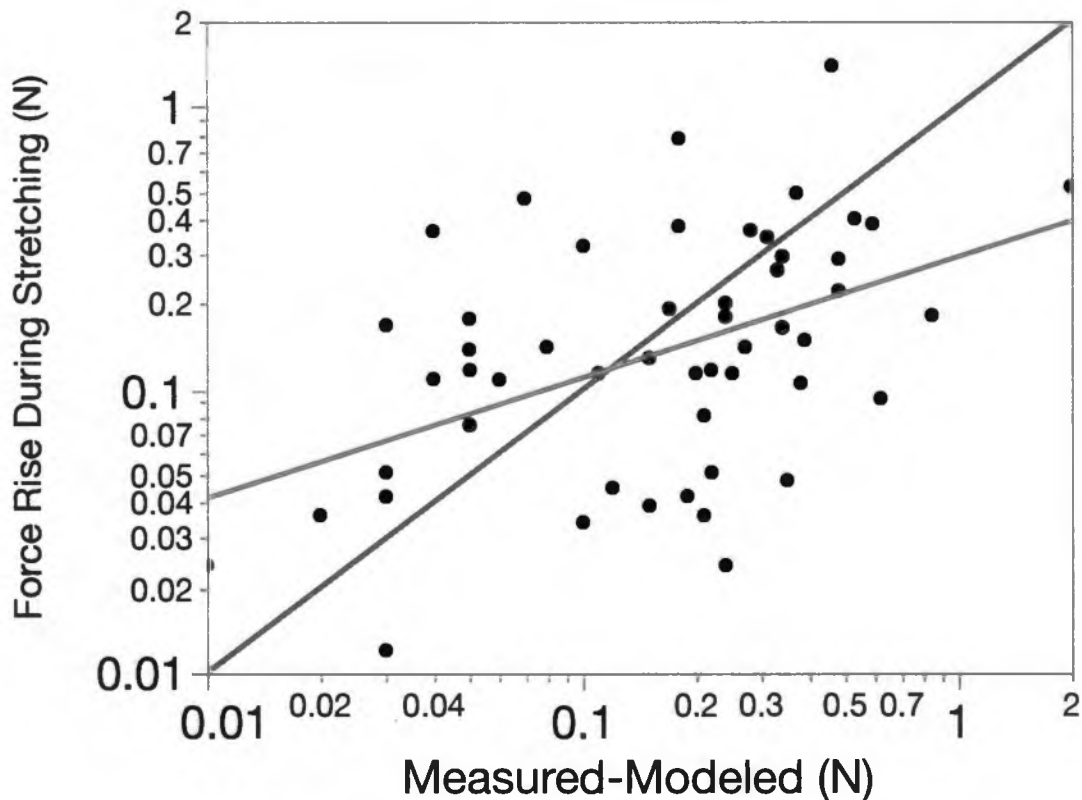


Figure 31) Force rise during stretching (N) and Measured-Modeled (N) comparison. This graph compares force rise during stretching (N) on the y-axis with Measured-Modeled (N) on the x-axis with both axis log transformed. The blue line is a one to one line and the is the trendline for the data. The results show that smaller rocks have higher force rise during stretching (N) values and larger rocks have a smaller force rise during stretching (N) values when compared to Measured-Modeled (N).

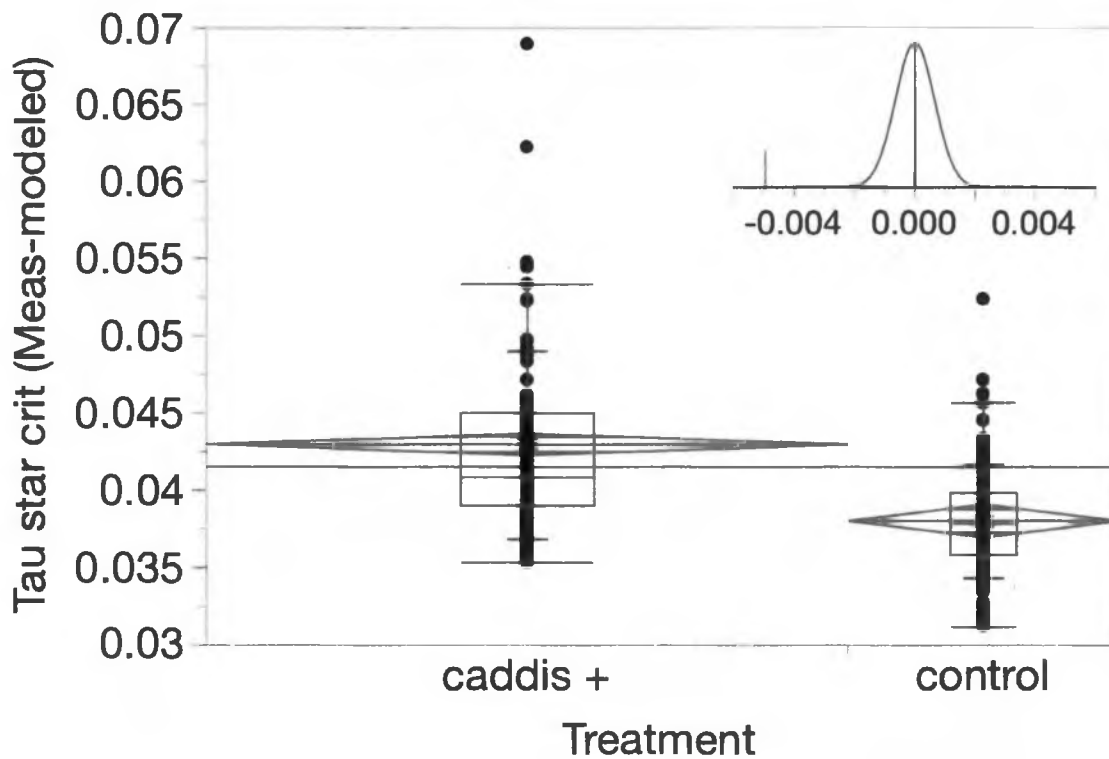


Figure 32) T-test of τ^* (Measured - Modeled) for all rock pulls. This T-test shows a statistically significant increase for caddisfly pulls above controls ($p = 0.0001$).

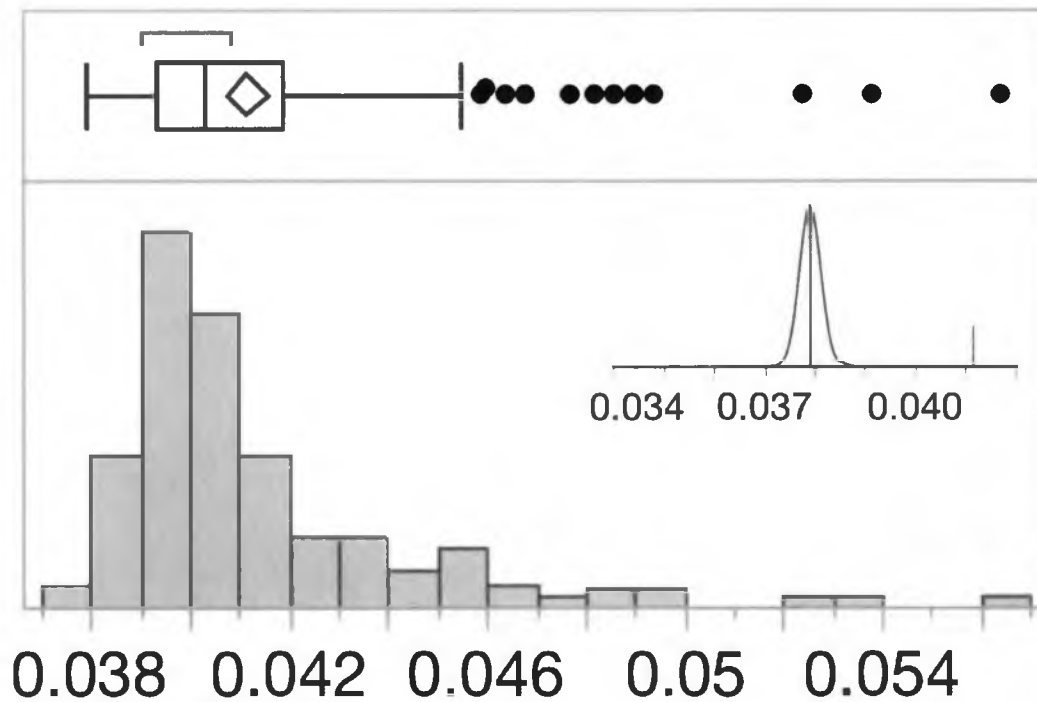


Figure 33) Distribution of τ^* (Force rise during stretching) and hypothetical mean comparison. The mean of the distribution of τ^* (Force rise during stretching) is compared to a hypothesized mean of 0.0379 which is the value the Albertson et al. model calculates without the caddisfly parameter and shows a statistically significant increase for caddisfly pulls ($p=0.0001$).

10.0 APPENDIX

Appendix 1. Raw Peak Force Analysis

Time Block	Flume # Rock #	Treatment	Grain Treatment	Rock Photo #	Weight(g)	Buoyant Weight (N)	Raw Peak Force (N)
1	Flume 1 Rock 1	Control	40	2	139	0.818	1.125
1	Flume 1 Rock 2	Control	40	3	155.4	0.915	1.287
1	Flume 1 Rock 3	Control	40	5	78	0.459	0.696
1	Flume 1 Rock 4	Control	40	6	198.8	1.170	2.400
1	Flume 1 Rock 5	Control	40	7	188.5	1.110	1.992
1	Flume 1 Rock 6	Control	40	11	93.3	0.549	1.305
1	Flume 1 Rock 7	Control	40	12	167.3	0.985	1.293
1	Flume 1 Rock 8	Control	40	13	153	0.901	1.257
1	Flume 10 Rock 1 (lasso slip)	Caddisfly	60	1	193.8	1.141	1.725
1	Flume 10 Rock 2	Caddisfly	60	2	161.3	0.949	2.643
1	Flume 10 Rock 3	Caddisfly	60	3	447.1	2.632	2.820
1	Flume 10 Rock 4	Caddisfly	60	4	321.8	1.894	1.632
1	Flume 10 Rock 5	Caddisfly	60	5	437.6	2.576	2.535
1	Flume 10 Rock 6	Caddisfly	60	6	314.3	1.850	1.977
1	Flume 10 Rock 7	Caddisfly	60	7	322.3	1.897	2.238
1	Flume 10 Rock 8	Caddisfly	60	8	302.9	1.783	2.634
1	Flume 10 Rock 9	Caddisfly	60	9	306.1	1.802	2.280
1	Flume 2 Rock 2	Caddisfly	40	3	137.5	0.809	1.548
1	Flume 2 Rock 3	Caddisfly	40	5	85.7	0.504	1.380
1	Flume 2 Rock 4	Caddisfly	40	6	138.9	0.818	0.897
1	Flume 2 Rock 5	Caddisfly	40	7	103.2	0.607	1.329

Time Block	Flume # Rock #	Treatment	Grain Treatment	Rock Photo #	Weight(g)	Buoyant Weight (N)	Raw Peak Force (N)
1	Flume 2 Rock 6	Caddisfly	40	11	166.7	0.981	3.747
1	Flume 2 Rock 7	Caddisfly	40	12	137.2	0.808	1.185
1	Flume 2 Rock 8	Caddisfly	40	13	99.8	0.587	1.023
1	Flume 3 Rock 1	Caddisfly	55	2	137.2	0.808	1.227
1	Flume 3 Rock 2	Caddisfly	55	1		0.000	0.000
1	Flume 3 Rock 3	Caddisfly	55	5	275.8	1.623	2.253
1	Flume 3 Rock 4	Caddisfly	55	6	193.9	1.141	1.398
1	Flume 3 Rock 5	Caddisfly	55	7	215.3	1.267	2.835
1	Flume 3 Rock 6	Caddisfly	55	11	215.3	1.267	1.110
1	Flume 3 Rock 7	Caddisfly	55	12	249	1.466	1.893
1	Flume 3 Rock 8	Caddisfly	55	13	163.9	0.965	1.836
1	Flume 3 Rock 9	Caddisfly	55	10	143.2	0.843	3.219
1	Flume 4 Rock 1	Control	55	8	181.2	1.067	0.000
1	Flume 4 Rock 2	Control	55	9	182.8	1.076	0.000
1	Flume 4 Rock 3	Control	55	5	277.8	1.635	1.995
1	Flume 4 Rock 4	Control	55	10	186.5	1.098	0.000
1	Flume 4 Rock 5	Control	55	7	188.8	1.111	1.566
1	Flume 4 Rock 6	Control	55	11	310.8	1.829	2.277
1	Flume 4 Rock 7	Control	55	12	202.6	1.193	2.517
1	Flume 4 Rock 8	Control	55	13	166.4	0.979	2.070
1	Flume 5 Rock 1	Caddisfly	30	2	55.9	0.329	0.621
1	Flume 5 Rock 2	Caddisfly	30	3		0.000	0.000
1	Flume 5 Rock 3	Caddisfly	30	4	67.8	0.399	0.528
1	Flume 5 Rock 4	Caddisfly	30	7	66.6	0.392	0.804

Time Block	Flume # Rock #	Treatment	Grain Treatment	Rock Photo #	Weight(g)	Buoyant Weight (N)	Raw Peak Force (N)
1	Flume 5 Rock 5	Caddisfly	30	9	84.9	0.500	0.639
1	Flume 5 Rock 6	Caddisfly	30	10	46.9	0.276	1.227
1	Flume 5 Rock 7	Caddisfly	30	12	57.7	0.340	1.704
1	Flume 5 Rock 8	Caddisfly	30	14	49.2	0.290	0.417
1	Flume 5 Rock 9	Caddisfly	30	13	42.8	0.252	0.309
1	Flume 6 Rock 1	Control	30	2		0.000	0.000
1	Flume 6 Rock 10	Control	30	11	38.1	0.224	0.000
1	Flume 6 Rock 11	Control	30	3	50.3	0.296	0.381
1	Flume 6 Rock 2	Control	30	4	38.2	0.225	0.546
1	Flume 6 Rock 3	Control	30	7		0.000	0.330
1	Flume 6 Rock 4	Control	30	9	50.3	0.296	0.000
1	Flume 6 Rock 5	Control	30	10	82.3	0.484	0.537
1	Flume 6 Rock 6	Control	30	12	75.6	0.445	0.492
1	Flume 6 Rock 7	Control	30	14	96.6	0.569	0.483
1	Flume 6 Rock 8	Control	30	13	49	0.288	0.516
1	Flume 6 Rock 9	Control	30	8		0.000	0.429
1	Flume 7 Rock 1	Control	50			0.000	0.000
1	Flume 7 Rock 10	Control	50	8	207.9	1.224	1.500
1	Flume 7 Rock 11	Control	50	11	212	1.248	2.118
1	Flume 7 Rock 2	Control	50			0.000	0.000
1	Flume 7 Rock 3	Control	50	3	213.6	1.257	1.419
1	Flume 7 Rock 4	Control	50	7	205.4	1.209	2.028
1	Flume 7 Rock 5	Control	50			0.000	0.000
1	Flume 7 Rock 6	Control	50	6	223.5	1.316	1.533

Time Block	Flume # Rock #	Treatment	Grain Treatment	Rock Photo #	Weight(g)	Buoyant Weight (N)	Raw Peak Force (N)
1	Flume 7 Rock 7	Control	50	9	164.4	0.968	1.068
1	Flume 7 Rock 8	Control	50	4	109.8	0.646	1.632
1	Flume 7 Rock 9	Control	50	5	217.2	1.278	2.004
1	Flume 8 Rock 1	Caddisfly	50	1	124.8	0.735	1.200
1	Flume 8 Rock 10	Caddisfly	50	8	193.3	1.138	1.659
1	Flume 8 Rock 11	Caddisfly	50	11	177.5	1.045	1.137
1	Flume 8 Rock 2	Caddisfly	50	2	91.2	0.537	1.983
1	Flume 8 Rock 3	Caddisfly	50	3	78.4	0.461	0.897
1	Flume 8 Rock 4	Caddisfly	50	4	187.8	1.105	2.325
1	Flume 8 Rock 5	Caddisfly	50	5		0.000	0.000
1	Flume 8 Rock 6	Caddisfly	50	6	72.2	0.425	2.139
1	Flume 8 Rock 7	Caddisfly	50	7		0.000	0.000
1	Flume 8 Rock 8	Caddisfly	50	9		0.000	0.000
1	Flume 8 Rock 9	Caddisfly	50	10	125.6	0.739	1.347
1	Flume 9 Rock 1	Control	60	1	186.3	1.097	0.837
1	Flume 9 Rock 2	Control	60	2	250.4	1.474	1.986
1	Flume 9 Rock 3	Control	60	3	334.3	1.968	1.878
1	Flume 9 Rock 4	Control	60	4	316.3	1.862	1.269
1	Flume 9 Rock 5	Control	60	5	476.2	2.803	3.201
1	Flume 9 Rock 6	Control	60	6	206.6	1.216	1.155
1	Flume 9 Rock 7 (tension start)	Control	60	7	401.9	2.366	2.268
1	Flume 9 Rock 8	Control	60	8	377.3	2.221	2.082
1	Flume 9 Rock 9	Control	60	9	330.6	1.946	2.448

Time Block	Flume # Rock #	Treatment	Grain Treatment	Rock Photo #	Weight(g)	Buoyant Weight (N)	Raw Peak Force (N)
2	Flume 1 Rock 1	Caddisfly	55	2	181.5	1.068	1.209
2	Flume 1 Rock 2	Caddisfly	55	3	200.8	1.182	1.755
2	Flume 1 Rock 3	Caddisfly	55	4	258.3	1.520	1.761
2	Flume 1 Rock 4	Caddisfly	55	5	357.7	2.105	3.390
2	Flume 1 Rock 5	Caddisfly	55	6	171	1.007	3.465
2	Flume 1 Rock 6	Caddisfly	55	7	194.1	1.142	1.698
2	Flume 1 Rock 7	Caddisfly	55	8	210.3	1.238	1.881
2	Flume 1 Rock 8	Caddisfly	55	11	238.9	1.406	1.839
2	Flume 10 Rock 1	Caddisfly	30	1	64	0.377	0.765
2	Flume 10 Rock 2	Caddisfly	30	3	62.4	0.367	0.351
2	Flume 10 Rock 3	Caddisfly	30	6	41.1	0.242	0.339
2	Flume 10 Rock 4	Caddisfly	30	8	75.9	0.447	0.471
2	Flume 10 Rock 5	Caddisfly	30	9	54.5	0.321	0.552
2	Flume 10 Rock 6	Caddisfly	30	10	45.2	0.266	0.498
2	Flume 10 Rock 7(Pocket altered by previous pull)	Caddisfly	30	11	48.6	0.286	0.270
2	Flume 10 Rock 8	Caddisfly	30	12	116.7	0.687	0.600
2	Flume 10 Rock 9	Caddisfly	30	2	70.9	0.417	0.510
2	Flume 2 Rock 1	Control	55	2	202.2	1.190	1.290
2	Flume 2 Rock 2	Control	55	3	214.8	1.264	1.647
2	Flume 2 Rock 3	Control	55	4	366.8	2.159	2.358
2	Flume 2 Rock 4	Control	55	5	230	1.354	1.434
2	Flume 2 Rock 5	Control	55	6	401.6	2.364	2.379

Time Block	Flume # Rock #	Treatment	Grain Treatment	Rock Photo #	Weight(g)	Buoyant Weight (N)	Raw Peak Force (N)
2	Flume 2 Rock 6	Control	55	7	287.1	1.690	1.773
2	Flume 2 Rock 7	Control	55	8	355	2.090	2.640
2	Flume 2 Rock 8	Control	55	11	166.9	0.982	4.113
2	Flume 2 Rock 9	Control	55	12	168.4	0.991	1.374
2	Flume 3 Rock 1	Caddisfly	50	2	175.5	1.033	1.857
2	Flume 3 Rock 2	Caddisfly	50	3	139.7	0.822	1.293
2	Flume 3 Rock 3	Caddisfly	50	4	96.2	0.566	1.569
2	Flume 3 Rock 4	Caddisfly	50	5	70.7	0.416	2.328
2	Flume 3 Rock 5	Caddisfly	50	6	197.7	1.164	1.536
2	Flume 3 Rock 6	Caddisfly	50	7	310.7	1.829	2.259
2	Flume 3 Rock 7	Caddisfly	50	8	172.4	1.015	2.796
2	Flume 3 Rock 8	Caddisfly	50	11	141.5	0.833	1.923
2	Flume 4 Rock 1	Control	50	2	215.9	1.271	1.464
2	Flume 4 Rock 2	Control	50	3	214.3	1.261	2.193
2	Flume 4 Rock 3	Control	50	4	175.7	1.034	2.082
2	Flume 4 Rock 4	Control	50	5	176.5	1.039	1.755
2	Flume 4 Rock 5	Control	50	6	301.1	1.772	2.130
2	Flume 4 Rock 6	Control	50	7	240.4	1.415	1.317
2	Flume 4 Rock 7	Control	50	8	122.3	0.720	1.281
2	Flume 4 Rock 8	Control	50	11	275.8	1.623	2.085
2	Flume 5 Rock 1	Control	60	1	490.8	2.889	3.438
2	Flume 5 Rock 2	Control	60	3	243.3	1.432	1.515
2	Flume 5 Rock 3	Control	60	4	228.1	1.343	1.431
2	Flume 5 Rock 4	Control	60	5	352.2	2.073	2.802

Time Block	Flume # Rock #	Treatment	Grain Treatment	Rock Photo #	Weight(g)	Buoyant Weight (N)	Raw Peak Force (N)
2	Flume 5 Rock 5	Control	60	6	284.9	1.677	2.214
2	Flume 5 Rock 6	Control	60	7	302.2	1.779	2.736
2	Flume 5 Rock 7(shifted pocket of downstream rock)	Control	60	8	255.3	1.503	1.527
2	Flume 5 Rock 8	Control	60	9	185.2	1.090	1.449
2	Flume 5 Rock 9	Control	60	10	536.1	3.155	3.438
2	Flume 6 Rock 1	Caddisfly	60	1	320.6	1.887	4.326
2	Flume 6 Rock 10	Caddisfly	60	5	224.1	1.319	1.899
2	Flume 6 Rock 2	Caddisfly	60	3	376.3	2.215	3.471
2	Flume 6 Rock 3	Caddisfly	60	4	317.1	1.866	3.183
2	Flume 6 Rock 4	Caddisfly	60	8	319.2	1.879	3.606
2	Flume 6 Rock 5	Caddisfly	60	9	296.6	1.746	1.758
2	Flume 6 Rock 6	Caddisfly	60	10	231.5	1.363	2.364
2	Flume 6 Rock 7	Caddisfly	60	11		0.000	0.000
2	Flume 6 Rock 8	Caddisfly	60	12		0.000	0.000
2	Flume 6 Rock 9	Caddisfly	60	13	293.7	1.729	3.966
2	Flume 7 Rock 1	Caddisfly	40	1	98.6	0.580	1.245
2	Flume 7 Rock 2	Caddisfly	40	3	172.7	1.017	2.109
2	Flume 7 Rock 3	Caddisfly	40	6	86.3	0.508	1.314
2	Flume 7 Rock 4	Caddisfly	40	4	92.9	0.547	0.915
2	Flume 7 Rock 5	Caddisfly	40	5	104.8	0.617	0.852
2	Flume 7 Rock 6	Caddisfly	40	10	143.4	0.844	0.756
2	Flume 7 Rock 7	Caddisfly	40	11	143.9	0.847	1.398

Time Block	Flume # Rock #	Treatment	Grain Treatment	Rock Photo #	Weight(g)	Buoyant Weight (N)	Raw Peak Force (N)
2	Flume 7 Rock 8	Caddisfly	40	12	88	0.518	0.450
2	Flume 8 Rock 1	Control	40	1	114.1	0.672	0.720
2	Flume 8 Rock 10	Control	40	7	107	0.630	1.611
2	Flume 8 Rock 2 (use first peak)	Control	40	3	165	0.971	1.281
2	Flume 8 Rock 3	Control	40	6	108.2	0.637	1.146
2	Flume 8 Rock 4	Control	40	8	106.1	0.625	1.137
2	Flume 8 Rock 5	Control	40	9	109.8	0.646	1.014
2	Flume 8 Rock 6	Control	40	10	236.3	1.391	NaN
2	Flume 8 Rock 7 (started with wire tension)	Control	40	11	134.7	0.793	0.645
2	Flume 8 Rock 8	Control	40	2	249.6	1.469	1.341
2	Flume 8 Rock 9	Control	40	5	153.3	0.902	1.317
2	Flume 9 Rock 1	Control	30	1	62.4	0.367	0.588
2	Flume 9 Rock 2	Control	30	3	78.4	0.461	0.486
2	Flume 9 Rock 3	Control	30	6	66	0.388	0.555
2	Flume 9 Rock 4	Control	30	8	63.8	0.376	0.582
2	Flume 9 Rock 5	Control	30	9	49.8	0.293	0.489
2	Flume 9 Rock 6	Control	30	10	87.5	0.515	0.645
2	Flume 9 Rock 7	Control	30	11	75.2	0.443	0.678
2	Flume 9 Rock 8	Control	30	5	101.2	0.596	0.678
3	Flume 1 Rock 1	Caddisfly	60	1	226.8	1.335	2.118
3	Flume 1 Rock 2	Caddisfly	60	3	450.7	2.653	2.211
3	Flume 1 Rock 3	Caddisfly	60	6	465.6	2.741	2.586

Time Block	Flume # Rock #	Treatment	Grain Treatment	Rock Photo #	Weight(g)	Buoyant Weight (N)	Raw Peak Force (N)
3	Flume 1 Rock 4	Caddisfly	60	8	329	1.936	1.683
3	Flume 1 Rock 5	Caddisfly	60	9	479.6	2.823	3.288
3	Flume 1 Rock 6	Caddisfly	60	10	420.3	2.474	2.865
3	Flume 1 Rock 7	Caddisfly	60	11	195	1.148	1.947
3	Flume 1 Rock 8	Caddisfly	60	12	190.7	1.122	1.326
3	Flume 10 Rock 1	Caddisfly	50	1	193.2	1.137	2.259
3	Flume 10 Rock 2	Caddisfly	50	3	390.9	2.301	2.022
3	Flume 10 Rock 3	Caddisfly	50	4	236.2	1.390	1.413
3	Flume 10 Rock 4	Caddisfly	50	6	215	1.265	2.583
3	Flume 10 Rock 5	Caddisfly	50	8	178.1	1.048	1.866
3	Flume 10 Rock 6	Caddisfly	50	9	184.5	1.086	1.323
3	Flume 10 Rock 7	Caddisfly	50	10	308.5	1.816	2.565
3	Flume 10 Rock 8(Epoxy Failure)	Caddisfly	50	11		0.000	NaN
3	Flume 10 Rock 9)	Caddisfly	50	5	102.2	0.602	1.641
3	Flume 2 Rock 1	Control	60	1	251.6	1.481	2.670
3	Flume 2 Rock 2	Control	60	3	261.2	1.537	1.764
3	Flume 2 Rock 3	Control	60	6	432	2.543	3.516
3	Flume 2 Rock 4	Control	60	8	360.9	2.124	2.010
3	Flume 2 Rock 5	Control	60	9	288.8	1.700	2.031
3	Flume 2 Rock 6	Control	60	10	385.6	2.270	4.860
3	Flume 2 Rock 7	Control	60	11	357.9	2.107	3.084
3	Flume 2 Rock 8	Control	60	4	187.7	1.105	1.338
3	Flume 3 Rock 1	Caddisfly	30	1	67.8	0.399	0.450

Time Block	Flume # Rock #	Treatment	Grain Treatment	Rock Photo #	Weight(g)	Buoyant Weight (N)	Raw Peak Force (N)
3	Flume 3 Rock 2	Caddisfly	30	3	69.7	0.410	0.417
3	Flume 3 Rock 3	Caddisfly	30	6	62.2	0.366	0.546
3	Flume 3 Rock 4	Caddisfly	30	8	30.5	0.180	0.435
3	Flume 3 Rock 5	Caddisfly	30	9	39.5	0.232	0.192
3	Flume 3 Rock 6	Caddisfly	30	10	45.3	0.267	0.291
3	Flume 3 Rock 7	Caddisfly	30	11	69	0.406	0.633
3	Flume 3 Rock 8	Caddisfly	30	4	48.5	0.285	0.441
3	Flume 4 Rock 1(epoxy fail)	Control	30	1		0.000	NaN
3	Flume 4 Rock 10	Control	30	3	47.3	0.278	0.531
3	Flume 4 Rock 11	Control	30	4	35.8	0.211	0.486
3	Flume 4 Rock 2	Control	30	6	78.7	0.463	0.285
3	Flume 4 Rock 3	Control	30	8		0.000	0.306
3	Flume 4 Rock 4	Control	30	9		0.000	0.561
3	Flume 4 Rock 5(Lasso slip)	Control	30	10	60.9	0.358	NaN
3	Flume 4 Rock 6(epoxy fail)	Control	30	11	71.9	0.423	NaN
3	Flume 4 Rock 7	Control	30	2	70.6	0.416	0.309
3	Flume 4 Rock 8	Control	30	5	91	0.536	0.528
3	Flume 4 Rock 9	Control	30	7	60.1	0.354	0.357
3	Flume 5 Rock 1	Control	40	1	114.8	0.676	0.819
3	Flume 5 Rock 2	Control	40	3	103.4	0.609	0.714
3	Flume 5 Rock 3	Control	40	4	96.8	0.570	0.741
3	Flume 5 Rock 4	Control	40	6	109.7	0.646	0.591

Time Block	Flume # Rock #	Treatment	Grain Treatment	Rock Photo #	Weight(g)	Buoyant Weight (N)	Raw Peak Force (N)
3	Flume 5 Rock 5	Control	40	8	73.3	0.431	0.630
3	Flume 5 Rock 6	Control	40	9	110.3	0.649	1.158
3	Flume 5 Rock 7	Control	40	10	132.4	0.779	0.903
3	Flume 5 Rock 8	Control	40	11	139.7	0.822	0.876
3	Flume 6 Rock 1	Caddisfly	40	1	122	0.718	1.107
3	Flume 6 Rock 2	Caddisfly	40	3	118.5	0.697	1.056
3	Flume 6 Rock 3	Caddisfly	40	4	169.4	0.997	1.077
3	Flume 6 Rock 4	Caddisfly	40	6	87.9	0.517	1.029
3	Flume 6 Rock 5	Caddisfly	40	8	127.2	0.749	0.948
3	Flume 6 Rock 6	Caddisfly	40	9	70.8	0.417	1.002
3	Flume 6 Rock 7	Caddisfly	40	10	89.7	0.528	0.471
3	Flume 6 Rock 8	Caddisfly	40	11	100.9	0.594	1.050
3	Flume 7 Rock 1	Caddisfly	55	1	225.6	1.328	1.860
3	Flume 7 Rock 2	Caddisfly	55	3	226.2	1.331	1.929
3	Flume 7 Rock 3	Caddisfly	55	4	217.9	1.283	1.515
3	Flume 7 Rock 4	Caddisfly	55	6	180.8	1.064	1.914
3	Flume 7 Rock 5	Caddisfly	55	8	239.9	1.412	2.502
3	Flume 7 Rock 6	Caddisfly	55	9	337.6	1.987	2.976
3	Flume 7 Rock 7	Caddisfly	55	10	292	1.719	2.217
3	Flume 7 Rock 8	Caddisfly	55	11	432.8	2.547	2.901
3	Flume 8 Rock 1	Control	55	1	257.5	1.516	1.887
3	Flume 8 Rock 2	Control	55	3	73.3	0.431	0.417
3	Flume 8 Rock 3	Control	55	4	358.4	2.110	2.835
3	Flume 8 Rock 4	Control	55	6	132	0.777	1.602

Time Block	Flume # Rock #	Treatment	Grain Treatment	Rock Photo #	Weight(g)	Buoyant Weight (N)	Raw Peak Force (N)
3	Flume 8 Rock 5	Control	55	8	199	1.171	3.756
3	Flume 8 Rock 6	Control	55	9	424.9	2.501	3.219
3	Flume 8 Rock 7	Control	55	10	321.7	1.894	2.805
3	Flume 8 Rock 8	Control	55	11	251	1.477	1.356
3	Flume 9 Rock 1	Control	50	1	268.1	1.578	1.746
3	Flume 9 Rock 2	Control	50	3	200.2	1.178	0.960
3	Flume 9 Rock 3	Control	50	4	299.7	1.764	3.270
3	Flume 9 Rock 4	Control	50	6	199.5	1.174	1.272
3	Flume 9 Rock 5	Control	50	8	291.5	1.716	1.650
3	Flume 9 Rock 6	Control	50	9	169.5	0.998	1.074
3	Flume 9 Rock 7	Control	50	10	114.4	0.673	1.428
3	Flume 9 Rock 8	Control	50	11	255.2	1.502	1.452
4	Flume 1 Rock 1	Caddisfly	60	1	295.6	1.740	1.494
4	Flume 1 Rock 2	Caddisfly	60	2	228.8	1.347	2.457
4	Flume 1 Rock 3	Caddisfly	60	4	147.9	0.871	1.281
4	Flume 1 Rock 4	Caddisfly	60	5	358.7	2.111	2.763
4	Flume 1 Rock 5	Caddisfly	60	6	366.3	2.156	2.295
4	Flume 1 Rock 6	Caddisfly	60	7	250.8	1.476	4.971
4	Flume 1 Rock 7	Caddisfly	60	9	256.4	1.509	1.584
4	Flume 1 Rock 8	Caddisfly	60	10	284.7	1.676	1.527
4	Flume 10 Rock 1	Caddisfly	40	1	103.4	0.609	0.717
4	Flume 10 Rock 2	Caddisfly	40	2	73.1	0.430	0.393
4	Flume 10 Rock 3	Caddisfly	40	4	105.1	0.619	0.723
4	Flume 10 Rock 4	Caddisfly	40	5	60.6	0.357	0.288

Time Block	Flume # Rock #	Treatment	Grain Treatment	Rock Photo #	Weight(g)	Buoyant Weight (N)	Raw Peak Force (N)
4	Flume 10 Rock 5	Caddisfly	40	6	194.2	1.143	1.383
4	Flume 10 Rock 6	Caddisfly	40	7	85.3	0.502	0.516
4	Flume 10 Rock 7	Caddisfly	40	9	325.9	1.918	2.352
4	Flume 10 Rock 8	Caddisfly	40	10	125.7	0.740	1.089
4	Flume 2 Rock 1	Control	60	1	259.2	1.526	2.337
4	Flume 2 Rock 2	Control	60	2	238.2	1.402	2.313
4	Flume 2 Rock 3	Control	60	4	216.8	1.276	1.539
4	Flume 2 Rock 4	Control	60	5	271.8	1.600	4.128
4	Flume 2 Rock 5	Control	60	6	220.3	1.297	1.116
4	Flume 2 Rock 6	Control	60	7	432.3	2.545	2.400
4	Flume 2 Rock 7	Control	60	9	316.3	1.862	4.446
4	Flume 2 Rock 8	Control	60	10	392.1	2.308	2.253
4	Flume 3 Rock 1	Control	50	1	144.8	0.852	1.830
4	Flume 3 Rock 2	Control	50	2	213.7	1.258	1.386
4	Flume 3 Rock 3	Control	50	4	250.1	1.472	1.374
4	Flume 3 Rock 4	Control	50	5	282.1	1.660	1.998
4	Flume 3 Rock 5	Control	50	6	83.2	0.490	1.038
4	Flume 3 Rock 6	Control	50	7	308.8	1.818	2.619
4	Flume 3 Rock 7	Control	50	9	29.4	0.173	1.104
4	Flume 3 Rock 8	Control	50	10	118.4	0.697	1.410
4	Flume 4 Rock 1	Caddisfly	50	1	276.7	1.629	1.590
4	Flume 4 Rock 2	Caddisfly	50	2	159.6	0.939	1.215
4	Flume 4 Rock 3	Caddisfly	50	4	235	1.383	1.464
4	Flume 4 Rock 4	Caddisfly	50	5	258.9	1.524	1.710

Time Block	Flume # Rock #	Treatment	Grain Treatment	Rock Photo #	Weight(g)	Buoyant Weight (N)	Raw Peak Force (N)
4	Flume 4 Rock 5	Caddisfly	50	6	132.2	0.778	0.642
4	Flume 4 Rock 6	Caddisfly	50	7	144.4	0.850	0.972
4	Flume 4 Rock 7	Caddisfly	50	9	157.3	0.926	2.829
4	Flume 4 Rock 8	Caddisfly	50	10	266.5	1.569	1.965
4	Flume 5 Rock 1	Caddisfly	30	1	46.4	0.273	0.546
4	Flume 5 Rock 2	Caddisfly	30	2	73.6	0.433	0.525
4	Flume 5 Rock 3	Caddisfly	30	4	103.8	0.611	0.924
4	Flume 5 Rock 4	Caddisfly	30	5	47.7	0.281	0.423
4	Flume 5 Rock 5	Caddisfly	30	6	35.9	0.211	0.918
4	Flume 5 Rock 6	Caddisfly	30	7	34.8	0.205	0.234
4	Flume 5 Rock 7	Caddisfly	30	9	75.1	0.442	0.741
4	Flume 5 Rock 8	Caddisfly	30	10	40.6	0.239	0.507
4	Flume 6 Rock 1	Control	30	1	78.1	0.460	0.384
4	Flume 6 Rock 2	Control	30	2	86.7	0.510	0.534
4	Flume 6 Rock 3	Control	30	4	60	0.353	0.420
4	Flume 6 Rock 4	Control	30	5	74.8	0.440	0.672
4	Flume 6 Rock 5	Control	30	6	58.1	0.342	0.441
4	Flume 6 Rock 6	Control	30	7		0.000	NaN
4	Flume 6 Rock 7	Control	30	9	55.6	0.327	0.234
4	Flume 6 Rock 8	Control	30	10	77.4	0.456	0.987
4	Flume 6 Rock 9	Control	30	11	101.3	0.596	0.645
4	Flume 7 Rock 1	Caddisfly	55	1	157.6	0.928	0.828
4	Flume 7 Rock 2	Caddisfly	55	2	320.1	1.884	2.031
4	Flume 7 Rock 3	Caddisfly	55	4	271.6	1.599	1.731

Time Block	Flume # Rock #	Treatment	Grain Treatment	Rock Photo #	Weight(g)	Buoyant Weight (N)	Raw Peak Force (N)
4	Flume 7 Rock 4	Caddisfly	55	5	264.8	1.559	1.980
4	Flume 7 Rock 5	Caddisfly	55	6	217.4	1.280	3.003
4	Flume 7 Rock 6	Caddisfly	55	7	213.5	1.257	3.336
4	Flume 7 Rock 7 (lasso slid along hook)	Caddisfly	55	9	287.3	1.691	2.013
4	Flume 7 Rock 8	Caddisfly	55	10	219.2	1.290	1.800
4	Flume 7 Rock 9	Caddisfly	55	3	189.3	1.114	1.830
4	Flume 8 Rock 1	Control	55	1	280.6	1.652	1.959
4	Flume 8 Rock 10	Control	55	10	291.1	1.713	1.692
4	Flume 8 Rock 2	Control	55	2	267.8	1.576	1.650
4	Flume 8 Rock 3	Control	55	3	279.4	1.645	1.647
4	Flume 8 Rock 4	Control	55	4	255.6	1.504	1.917
4	Flume 8 Rock 5	Control	55	5	epoxy fail	#####	NaN
4	Flume 8 Rock 6	Control	55	6	122.7	0.722	2.706
4	Flume 8 Rock 7	Control	55	7	epoxy fail	#####	NaN
4	Flume 8 Rock 8	Control	55	8	194.4	1.144	3.291
4	Flume 8 Rock 9	Control	55	9	213.9	1.259	2.241
4	Flume 9 Rock 1	Control	40	1	177.4	1.044	1.035
4	Flume 9 Rock 2	Control	40	2	150.7	0.887	1.026
4	Flume 9 Rock 3	Control	40	4	141.6	0.833	0.636
4	Flume 9 Rock 4	Control	40	5	111.9	0.659	0.609
4	Flume 9 Rock 5	Control	40	6	83.9	0.494	0.558

Time Block	Flume # Rock #	Treatment	Grain Treatment	Rock Photo #	Weight(g)	Buoyant Weight (N)	Raw Peak Force (N)
4	Flume 9 Rock 6	Control	40	7	196.4	1.156	0.945
4	Flume 9 Rock 7	Control	40	9	99	0.583	1.080
4	Flume 9 Rock 8	Control	40	11	99.9	0.588	0.591
5	Flume 1 Rock 1	Caddisfly	50	1	99.3	0.584	0.684
5	Flume 1 Rock 2	Caddisfly	50	2	182.1	1.072	1.038
5	Flume 1 Rock 3	Caddisfly	50	3	366.1	2.155	1.971
5	Flume 1 Rock 4	Caddisfly	50	4	204.4	1.203	1.971
5	Flume 1 Rock 5	Caddisfly	50	6	223.6	1.316	2.652
5	Flume 1 Rock 6	Caddisfly	50	7	223	1.313	1.440
5	Flume 1 Rock 7	Caddisfly	50	9	201.4	1.185	1.275
5	Flume 1 Rock 8	Caddisfly	50	10	111.7	0.657	1.782
5	Flume 10 Rock 1	Caddisfly	60	1	388	2.284	2.004
5	Flume 10 Rock 2	Caddisfly	60	2	448.9	2.642	4.053
5	Flume 10 Rock 3	Caddisfly	60	3	166	0.977	1.929
5	Flume 10 Rock 4	Caddisfly	60	4	326.3	1.921	2.052
5	Flume 10 Rock 5	Caddisfly	60	6	293.5	1.728	NaN
5	Flume 10 Rock 6	Caddisfly	60	7	383	2.254	1.956
5	Flume 10 Rock 7	Caddisfly	60	8	251.7	1.482	1.326
5	Flume 10 Rock 8	Caddisfly	60	11	374	2.201	3.831
5	Flume 10 Rock 9	Caddisfly	60	5	376	2.213	1.980
5	Flume 2 Rock 1	Control	50	1	129.2	0.760	3.414
5	Flume 2 Rock 2	Control	50	2	261.2	1.537	1.275
5	Flume 2 Rock 3	Control	50	3	217.5	1.280	1.992
5	Flume 2 Rock 4	Control	50	4	184.4	1.085	1.902

Time Block	Flume # Rock #	Treatment	Grain Treatment	Rock Photo #	Weight(g)	Buoyant Weight (N)	Raw Peak Force (N)
5	Flume 2 Rock 5	Control	50	6	133.6	0.786	1.065
5	Flume 2 Rock 6	Control	50	7	277.5	1.633	1.389
5	Flume 2 Rock 7	Control	50	8	203.8	1.200	1.350
5	Flume 2 Rock 8	Control	50	10	176.3	1.038	1.014
5	Flume 3 Rock 1	Control	40	11	102.3	0.602	0.918
5	Flume 3 Rock 2	Control	40	8	140.9	0.829	0.825
5	Flume 3 Rock 3	Control	40	7	155.4	0.915	1.407
5	Flume 3 Rock 4	Control	40	6	102.2	0.602	0.843
5	Flume 3 Rock 5	Control	40	4	84.5	0.497	0.564
5	Flume 3 Rock 6	Control	40	3	111	0.653	0.507
5	Flume 3 Rock 7	Control	40	2	146.1	0.860	0.858
5	Flume 3 Rock 8	Control	40	1	90.7	0.534	0.909
5	Flume 4 Rock 1	Caddisfly	40	1	99.9	0.588	0.513
5	Flume 4 Rock 2	Caddisfly	40	2	100.1	0.589	0.684
5	Flume 4 Rock 3	Caddisfly	40	3	58.5	0.344	0.543
5	Flume 4 Rock 4	Caddisfly	40	4	112.1	0.660	0.558
5	Flume 4 Rock 5	Caddisfly	40	6	72.3	0.426	0.459
5	Flume 4 Rock 6	Caddisfly	40	7	91	0.536	0.951
5	Flume 4 Rock 7	Caddisfly	40	8	100.7	0.593	0.705
5	Flume 4 Rock 8	Caddisfly	40	11	74.5	0.439	0.444
5	Flume 4 Rock 9	Caddisfly	40	12	103.6	0.610	1.434
5	Flume 5 Rock 1	Control	55	1	56.1	0.330	0.381
5	Flume 5 Rock 2	Control	55	2	237.9	1.400	1.266
5	Flume 5 Rock 3	Control	55	3	169.8	0.999	0.933

Time Block	Flume # Rock #	Treatment	Grain Treatment	Rock Photo #	Weight(g)	Buoyant Weight (N)	Raw Peak Force (N)
5	Flume 5 Rock 4	Control	55	4	160.5	0.945	1.563
5	Flume 5 Rock 5	Control	55	6	179.4	1.056	0.879
5	Flume 5 Rock 6	Control	55	7	157	0.924	1.752
5	Flume 5 Rock 7	Control	55	8	213.1	1.254	2.355
5	Flume 5 Rock 8	Control	55	11	223.2	1.314	1.458
5	Flume 6 Rock 1	Caddisfly	55	1	263.9	1.553	1.344
5	Flume 6 Rock 2	Caddisfly	55	2	161.1	0.948	0.801
5	Flume 6 Rock 3	Caddisfly	55	3	148.5	0.874	0.996
5	Flume 6 Rock 4	Caddisfly	55	4	234.4	1.380	1.950
5	Flume 6 Rock 5	Caddisfly	55	6	203.5	1.198	1.464
5	Flume 6 Rock 6	Caddisfly	55	7	383.5	2.257	3.438
5	Flume 6 Rock 7	Caddisfly	55	8	186.8	1.100	1.329
5	Flume 6 Rock 8	Caddisfly	55	11	184.5	1.086	1.746
5	Flume 7 Rock 1	Control	30	1	41.3	0.243	0.405
5	Flume 7 Rock 2	Control	30	2	78	0.459	0.435
5	Flume 7 Rock 3	Control	30	3	52	0.306	0.306
5	Flume 7 Rock 4	Control	30	4	64	0.377	1.266
5	Flume 7 Rock 5	Control	30	6	50.9	0.300	0.417
5	Flume 7 Rock 6	Control	30	7	124.8	0.735	0.768
5	Flume 7 Rock 7	Control	30	8	60.9	0.358	0.279
5	Flume 7 Rock 8	Control	30	11	63.5	0.374	0.318
5	Flume 7 Rock 9	Control	30	5	30.5	0.180	0.213
5	Flume 8 Rock 1	Caddisfly	30	1	40.2	0.237	0.309
5	Flume 8 Rock 2	Caddisfly	30	2	110.3	0.649	0.651

Time Block	Flume # Rock #	Treatment	Grain Treatment	Rock Photo #	Weight(g)	Buoyant Weight (N)	Raw Peak Force (N)
5	Flume 8 Rock 3	Caddisfly	30	3	58.1	0.342	0.468
5	Flume 8 Rock 4	Caddisfly	30	4	64.8	0.381	0.399
5	Flume 8 Rock 5	Caddisfly	30	6	57.9	0.341	0.456
5	Flume 8 Rock 6	Caddisfly	30	7	63.7	0.375	0.540
5	Flume 8 Rock 7	Caddisfly	30	8	56.4	0.332	0.240
5	Flume 8 Rock 8	Caddisfly	30	11	41.1	0.242	0.240
5	Flume 9 Rock 1	Control	60	1	258.1	1.519	1.776
5	Flume 9 Rock 2	Control	60	2	350.7	2.064	2.487
5	Flume 9 Rock 3	Control	60	3	231.9	1.365	1.800
5	Flume 9 Rock 4 (loose pocket)	Control	60	4	351.8	2.071	3.654
5	Flume 9 Rock 5	Control	60	6	509.9	3.001	4.707
5	Flume 9 Rock 6	Control	60	7	256	1.507	2.037
5	Flume 9 Rock 7	Control	60	8	251	1.477	1.452
5	Flume 9 Rock 8	Control	60	11	381.8	2.247	3.492
5	Flume 9 Rock 9	Control	60	9	279.9	1.647	1.716

Appendix 2. Table Measured Versus Modeled

Block	Flume	Treatment	Grain Size Bin	Rock pull	Buoyant Weight (N)	B-axis (mm)	Notes	Difference in Force (N)	Normalized Difference	PHI (Friction Angle) in degrees
3	1	caddis +	60	1	1.45	54.34		1.14	1.16	22.48
3	1	caddis +	60	2	2.88	58.74		0.27	0.14	22.48
3	1	caddis +	60	3	2.97	66.86		0.33	0.15	28.89
3	1	caddis +	60	3	2.97	66.86		0.33	0.15	28.89
3	1	caddis +	60	4	2.10	67.25		0.26	0.19	22.48
3	1	caddis +	60	5	3.06	66.64	rock pushed downstream rock out of the way, and climbed halfway over, tilted and went off to the side between 20-29 sec in match-up, picked peak force before then	0.34	0.12	44.00
3	1	caddis +	60	5	3.06	66.64	rock pushed downstream rock out of the way, did not climb over	0.34	0.12	44.00
3	1	caddis +	60	6	2.68	64.55		0.28	0.11	44.00
3	1	caddis +	60	6	2.68	64.55		0.28	0.11	44.00
3	1	caddis +	60	6	2.68	64.55		0.28	0.11	44.00
3	1	caddis +	60	6	2.68	64.55		0.28	0.11	44.00
3	1	caddis +	60	6	2.68	64.55		0.28	0.11	44.00
3	1	caddis +	60	7	1.24	62.05	lifted back rock drops at 8 sec	0.22	0.30	15.42
3	1	caddis +	60	8	1.22	63.74	rock rotates to vertical	0.31	0.31	34.60

Block	Flume	Treatment	Grain Size Bin	Rock pull	Buoyant Weight (N)	B-axis (mm)	Notes	Difference in Force (N)	Normalized Difference	PHI (Friction Angle) in degrees
3	2	control	60	1	1.61	63.10	interference 14-17 sec in vid. rock on side being lifted drops at 18 sec. peak force taken after 18 sec	0.10	0.08	33.46
3	2	control	60	2	1.67	74.44	starts moving over second ds rock at 20 sec	0.05	0.04	32.87
3	2	control	60	3	2.76	60.38	from beginning of pull 16-21 sec overlapping back rock	1.08	0.44	38.42
3	2	control	60	4	2.30	65.80	toggles at first movement picked peak before rock rolls to side	0.15	0.08	32.87
3	2	control	60	5	1.84	62.50		0.09	0.05	49.95
3	2	control	60	6	2.46	68.36	from beginning of pull 10 -12 sec, back rock being lifted drops after 13 sec. chose peak force after 13 sec	0.07	0.03	46.60
3	2	control	60	7	2.28	70.44	snagged under side rock from 10 to 16 secs	0.04	0.02	52.89
3	2	control	60	8	1.20	65.14	jumps then lifts front rock from 10 to 15 sec	0.02	0.02	21.63
3	3	caddis +	30	1	0.43	35.43		0.11	0.33	21.75
3	3	caddis +	30	2	0.44	33.89		0.00	-0.01	33.62
3	3	caddis +	30	3	0.40	35.21	pull starts at 6 sec. side rock drops at 8 sec	0.11	0.26	42.94

Block	Flume	Treatment	Grain Size Bin	Rock pull	Buoyant Weight (N)	B-axis (mm)	Notes	Difference in Force (N)	Normalized Difference	PHI (Friction Angle) in degrees
3	3	caddis +	30	3	0.40	35.21	pull starts at 6 sec. side rock drops at 8 sec	0.11	0.26	42.94
3	3	caddis +	30	3	0.40	35.21	pull starts at 6 sec. side rock drops at 8 sec	0.11	0.26	42.94
3	3	caddis +	30	4	0.19	27.37		0.22	1.05	42.94
3	3	caddis +	30	4	0.19	27.37	strong net attached; moves attached rock	0.22	1.06	42.94
3	3	caddis +	30	4	0.19	27.37	strong net attached; moves attached rock	0.22	1.06	42.94
3	3	caddis +	30	4	0.19	27.37	strong net attached; moves attached rock	0.22	1.06	42.94
3	3	caddis +	30	5	0.25	35.20		-0.03	-0.12	28.01
3	3	caddis +	30	5	0.25	35.20		-0.03	-0.12	28.01
3	3	caddis +	30	5	0.25	35.20		-0.03	-0.12	28.01
3	3	caddis +	30	6	0.29	36.25		0.04	0.16	28.01
3	3	caddis +	30	6	0.29	36.25		0.04	0.16	28.01
3	3	caddis +	30	7	0.44	37.05		0.16	0.31	46.77
3	3	caddis +	30	8	0.31	36.42	pull starts at 5 sec. front rock lifts at 8 sec. rock drops at 10 sec. picked peak after rock drop	0.10	0.28	42.94
3	4	control	30	1	0.00				#DIV/0!	32.92
3	4	control	30	2	0.30	33.52		0.02	0.06	29.97
3	4	control	30	3	0.23	32.31	rock drops at 6-7 sec	0.02	0.07	37.84
3	4	control	30	4	0.50	39.82	rock ds lifts up after 16 sec	0.02	0.03	35.38
3	4	control	30	5	0.00			#DIV/0!	#DIV/0!	

Block	Flume	Treatment	Grain Size Bin	Rock pull	Buoyant Weight (N)	B-axis (mm)	Notes	Difference in Force (N)	Normalized Difference	PHI (Friction Angle) in degrees
3	4	control	30	6	0.00			#DIV/0!	#DIV/0!	
3	4	control	30	7	0.39	48.06	rock being lifted	-0.08	-0.21	32.92
3	4	control	30	8	0.46	31.39	drops after 5 sec pull starts at 10 sec. front rock lifts at 12 rock drops at 16 sec. picked peak after rock drop	-0.05	-0.11	42.18
3	4	control	30	9	0.45	38.07	side rock lifts at 9 sec and drops at 13	-0.02	-0.05	25.39
3	4	control	30	10	0.58	41.89	lifts rock at 12 drops at 13 sec	0.03	0.07	19.78
3	4	control	30	11	0.38	39.95		0.10	0.25	38.31
3	5	control	40	1	0.73	48.82	pull starts at 6 sec. front rock lifts at 12 rock drops at 15 sec. picked peak after rock drop	-0.10	-0.15	34.60
3	5	control	40	2	0.66	49.82	rock rotates vertical before being lifted out	-0.06	-0.07	47.51
3	5	control	40	3	0.62	43.73	picked highest force before downstream rock lifted up by pull after 10 sec.	-0.16	-0.25	42.18
3	5	control	40	4	0.70	46.04	lifts rock up at 13 sec drops at 15 sec. picked force before 13 sec	-0.01	-0.02	27.50
3	5	control	40	5	0.47	45.89	side rock drops at 15 sec	-0.04	-0.06	47.82
3	5	control	40	6	0.70	45.51	experiencing interference the whole time			

Block	Flume	Treatment	Grain Size Bin	Rock pull	Buoyant Weight (N)	B-axis (mm)	Notes	Difference in Force (N)	Normalized Difference	PHI (Friction Angle) in degrees
3	5	control	40	7	0.84	46.41	rock is jolted out of stuck position at beginning of pull.	-0.26	-0.23	57.64
3	5	control	40	8	0.89	53.68		-0.28	-0.24	54.18
3	6	caddis +	40	1	0.78	42.42	pull starts at 5 sec. side rock drops at 9 sec	0.20	0.31	26.37
3	6	caddis +	40	2	0.76	43.41		0.42	0.65	26.37
3	6	caddis +	40	3	1.08	55.84		0.08	0.08	31.79
3	6	caddis +	40	3	1.08	55.84		0.08	0.08	31.79
3	6	caddis +	40	3	1.08	55.84		0.08	0.08	31.79
3	6	caddis +	40	4	0.56	41.44	pull starts at 9 sec. moves out of way of side rock at 11 sec	0.38	0.80	26.37
3	6	caddis +	40	5	0.81	47.63		0.20	0.27	31.79
3	6	caddis +	40	5	0.81	47.63		0.20	0.27	31.79
3	6	caddis +	40	5	0.81	47.63		0.20	0.27	31.79
3	6	caddis +	40	5	0.81	47.63		0.20	0.27	31.79
3	6	caddis +	40	6	0.45	37.42	pull starts at 3 sec. front rock drops at 9 sec	-0.02	-0.05	26.37
3	6	caddis +	40	7	0.57	43.41		0.03	0.07	20.40
3	6	caddis +	40	7	0.57	43.41		0.03	0.07	20.40
3	6	caddis +	40	7	0.57	43.41		0.03	0.07	20.40
3	6	caddis +	40	7	0.57	43.41		0.03	0.07	20.40
3	6	caddis +	40	8	0.64	41.47	side rock shuffled during beginning net break	0.19	0.36	26.37

Block	Flume	Treatment	Grain Size Bin	Rock pull	Buoyant Weight (N)	B-axis (mm)	Notes	Difference in Force (N)	Normalized Difference	PHI (Friction Angle) in degrees
3	6	caddis +	40	8	0.64	41.47	side rock shuffled during beginning net break	0.19	0.36	26.37
3	6	caddis +	40	8	0.64	41.47	side rock shuffled during beginning net break	0.19	0.36	26.37
3	7	caddis +	55	1	1.44	58.01	pull starts at 6 sec. Pull rock finishes rotating out of tight spot at 12 sec	0.62	0.50	27.55
3	7	caddis +	55	2	1.44	58.21	toggles the downstream rock while the pull rock is pulled over it	0.53	0.38	35.50
3	7	caddis +	55	2	1.44	58.21	toggles the downstream rock while the pull rock is pulled over it	0.53	0.38	35.50
3	7	caddis +	55	3	1.39	51.46	pull starts at 3 sec. front rock drops at 6 sec	-0.14	-0.12	25.32
3	7	caddis +	55	4	1.15	60.62	pull starts at 6 sec. front rock begins to lift at 9 and drops at 11 sec. pick peak force before	0.31	0.26	39.56
3	7	caddis +	55	5	1.53	56.05	side rock lifts up at 9 and drops at 11 sec, picked peak force after side rock drop when nets when still attached	0.10	0.08	25.43

Block	Flume	Treatment	Grain Size Bin	Rock pull	Buoyant Weight (N)	B-axis (mm)	Notes	Difference in Force (N)	Normalized Difference	PHI (Friction Angle) in degrees
3	7	caddis +	55	5	1.53	56.05	side rock lifts up at 5 and drops at 7 sec, picked peak force after side rock drop when nets when still attached	0.10	0.08	25.43
3	7	caddis +	55	6	2.15	63.33		0.48	0.19	46.94
3	7	caddis +	55	6	2.15	63.33		0.48	0.19	46.94
3	7	caddis +	55	7	1.86	63.58	pull starts at 3 sec. side rock drops at 7 sec	0.08	0.06	17.15
3	7	caddis +	55	8	2.76	69.72		0.04	0.01	39.77
3	7	caddis +	55	8	2.76	69.72		0.04	0.01	39.77
3	8	control	55	1	1.64	58.68		0.71	0.61	25.53
3	8	control	55	2	0.47	51.95		-0.04	-0.10	43.69
3	8	control	55	3	2.29	58.67		0.53	0.23	47.07
3	8	control	55	4	0.84	60.26		-0.03	-0.04	35.62
3	8	control	55	5	1.27	76.54	back rock lifted and dropped at 6 sec. peak force picked after 6 sec	0.13	0.06	74.40
3	8	control	55	6	2.71	58.94	higher peak force too late in time series	0.51	0.29	19.71
3	8	control	55	7	2.05	55.70	rotates to vert then begins moving over DS rock at 8 sec	0.10	0.05	43.69
3	8	control	55	8	1.60	55.82		0.00	0.00	35.62
3	9	control	50	1	1.71	53.75	takes route over shorter less steep rock	-0.42	-0.20	52.72
3	9	control	50	2	1.28	56.56		-0.37	-0.28	39.89

Block	Flume	Treatment	Grain Size Bin	Rock pull	Buoyant Weight (N)	B-axis (mm)	Notes	Difference in Force (N)	Normalized Difference	PHI (Friction Angle) in degrees
3	9	control	50	3	1.91	61.67	experiencing interference the whole time			25.53
3	9	control	50	4	1.27	55.71	rotates to vert then begins moving over DS rock at 13 sec	-0.13	-0.09	43.69
3	9	control	50	5	1.86	51.32		-0.39	-0.31	13.43
3	9	control	50	6	1.08	57.05		-0.19	-0.15	47.07
3	9	control	50	7	0.73	44.88	drops lifted side rock at 6 sec	-0.16	-0.22	35.62
3	9	control	50	8	1.63	45.97		-0.04	-0.03	30.84
3	10	caddis +	50	1	1.23	59.70	rock pull starts at 9 front rock drops at 13	0.39	0.27	48.92
3	10	caddis +	50	2	2.49	60.49	takes route over shorter less steep rock	-0.20	-0.09	29.84
3	10	caddis +	50	2	2.49	60.49	takes route over shorter less steep rock	-0.20	-0.09	29.84
3	10	caddis +	50	2	2.49	60.49	takes route over shorter less steep rock	-0.20	-0.09	29.84
3	10	caddis +	50	2	2.49	60.49	takes route over shorter less steep rock	-0.20	-0.09	29.84
3	10	caddis +	50	3	1.51	62.15		0.17	0.14	24.65
3	10	caddis +	50	3	1.51	62.15		0.17	0.14	24.65
3	10	caddis +	50	4	1.37	51.06	lifted front rock drops at 9 seconds	0.07	0.06	24.65
3	10	caddis +	50	5	1.14	45.24	lifted back rock drops at 6 sec	0.12	0.10	42.54
3	10	caddis +	50	5	1.14	45.24	lifted back rock drops at 6 sec	0.12	0.10	42.54

Block	Flume	Treatment	Grain Size Bin	Rock pull	Buoyant Weight (N)	B-axis (mm)	Notes	Difference in Force (N)	Normalized Difference	PHI (Friction Angle) in degrees
3	10	caddis +	50	6	1.18	42.16		0.05	0.04	34.54
3	10	caddis +	50	6	1.18	42.16		0.05	0.04	34.54
3	10	caddis +	50	7	1.97	62.34		0.01	0.01	54.01
3	10	caddis +	50	8	0.00			#DIV/0!	#DIV/0!	
3	10	caddis +	50	9	0.65	51.95	pull starts at 6 sec. front rock begins to lift at 8 and drops at 14 sec	0.33	0.53	34.54
4	1	caddis +	60	1	1.89	67.66		-0.08	-0.05	34.81
4	1	caddis +	60	1	1.89	67.66		-0.08	-0.05	34.81
4	1	caddis +	60	2	1.46	59.73				
4	1	caddis +	60	3	0.94	64.99				
4	1	caddis +	60	4	2.29	67.37		0.85	0.44	34.92
4	1	caddis +	60	4	2.29	67.37		0.85	0.44	34.92
4	1	caddis +	60	4	2.29	67.37		0.85	0.44	34.92
4	1	caddis +	60	4	2.29	67.37		0.85	0.44	34.92
4	1	caddis +	60	5	2.34	67.60	lifted back rock drops at 21 sec	0.44	0.24	31.70
4	1	caddis +	60	5	2.34	67.60	lifted back rock drops at 21 sec	0.44	0.24	31.70
4	1	caddis +	60	5	2.34	67.60	lifted back rock drops at 21 sec	0.44	0.24	31.70
4	1	caddis +	60	6	1.60	58.98	lifted side rocks drop at 5 sec	0.46	0.40	25.57
4	1	caddis +	60	7	1.64	58.88		0.38	0.41	13.77
4	1	caddis +	60	8	1.82	66.25		0.24	0.19	24.91
4	2	control	60	1	1.65	61.10		-0.01	0.00	59.27
4	2	control	60	2	1.52	74.90	starts lifting at 5 sec. stops pushing side rock at 12 sec	0.35	0.33	25.32

Block	Flume	Treatment	Grain Size Bin	Rock pull	Buoyant Weight (N)	B-axis (mm)	Notes	Difference in Force (N)	Normalized Difference	PHI (Friction Angle) in degrees
4	2	control	60	3	1.38	54.93		-0.07	-0.07	27.86
4	2	control	60	4	1.73	67.63	lifted back rock drops at 14 sec	0.20	0.15	30.62
4	2	control	60	5	1.41	52.85	nose is extra heavy causing back end to rotate up; higher peak force too late in time series	0.09	0.11	19.41
4	2	control	60	6	2.76	84.91	side rock drops at 17 sec	0.24	0.15	13.31
4	2	control	60	7	2.02	69.25	lifted side and back rock drops at 12 and 17 sec respectively	0.13	0.10	20.84
4	2	control	60	8	2.50	50.32	slides against side rock. Pull rock shifts at 10 sec	-0.17	-0.09	25.32
4	3	control	50	1	0.92	49.66	lifted side rock drops at 15 sec	0.10	0.11	33.61
4	3	control	50	2	1.36	49.56		0.27	0.24	24.61
4	3	control	50	3	1.60	54.11		-0.15	-0.10	34.49
4	3	control	50	4	1.80	55.49		0.30	0.18	33.49
4	3	control	50	5	0.53	59.60	lifted back rock drops at 14 sec	0.19	0.37	35.78
4	3	control	50	6	1.97	57.17	side rock drops at 11 sec	0.49	0.33	19.82
4	3	control	50	7	0.19	51.50	pull starts at 8 but is snug in pocket. Leaves pocket at 11, possible error in weight			31.24
4	3	control	50	8	0.76	53.31		-0.06	-0.12	12.20
4	4	caddis +	50	1	1.77	59.78		0.22	0.16	21.23
4	4	caddis +	50	1	1.77	59.78		0.22	0.16	21.23
4	4	caddis +	50	1	1.77	59.78		0.22	0.16	21.23

Block	Flume	Treatment	Grain Size Bin	Rock pull	Buoyant Weight (N)	B-axis (mm)	Notes	Difference in Force (N)	Normalized Difference	PHI (Friction Angle) in degrees
4	4	caddis +	50	1	1.77	59.78		0.22	0.16	21.23
4	4	caddis +	50	1	1.77	59.78		0.22	0.16	21.23
4	4	caddis +	50	1	1.77	59.78		0.22	0.16	21.23
4	4	caddis +	50	2	1.02	59.30		0.24	0.25	34.44
4	4	caddis +	50	2	1.02	59.30		0.24	0.25	34.44
4	4	caddis +	50	3	1.50	40.49		-0.03	-0.03	22.45
4	4	caddis +	50	3	1.50	40.49		-0.03	-0.03	22.45
4	4	caddis +	50	4	1.65	57.13		0.62	0.56	12.20
4	4	caddis +	50	4	1.65	57.13		0.62	0.56	12.20
4	4	caddis +	50	5	0.84	43.75		0.03	0.05	17.15
4	4	caddis +	50	5	0.84	43.75		0.03	0.05	17.15
4	4	caddis +	50	6	0.92	44.14			#DIV/0!	
4	4	caddis +	50	7	1.00	59.66		0.00	#DIV/0!	
4	4	caddis +	50	8	1.70	55.75		0.00	#DIV/0!	
4	5	caddis +	30	1	0.30	28.79	too merky to see in vid	0.02	0.10	24.00
4	5	caddis +	30	2	0.47	36.90	too merky to see in vid	-0.06	-0.15	24.52
4	5	caddis +	30	3	0.66	32.31	too murky to see in vid	0.17	0.31	23.39
4	5	caddis +	30	4	0.30	32.08		0.21	0.95	16.08
4	5	caddis +	30	4	0.30	32.08		0.21	0.95	16.08
4	5	caddis +	30	4	0.30	32.08		0.21	0.95	16.08
4	5	caddis +	30	4	0.30	32.08		0.21	0.95	16.08
4	5	caddis +	30	5	0.23	28.45	lifted side and back rock drop at 9 sec	0.05	0.26	25.32
4	5	caddis +	30	5	0.23	28.45	lifted side and back rock drop at 9 sec	0.05	0.26	25.32
4	5	caddis +	30	6	0.22	35.85		0.07	0.46	16.76

Block	Flume	Treatment	Grain Size Bin	Rock pull	Buoyant Weight (N)	B-axis (mm)	Notes	Difference in Force (N)	Normalized Difference	PHI (Friction Angle) in degrees
4	5	caddis +	30	6	0.22	35.85		0.07	0.46	16.76
4	5	caddis +	30	6	0.22	35.85		0.07	0.46	16.76
4	5	caddis +	30	6	0.22	35.85		0.07	0.46	16.76
4	5	caddis +	30	6	0.22	35.85		0.07	0.46	16.76
4	5	caddis +	30	7	0.48	38.97	rock attached by net is lifted during rock pull	0.35	0.88	24.61
4	5	caddis +	30	7	0.48	38.97	rock attached by net is lifted during rock pull	0.35	0.88	24.61
4	5	caddis +	30	7	0.48	38.97	rock attached by net is lifted during rock pull	0.35	0.88	24.61
4	5	caddis +	30	7	0.48	38.97	rock attached by net is lifted during rock pull	0.37	1.01	20.47
4	5	caddis +	30	7	0.48	38.97	rock attached by net is lifted during rock pull	0.37	1.01	20.47
4	5	caddis +	30	7	0.48	38.97	rock attached by net is lifted during rock pull	0.37	1.01	20.47
4	5	caddis +	30	7	0.48	38.97	rock attached by net is lifted during rock pull	0.37	1.01	20.47
4	5	caddis +	30	8	0.26	32.82	side rock drops at 13 sec	0.14	0.69	19.82
4	5	caddis +	30	8	0.26	32.82	side rock drops at 13 sec	0.14	0.69	19.82
4	6	control	30	1	0.50	47.40	backside rotates up	-0.02	-0.04	23.39

Block	Flume	Treatment	Grain Size Bin	Rock pull	Buoyant Weight (N)	B-axis (mm)	Notes	Difference in Force (N)	Normalized Difference	PHI (Friction Angle) in degrees
4	6	control	30	2	0.55	46.24	wire taut at 6 sec rock lifts over 1st ds rock at 15 sec	0.06	0.13	27.35
4	6	control	30	3	0.38	30.52	backside rotates up. tire taut at 6 sec rock lifts over 1st ds rock at 14 sec	0.05	0.15	26.77
4	6	control	30	4	0.48	36.72	back and side interference	0.12	0.35	16.05
4	6	control	30	5	0.37	34.32	possible net break on control rock at 3 sec. picked peak after, backside rotates up	-0.01	-0.04	26.11
4	6	control	30	6	0.00	fail		#####	#####	
4	6	control	30	7	0.35	46.49		-0.02	-0.07	16.08
4	6	control	30	8	0.49	32.28	wire taut at 6 side rocks drop at 9 and 12	0.15	0.43	16.08
4	6	control	30	9	0.65	46.55	rock edge stuck going over ds rock at end of pull	0.10	0.19	23.39
4	7	caddis +	55	1	1.01	52.59		0.21	0.35	8.20
4	7	caddis +	55	1	1.01	52.59		0.21	0.35	8.20
4	7	caddis +	55	2	2.04	62.90		0.15	0.08	31.92
4	7	caddis +	55	2	2.04	62.90		0.15	0.08	31.92
4	7	caddis +	55	3	1.73	54.19	pull starts at 7, side rock drops at 13 sec	0.24	0.21	12.76
4	7	caddis +	55	4	1.69	56.18	back rock drops at 8 sec	0.24	0.18	19.82
4	7	caddis +	55	4	1.69	56.18	back rock drops at 8 sec	0.24	0.18	19.82
4	7	caddis +	55	4	1.69	56.18	back rock drops at 8 sec	0.24	0.18	19.82

Block	Flume	Treatment	Grain Size Bin	Rock pull	Buoyant Weight (N)	B-axis (mm)	Notes	Difference in Force (N)	Normalized Difference	PHI (Friction Angle) in degrees
4	7	caddis +	55	5	1.39	57.36	side and back rocks drops at 8 sec	0.18	0.19	13.31
4	7	caddis +	55	5	1.39	57.36	side and back rocks drops at 8 sec	0.18	0.19	13.31
4	7	caddis +	55	5	1.39	57.36	side and back rocks drops at 8 sec	0.18	0.19	13.31
4	7	caddis +	55	5	1.39	57.36	side and back rocks drops at 8 sec	0.18	0.19	13.31
4	7	caddis +	55	5	1.39	57.36	side and back rocks drops at 8 sec	0.18	0.19	13.31
4	7	caddis +	55	6	1.36	52.92	goes over side rock; looks vertical, nose may have gotten stuck on front rock	2.00	1.49	36.34
4	7	caddis +	55	6	1.36	52.92	goes over side rock looks vertical	2.00	1.49	36.34
4	7	caddis +	55	6	1.36	52.92	goes over side rock looks vertical	2.00	1.49	36.34
4	7	caddis +	55	6	1.36	52.92	goes over side rock looks vertical	2.00	1.49	36.34
4	7	caddis +	55	7	1.83	53.69	pull starts at 7 sec back rock lifts at 12 drops at 18 sec	0.01	0.01	25.24
4	7	caddis +	55	8	1.40	53.22		0.48	0.36	33.57
4	7	caddis +	55	8	1.40	53.22		0.48	0.36	33.57
4	7	caddis +	55	9	1.21	66.82		0.34	0.23	51.00
4	7	caddis +	55	9	1.21	66.82		0.34	0.23	51.00
4	7	caddis +	55	9	1.21	66.82		0.34	0.23	51.00
4	7	caddis +	55	9	1.21	66.82		0.34	0.23	51.00
4	7	caddis +	55	9	1.21	66.82		0.34	0.23	51.00
4	7	caddis +	55	9	1.21	66.82		0.34	0.23	51.00

Block	Flume	Treatment	Grain Size Bin	Rock pull	Buoyant Weight (N)	B-axis (mm)	Notes	Difference in Force (N)	Normalized Difference	PHI (Friction Angle) in degrees
4	7	caddis +	55	9	1.21	66.82		0.34	0.23	51.00
4	7	caddis +	55	9	1.21	66.82		0.34	0.23	51.00
4	7	caddis +	55	9	1.21	66.82		0.34	0.23	51.00
4	8	control	55	1	1.79	61.46	starts lifting side rock at 7 seconds, moves rock out of the way and stops at 12. picked a peak force before this	0.13	0.09	27.93
4	8	control	55	2	1.71	60.28	side rock drops at 13 sec, peak force at end is from going over 2nd rock ds of origin, too late in time series	-0.26	-0.18	36.26
4	8	control	55	3	1.78	70.08	side rock drops at 6 sec, peak force at end is from going over 2nd rock ds of origin too late in time series	-0.01	0.00	23.12
4	8	control	55	4	1.63	59.35	side rock drops at 9 sec	0.00	0.00	25.32
4	8	control	55	5	#####	fail		#####	#####	
4	8	control	55	6	0.78	54.58	side rocks drop at 6 sec	0.16	0.28	28.78
4	8	control	55	7	#####	fail		#####	#####	
4	8	control	55	8	1.24	64.85	interference from side rocks stops at 11 sec	0.01	0.01	19.82
4	8	control	55	9	1.36	53.82	wedged underneath back rock causing interference before 10 sec	0.15	0.15	26.77

Block	Flume	Treatment	Grain Size Bin	Rock pull	Buoyant Weight (N)	B-axis (mm)	Notes	Difference in Force (N)	Normalized Difference	PHI (Friction Angle) in degrees
4	8	control	55	10	1.86	60.33		0.40	0.31	24.00
4	9	control	40	1	1.13	49.40		0.09	0.10	25.32
4	9	control	40	2	0.96	44.19	side and front rock in way from beginning of lift at 7 sec to 11 sec	-0.01	-0.02	23.39
4	9	control	40	3	0.90	43.54		-0.01	-0.01	16.08
4	9	control	40	4	0.71	47.91		0.01	0.01	26.36
4	9	control	40	5	0.54	41.02	pushed small rock in front out of the way at 6 to 9 sec	-0.17	-0.31	39.63
4	9	control	40	6	1.25	47.34		-0.13	-0.12	26.77
4	9	control	40	7	0.63	50.84	gets stuck on front rock	0.01	0.02	30.60
4	9	control	40	8	0.64	46.32		0.01	0.02	30.60
4	10	caddis +	40	1	0.66	43.22	rock pull begins at 8 sec. side rock drops at 10 sec. out of pocket at 15	0.06	0.11	27.93
4	10	caddis +	40	1	0.66	43.22	rock pull begins at 8 sec. side rock drops at 10 sec. out of pocket at 16	0.06	0.11	27.93
4	10	caddis +	40	1	0.66	43.22	rock pull begins at 8 sec. side rock drops at 10 sec. out of pocket at 17	0.06	0.11	27.93
4	10	caddis +	40	1	0.66	43.22	rock pull begins at 8 sec. side rock drops at 10 sec. out of pocket at 18	0.06	0.11	27.93

Block	Flume	Treatment	Grain Size Bin	Rock pull	Buoyant Weight (N)	B-axis (mm)	Notes	Difference in Force (N)	Normalized Difference	PHI (Friction Angle) in degrees
4	10	caddis +	40	2	0.47	40.19	pull starts at 6 sec. side rock drops at 8 sec	-0.03	-0.09	26.52
4	10	caddis +	40	2	0.47	40.19	pull starts at 6 sec. side rock drops at 8 sec	-0.03	-0.09	26.52
4	10	caddis +	40	3	0.67	49.69	pull starts at 2 sec toggles side rock at 3 sec and back rock at 5 sec	0.05	0.10	19.82
4	10	caddis +	40	3	0.67	49.69	pull starts at 2 sec toggles side rock at 3 sec and back rock at 5 sec	0.05	0.10	19.82
4	10	caddis +	40	4	0.39	40.82		0.03	0.12	12.20
4	10	caddis +	40	5	1.24	48.08	side rock drops at 3 sec	0.02	0.02	19.82
4	10	caddis +	40	5	1.24	48.08	side rock drops at 3 sec	0.02	0.02	19.82
4	10	caddis +	40	5	1.24	48.08	side rock drops at 3 sec	0.02	0.02	19.82
4	10	caddis +	40	5	1.24	48.08	side rock drops at 3 sec	0.02	0.02	19.82
4	10	caddis +	40	6	0.54	37.87	higher peak force after rock left pocket	-0.02	-0.05	26.77
4	10	caddis +	40	7	2.08	49.16		0.59	0.34	25.42
4	10	caddis +	40	7	2.08	49.16		0.59	0.34	25.42
4	10	caddis +	40	7	2.08	49.16		0.59	0.34	25.42
4	10	caddis +	40	7	2.08	49.16		0.59	0.34	25.42
4	10	caddis +	40	7	2.08	49.16		0.59	0.34	25.42
4	10	caddis +	40	7	2.08	49.16		0.59	0.34	25.42

Block	Flume	Treatment	Grain Size Bin	Rock pull	Buoyant Weight (N)	B-axis (mm)	Notes	Difference in Force (N)	Normalized Difference	PHI (Friction Angle) in degrees
4	10	caddis +	40	7	2.08	49.16		0.59	0.34	25.42
4	10	caddis +	40	7	2.08	49.16		0.59	0.34	25.42
4	10	caddis +	40	8	0.80	46.31		0.39	0.57	27.93
4	10	caddis +	40	8	0.80	46.31		0.39	0.57	27.93
4	10	caddis +	40	8	0.80	46.31		0.39	0.57	27.93
4	10	caddis +	40	8	0.80	46.31		0.39	0.57	27.93
4	10	caddis +	40	8	0.80	46.31		0.39	0.57	27.93
4	10	caddis +	40	8	0.80	46.31		0.39	0.57	27.93
5	1	caddis +	50	1	0.63	53.33		0.11	0.18	31.37
5	1	caddis +	50	2	1.16	55.07		-0.02	-0.02	30.84
5	1	caddis +	50	2	1.16	55.07		-0.02	-0.02	30.84
5	1	caddis +	50	2	1.16	55.07		-0.02	-0.02	30.84
5	1	caddis +	50	3	2.34	56.55	pull starts at 8 sec back rock drops at 12 sec	-0.24	-0.11	30.60
5	1	caddis +	50	3	2.34	56.55	pull starts at 8 sec back rock drops at 12 sec	-0.24	-0.11	30.60
5	1	caddis +	50	3	2.34	56.55	pull starts at 8 sec back rock drops at 12 sec	-0.24	-0.11	30.60
5	1	caddis +	50	3	2.34	56.55	pull starts at 8 sec back rock drops at 12 sec	-0.24	-0.11	30.60
5	1	caddis +	50	4	1.30	47.15	pull starts at 6 sec back rock lifts at 8 drops at 16 sec	0.27	0.20	38.93
5	1	caddis +	50	4	1.30	47.15	pull starts at 6 sec back rock lifts at 8 drops at 16 sec	0.27	0.20	38.93

Block	Flume	Treatment	Grain Size Bin	Rock pull	Buoyant Weight (N)	B-axis (mm)	Notes	Difference in Force (N)	Normalized Difference	PHI (Friction Angle) in degrees
5	1	caddis +	50	4	1.30	47.15	pull starts at 6 sec back rock lifts at 8 drops at 16 sec	0.27	0.20	38.93
5	1	caddis +	50	4	1.30	47.15	pull starts at 6 sec back rock lifts at 8 drops at 16 sec	0.27	0.20	38.93
5	1	caddis +	50	5	1.43	52.34	pull starts at 8 sec overlapping side rock rubs until 14 sec	0.18	0.13	36.34
5	1	caddis +	50	5	1.43	52.34	pull starts at 8 sec overlapping side rock rubs until 14 sec	0.18	0.13	36.34
5	1	caddis +	50	5	1.43	52.34	pull starts at 8 sec overlapping side rock rubs until 14 sec	0.18	0.13	36.34
5	1	caddis +	50	5	1.43	52.34	pull starts at 8 sec overlapping side rock rubs until 14 sec	0.18	0.13	36.34
5	1	caddis +	50	6	1.42	52.09	rotates to vertical	0.15	0.12	30.84
5	1	caddis +	50	6	1.42	52.09	rotates to vertical	0.15	0.12	30.84
5	1	caddis +	50	6	1.42	52.09	rotates to vertical	0.15	0.12	30.84
5	1	caddis +	50	6	1.42	52.09	rotates to vertical	0.15	0.12	30.84
5	1	caddis +	50	6	1.42	52.09	rotates to vertical	0.15	0.12	30.84
5	1	caddis +	50	7	1.28	55.42		0.05	0.04	34.07
5	1	caddis +	50	7	1.28	55.42		0.05	0.04	34.07
5	1	caddis +	50	7	1.28	55.42		0.05	0.04	34.07
5	1	caddis +	50	7	1.28	55.42		0.05	0.04	34.07
5	1	caddis +	50	7	1.28	55.42		0.05	0.04	34.07
5	1	caddis +	50	7	1.28	55.42		0.05	0.04	34.07

Block	Flume	Treatment	Grain Size Bin	Rock pull	Buoyant Weight (N)	B-axis (mm)	Notes	Difference in Force (N)	Normalized Difference	PHI (Friction Angle) in degrees
5	1	caddis +	50	7	1.28	55.42		0.05	0.04	34.07
5	1	caddis +	50	7	1.28	55.42		0.05	0.04	34.07
5	1	caddis +	50	8	0.71	47.40	pull starts at 4 sec pull rock nose stuck on front side rock that drops at 14 sec,	0.03	0.05	33.57
5	1	caddis +	50	8	0.71	47.40	pull starts at 4 sec pull rock nose stuck on front side rock that drops at 14 sec,	0.03	0.05	33.57
5	1	caddis +	50	8	0.71	47.40	pull starts at 4 sec pull rock nose stuck on front side rock that drops at 14 sec,	0.03	0.05	33.57
5	2	control	50	1	0.82	54.50	pull starts at 2, front rock drops at 12, 2 back rocks drop at 15	0.09	0.12	30.70
5	2	control	50	2	1.67	55.23		-0.43	-0.25	39.05
5	2	control	50	3	1.39	59.80		0.94	0.90	19.54
5	2	control	50	4	1.18	54.35	pull starts at 3, back rocks drop at 7, front rock drops at 12	-0.12	-0.11	30.60
5	2	control	50	5	0.85	56.04	pull starts at 3 sec. side rock drops at 8 sec	-0.04	-0.04	40.91
5	2	control	50	6	1.77	66.56		-0.17	-0.11	28.60
5	2	control	50	7	1.30	50.52	pull starts at 3 sec. nose stuck on front rock and back side rotating up until 12 sec	-0.27	-0.19	41.45
5	2	control	50	8	1.12	52.40		-0.10	-0.09	36.54

Block	Flume	Treatment	Grain Size Bin	Rock pull	Buoyant Weight (N)	B-axis (mm)	Notes	Difference in Force (N)	Normalized Difference	PHI (Friction Angle) in degrees
5	3	control	40	1	0.65	40.54	picked initial peak force because rock gets stuck and turns on side during pull	-0.12	-0.16	45.89
5	3	control	40	2	0.90	49.76		0.00	0.00	31.69
5	3	control	40	3	0.99	46.38				
5	3	control	40	4	0.65	46.47				
5	3	control	40	5	0.54	43.49		-0.16	-0.33	30.60
5	3	control	40	6	0.71	42.81		-0.11	-0.18	28.60
5	3	control	40	7	0.93	52.71	picked initial peak because nose gets stuck on ds rock and is yanked out as it rotates to vertical during pull	-0.06	-0.08	23.12
5	3	control	40	8	0.58	45.22	pushing ds rock out of the way from 5 to 16 sec	-0.07	-0.13	37.49
5	4	caddis +	40	1	0.64	35.45		0.03	0.06	19.54
5	4	caddis +	40	1	0.64	35.45		0.03	0.06	19.54
5	4	caddis +	40	2	0.64	41.41		0.10	0.17	31.69
5	4	caddis +	40	2	0.64	41.41		0.10	0.17	31.69
5	4	caddis +	40	2	0.64	41.41		0.10	0.17	31.69
5	4	caddis +	40	3	0.37	46.72	pull starts at 5 sec. nose stuck on ds rock moves at 15 sec	0.09	0.29	28.60
5	4	caddis +	40	4	0.72	39.32		-0.01	-0.01	22.13
5	4	caddis +	40	5	0.46	41.51		0.01	0.03	35.36
5	4	caddis +	40	6	0.58	51.21		0.46	0.93	26.52
5	4	caddis +	40	7	0.64	42.04		0.25	0.54	16.13

Block	Flume	Treatment	Grain Size Bin	Rock pull	Buoyant Weight (N)	B-axis (mm)	Notes	Difference in Force (N)	Normalized Difference	PHI (Friction Angle) in degrees
5	4	caddis +	40	7	0.64	42.04		0.25	0.54	16.13
5	4	caddis +	40	7	0.64	42.04		0.25	0.54	16.13
5	4	caddis +	40	7	0.64	42.04		0.25	0.54	16.13
5	4	caddis +	40	7	0.64	42.04		0.25	0.54	16.13
5	4	caddis +	40	7	0.64	42.04		0.25	0.54	16.13
5	4	caddis +	40	8	0.48	43.55		-0.02	-0.05	36.34
5	4	caddis +	40	8	0.48	43.55		-0.03	-0.06	37.29
5	4	caddis +	40	8	0.48	43.55		-0.03	-0.06	37.29
5	4	caddis +	40	8	0.48	43.55		-0.03	-0.06	37.29
5	4	caddis +	40	8	0.48	43.55		-0.03	-0.06	37.29
5	4	caddis +	40	8	0.48	43.55		-0.03	-0.06	37.29
5	4	caddis +	40	8	0.48	43.55		-0.03	-0.06	37.29
5	4	caddis +	40	9	0.66	38.65	pull starts at 5 sec. side rocks moves at 6 sec	0.37	0.67	25.32
5	4	caddis +	40	9	0.66	38.65	pull starts at 5 sec. side rocks moves at 6 sec	0.37	0.67	25.32
5	4	caddis +	40	9	0.66	38.65	pull starts at 5 sec. side rocks moves at 6 sec	0.37	0.67	25.32
5	4	caddis +	40	9	0.66	38.65	pull starts at 5 sec. side rocks moves at 6 sec	0.37	0.67	25.32
5	4	caddis +	40	9	0.66	38.65	pull starts at 5 sec. side rocks moves at 6 sec	0.37	0.67	25.32
5	4	caddis +	40	9	0.66	38.65	pull starts at 5 sec. side rocks moves at 6 sec	0.37	0.67	25.32

Block	Flume	Treatment	Grain Size Bin	Rock pull	Buoyant Weight (N)	B-axis (mm)	Notes	Difference in Force (N)	Normalized Difference	PHI (Friction Angle) in degrees
5	4	caddis +	40	9	0.66	38.65	pull starts at 5 sec. side rocks moves at 6 sec	0.37	0.67	25.32
5	5	control	55	1	0.36	44.10	rock pull starts at 4 side rock drops at start of pull	0.01	0.04	40.49
5	5	control	55	2	1.52	66.34		0.28	0.29	19.54
5	5	control	55	3	1.08	65.50		-0.30	-0.26	51.77
5	5	control	55	4	1.02	59.44		-0.21	-0.22	41.81
5	5	control	55	5	1.14	60.78		0.00	0.01	29.34
5	5	control	55	6	1.00	47.34	pull starts at 10 sec, nosed drops front rock at 18 sec.	-0.15	-0.18	34.58
5	5	control	55	7	1.36	63.05	pull starts at 7 sec back rock drops at 14 sec	0.16	0.14	34.44
5	5	control	55	8	1.42	66.53	pull starts at 5 sec, gets snagged on side rock until 11	0.05	0.04	26.04

Appendix 3. Difference in Force

(Measured-FP)												
	Control				Caddisfly				T-Test			
Grain Treatment	#	Mean	Std Dev.	Std Error	#	Mean	Std Dev.	Std Error	Difference	Std Error of Difference	Degrees of Freedom	Prob > t
30	16	0.03	0.06	0.02	16	0.10	0.10	0.03	0.07	0.03	30	0.0109*
40	21	0.08	0.09	0.02	25	0.15	0.18	0.04	0.23	0.04	44	<.0001*
50	21	0.08	0.25	0.05	21	0.12	0.19	0.04	0.20	0.07	40	0.0061*
55	24	0.10	0.25	0.05	17	0.35	0.47	0.11	0.25	0.11	39	0.0171*
60	16	0.15	0.28	0.07	14	0.39	0.29	0.08	0.24	0.10	28	0.0139*
All	98	0.02	0.22	0.02	93	0.21	0.29	0.03	0.19	0.04	189	<.0001*

Appendix 4. Net Measurements

Block	Flume	Treatment	Grain Size Bin	Rock pull	Buoyant Weight (N)	B-axis (mm)	Net area (mm ²)	Net orientation (looking DS in pull direction)	Type of observation	Distance net stretched (mm)	Force rise during stretching (N)
2	10	caddis +	30	1	0.41	32.25	52.30	right	net break	10.00	0.28
2	10	caddis +	30	1	0.41	32.25	55.65	left			
2	10	caddis +	30	1	0.41	32.25	48.64	back			
2	10	caddis +	30	2	0.40	34.23	28.16	back	net break	0.80	0.02
2	10	caddis +	30	3	0.26	32.12	44.72	back	rock in the way	20.20	0.13
2	10	caddis +	30	4	0.48	38.72	55.92	back left	net break	20.60	0.17
2	10	caddis +	30	4	0.48	38.72	44.67	left			
2	10	caddis +	30	5	0.35	31.33		bottom	net break	1.80	0.10
2	10	caddis +	30	6	0.29	91.13	22.40	left	net break	2.40	0.08
2	10	caddis +	30	6	0.29	91.13	23.89	left	net break	0.60	0.06
2	10	caddis +	30	6	0.29	91.13	34.50	left	net break	0.90	0.05
2	10	caddis +	30	6	0.29	91.13		left	rock in the way	0.50	0.08
2	10	caddis +	30	7	0.31	48.35	17.23	right	net break	1.30	0.04
2	10	caddis +	30	7	0.31	48.35	84.71	left	net break	5.50	0.05
2	10	caddis +	30	7	0.31	48.35	84.71	left	net break	0.50	0.04
2	10	caddis +	30	8	0.75	36.40					
2	10	caddis +	30	9	0.45	36.27					
3	1	caddis +	60	1	1.45	54.34					
3	1	caddis +	60	2	2.88	58.74					
3	1	caddis +	60	3	2.97	66.86	88.35	right	net break	1.60	0.26
3	1	caddis +	60	3	2.97	66.86	97.28	back	net break	13.20	0.58
3	1	caddis +	60	4	2.10	67.25					
3	1	caddis +	60	5	3.06	66.64	51.74	back	net break	0.80	0.29
3	1	caddis +	60	5	3.06	66.64	87.99	back	net break	2.70	0.16
3	1	caddis +	60	6	2.68	64.55	16.47	back	net break	1.10	0.37

Block	Flume	Treatment	Grain Size Bin	Rock pull	Buoyant Weight (N)	B-axis (mm)	Net area (mm ²)	Net orientation (looking DS in pull direction)	Type of observation	Distance net stretched (mm)	Force rise during stretching (N)
3	1	caddis +	60	6	2.68	64.55	7.28	left	net break	0.90	0.22
3	1	caddis +	60	6	2.68	64.55	14.63	right	net break	1.70	0.33
3	1	caddis +	60	6	2.68	64.55	35.38	left	net break	4.60	0.27
3	1	caddis +	60	6	2.68	64.55	#####	right	net break	0.60	0.20
3	1	caddis +	60	7	1.24	62.05					
3	1	caddis +	60	8	1.22	63.74	21.10	right	net break	0.60	0.35
3	2	control	60	1	1.61	63.10					
3	2	control	60	2	1.67	74.44					
3	2	control	60	3	2.76	60.38					
3	2	control	60	4	2.30	65.80					
3	2	control	60	5	1.84	62.50					
3	2	control	60	6	2.46	68.36					
3	2	control	60	7	2.28	70.44					
3	2	control	60	8	1.20	65.14					
3	3	caddis +	30	1	0.43	35.43					
3	3	caddis +	30	2	0.45	33.89					
3	3	caddis +	30	3	0.40	35.21	2.13	back	net break	1.50	0.11
3	3	caddis +	30	3	0.40	35.21	2.59	right	thread break	2.10	0.16
3	3	caddis +	30	3	0.40	35.21	2.59	right	thread break	2.30	0.04
3	3	caddis +	30	4	0.20	27.37	3.04	right	net break	0.70	0.05
3	3	caddis +	30	4	0.20	27.37	14.63	right	net break	0.70	0.10
3	3	caddis +	30	4	0.20	27.37	12.73	left	net break	1.70	0.02
3	3	caddis +	30	4	0.20	27.37	38.66	left	net break	1.00	0.07
3	3	caddis +	30	5	0.25	35.20	5.29	back	net break	1.50	0.04
3	3	caddis +	30	5	0.25	35.20	2.44	back	net break	1.00	0.02
3	3	caddis +	30	5	0.25	35.20	2.73	right	net break	2.00	0.02

Block	Flume	Treatment	Grain Size Bin	Rock pull	Buoyant Weight (N)	B-axis (mm)	Net area (mm ²)	Net orientation (looking DS in pull direction)	Type of observation	Distance net stretched (mm)	Force rise during stretching (N)
3	3	caddis +	30	6	0.29	36.25	8.34	back	net break	1.60	0.11
3	3	caddis +	30	6	0.29	36.25	5.60	left	net break	4.60	0.05
3	6	caddis +	40	3	1.08	55.84	9.73	back	net break	0.80	0.14
3	6	caddis +	40	3	1.08	55.84	9.16	left	net break	0.60	0.02
3	6	caddis +	40	3	1.08	55.84	20.44	left	net break	2.30	0.09
3	6	caddis +	40	4	0.56	41.44					
3	6	caddis +	40	5	0.81	47.63	7.96	back	thread break	0.30	0.11
3	6	caddis +	40	5	0.81	47.63	3.76	back	thread break	1.20	0.04
3	6	caddis +	40	5	0.81	47.63	1.98	left	net break	4.20	0.05
3	6	caddis +	40	5	0.81	47.63	7.80	back	thread break	1.00	0.15
3	6	caddis +	40	6	0.45	37.42					
3	6	caddis +	40	7	0.57	43.41	10.90	right	thread break	5.60	0.01
3	6	caddis +	40	7	0.57	43.41	21.83	left	net break	1.90	0.03
3	6	caddis +	40	7	0.57	43.41	22.21	right	net break	2.60	0.02
3	6	caddis +	40	7	0.57	43.41	55.00	left	net break	0.50	0.09
3	6	caddis +	40	8	0.64	41.47	20.46	right	net break	0.50	0.04
3	6	caddis +	40	8	0.64	41.47	34.89	right	net tear	2.90	0.05
3	6	caddis +	40	8	0.64	41.47	82.62	left	net tear	0.50	0.06
3	7	caddis +	55	1	1.44	58.01					
3	7	caddis +	55	2	1.44	58.21	57.41	right	net break	2.60	0.40
3	7	caddis +	55	2	1.44	58.21	11.77	right	net break	1.90	0.25
3	7	caddis +	55	3	1.39	51.46					
3	7	caddis +	55	4	1.15	60.62					
3	7	caddis +	55	5	1.53	56.05	72.06	back	net break	1.20	0.32

Block	Flume	Treatment	Grain Size Bin	Rock pull	Buoyant Weight (N)	B-axis (mm)	Net area (mm ²)	Net orientation (looking DS in pull direction)	Type of observation	Distance net stretched (mm)	Force rise during stretching (N)
3	7	caddis +	55	5	1.53	56.05	26.84	right	net break	1.10	0.15
3	7	caddis +	55	6	2.15	63.33	24.38	left	net break	0.70	0.29
3	7	caddis +	55	6	2.15	63.33	48.68	right	net break	1.80	0.15
3	7	caddis +	55	7	1.86	63.58					
3	7	caddis +	55	8	2.76	69.72	47.47	left	net break	0.80	0.36
3	7	caddis +	55	8	2.76	69.72	38.90	right	net break	3.30	0.10
3	10	caddis +	50	1	1.23	59.70					
3	10	caddis +	50	2	2.49	60.49	6.42	right	thread break	0.20	0.12
3	10	caddis +	50	2	2.49	60.49	13.40	right	net break	0.60	0.11
3	10	caddis +	50	2	2.49	60.49	29.59	left	net tear	0.40	0.03
3	10	caddis +	50	2	2.49	60.49	29.59	left	net break	0.80	0.30
3	10	caddis +	50	3	1.51	62.15	19.24	back	thread break	0.50	0.19
3	10	caddis +	50	3	1.51	62.15	19.24	back	thread break	1.20	0.12
3	10	caddis +	50	4	1.37	51.06	23.48	left	net break	2.00	0.47
3	10	caddis +	50	5	1.14	45.24	27.71	back	thread break	1.40	0.05
3	10	caddis +	50	5	1.14	45.24	3.35	back	thread break	0.20	0.07
3	10	caddis +	50	6	1.18	42.16	22.41	right	net break	0.60	0.12
3	10	caddis +	50	6	1.18	42.16	35.08	right	net break	10.90	0.19
3	10	caddis +	50	7	1.97	62.34					
3	10	caddis +	50	8	0.00						
3	10	caddis +	50	9	0.65	51.95					
4	1	caddis +	60	1	1.89	67.66	24.75	back	net break	1.80	0.07
4	1	caddis +	60	1	1.89	67.66	57.89	back left	net break	0.30	0.17
4	1	caddis +	60	2	1.46	59.73					

Block	Flume	Treatment	Grain Size Bin	Rock pull	Buoyant Weight (N)	B-axis (mm)	Net area (mm ²)	Net orientation (looking DS in pull direction)	Type of observation	Distance net stretched (mm)	Force rise during stretching (N)
4	1	caddis +	60	3	0.94	64.99					
4	1	caddis +	60	4	2.29	67.37	37.16	back	thread break	0.40	0.18
4	1	caddis +	60	4	2.29	67.37	37.16	back	thread break	1.10	0.56
4	1	caddis +	60	4	2.29	67.37	37.16	back	thread break	3.20	0.79
4	1	caddis +	60	4	2.29	67.37	37.16	back	net break	2.70	0.80
4	1	caddis +	60	5	2.34	67.60	29.34	front			
4	1	caddis +	60	5	2.34	67.60	62.60	front			
4	1	caddis +	60	5	2.34	67.60	26.93	back	net break	1.80	0.28
4	1	caddis +	60	6	1.60	58.98	88.51	back	net break	2.80	1.40
4	1	caddis +	60	7	1.64	58.88	47.22	left	thread break	1.10	0.11
4	1	caddis +	60	8	1.82	66.25	23.15	left	net break	3.10	0.20
4	4	caddis +	50	1	1.77	59.78	91.10	left	net break	0.70	0.12
4	4	caddis +	50	1	1.77	59.78	26.50	left	net break	0.60	0.14
4	4	caddis +	50	1	1.77	59.78	10.57	right	net break	1.80	0.15
4	4	caddis +	50	1	1.77	59.78	80.11	right	net break	0.90	0.14
4	4	caddis +	50	1	1.77	59.78	3.11	back	thread break	2.10	0.39
4	4	caddis +	50	1	1.77	59.78	3.01	back	thread break	4.70	0.22
4	4	caddis +	50	2	1.02	59.30	5.56	back left	thread break	0.40	0.18
4	4	caddis +	50	2	1.02	59.30	5.56	back left	thread break	1.50	0.11
4	4	caddis +	50	3	1.50	40.49	#####	back	thread break		
4	4	caddis +	50	3	1.50	40.49	26.49	back	thread break	1.00	0.02

Block	Flume	Treatment	Grain Size Bin	Rock pull	Buoyant Weight (N)	B-axis (mm)	Net area (mm ²)	Net orientation (looking DS in pull direction)	Type of observation	Distance net stretched (mm)	Force rise during stretching (N)
4	4	caddis +	50	4	1.65	57.13	15.16	back left	net break	5.40	0.09
4	4	caddis +	50	4	1.65	57.13	8.97	back left	net break	0.30	0.15
4	4	caddis +	50	5	0.84	43.75	#####	back left	net tear	0.40	0.05
4	4	caddis +	50	5	0.84	43.75	#####	back left	net break	1.20	0.03
4	4	caddis +	50	6	0.92	44.14					
4	4	caddis +	50	7	1.00	59.66	#####	left	net break	0.70	0.12
4	4	caddis +	50	8	1.70	55.75	3.98	back	thread break	0.40	0.11
4	5	caddis +	30	1	0.30	28.79					
4	5	caddis +	30	2	0.47	36.90					
4	5	caddis +	30	3	0.66	32.31					
4	5	caddis +	30	4	0.30	32.08	10.69	left	net break	0.20	0.04
4	5	caddis +	30	4	0.30	32.08	11.19	left	net break	2.60	0.10
4	5	caddis +	30	4	0.30	32.08	24.25	right	net break	1.80	0.07
4	5	caddis +	30	4	0.30	32.08	24.25	right	net break	1.40	0.03
4	5	caddis +	30	5	0.23	28.45	23.49	left	net break	0.30	0.08
4	5	caddis +	30	5	0.23	28.45	27.17	right	net break	6.20	0.10
4	5	caddis +	30	6	0.22	35.85	37.08	front			
4	5	caddis +	30	6	0.22	35.85	9.23	back	net break	0.20	0.02
4	5	caddis +	30	6	0.22	35.85	24.07	back right	net break	1.70	0.03
4	5	caddis +	30	6	0.22	35.85	5.12	back left	net break	1.10	0.02
4	5	caddis +	30	6	0.22	35.85	24.07	back right	net break	1.00	0.02
4	5	caddis +	30	7	0.48	38.97	21.08	back right	net tear	0.30	0.05
4	5	caddis +	30	7	0.48	38.97	21.08	back right	net break	0.50	0.02
4	5	caddis +	30	7	0.48	38.97	25.77	back right	net tear	0.60	0.16
4	5	caddis +	30	7	0.48	38.97	14.34	back	net tear	0.20	0.04
4	5	caddis +	30	7	0.48	38.97	25.77	back right	net tear	0.20	0.05

Block	Flume	Treatment	Grain Size Bin	Rock pull	Buoyant Weight (N)	B-axis (mm)	Net area (mm ²)	Net orientation (looking DS in pull direction)	Type of observation	Distance net stretched (mm)	Force rise during stretching (N)
4	5	caddis +	30	7	0.48	38.97	14.34	back	net break	0.40	0.16
4	5	caddis +	30	7	0.48	38.97	34.04				
4	5	caddis +	30	8	0.26	32.82	38.13				
4	5	caddis +	30	8	0.26	32.82	28.81	back left	thread break	0.50	0.12
4	7	caddis +	55	1	1.01	52.59	41.71	back left	net tear	0.80	0.08
4	7	caddis +	55	1	1.01	52.59	41.71	back left	net break	0.30	0.05
4	7	caddis +	55	2	2.04	62.90	7.42	back left	net tear	3.60	0.13
4	7	caddis +	55	2	2.04	62.90	7.42	back left	net break	4.40	0.13
4	7	caddis +	55	3	1.73	54.19	52.84	front			
4	7	caddis +	55	4	1.69	56.18	20.80	left	net break	0.30	0.02
4	7	caddis +	55	4	1.69	56.18	33.92	back	net break	2.80	0.35
4	7	caddis +	55	4	1.69	56.18	35.29	front			
4	7	caddis +	55	5	1.39	57.36	14.38	left	net break	1.60	0.38
4	7	caddis +	55	5	1.39	57.36	16.50	left	net break	1.80	0.50
4	7	caddis +	55	5	1.39	57.36	7.85	left	thread break	1.80	0.16
4	7	caddis +	55	5	1.39	57.36	26.94	right			
4	7	caddis +	55	5	1.39	57.36	78.04	front			
4	7	caddis +	55	6	1.36	52.92	56.79	right	net break	1.90	0.52
4	7	caddis +	55	6	1.36	52.92	54.14	left	net break	2.70	0.43
4	7	caddis +	55	6	1.36	52.92	56.79	right	net break	0.60	0.37
4	7	caddis +	55	6	1.36	52.92	39.25	front			
4	7	caddis +	55	7	1.83	53.69					
4	7	caddis +	55	8	1.40	53.22	8.55	back	thread break	0.40	0.22
4	7	caddis +	55	8	1.40	53.22	87.67	right	net break	0.70	0.05
4	7	caddis +	55	9	1.21	66.82	55.16	left	net break	0.60	0.17

Block	Flume	Treatment	Grain Size Bin	Rock pull	Buoyant Weight (N)	B-axis (mm)	Net area (mm ²)	Net orientation (looking DS in pull direction)	Type of observation	Distance net stretched (mm)	Force rise during stretching (N)
4	7	caddis +	55	9	1.21	66.82	15.42	left	net break	0.80	0.10
4	7	caddis +	55	9	1.21	66.82	27.11	back	net break	1.30	0.27
4	7	caddis +	55	9	1.21	66.82	90.34	left	net tear	1.70	0.26
4	7	caddis +	55	9	1.21	66.82	90.34	left	net break	1.10	0.19
4	7	caddis +	55	9	1.21	66.82	49.87	right	net break	1.40	0.13
4	7	caddis +	55	9	1.21	66.82	53.37	right	net break	0.50	0.08
4	7	caddis +	55	9	1.21	66.82	57.53	front	net break	5.30	0.14
4	7	caddis +	55	9	1.21	66.82	96.21	right	net break	3.70	0.17
4	10	caddis +	40	1	0.66	43.22	40.01	back right	net break	0.80	0.11
4	10	caddis +	40	1	0.66	43.22	47.41	back left	net break	0.30	0.09
4	10	caddis +	40	1	0.66	43.22	42.45	back left	thread break	0.20	0.02
4	10	caddis +	40	1	0.66	43.22	6.51	right			
4	10	caddis +	40	2	0.47	40.19	20.06	right	net break	0.30	0.02
4	10	caddis +	40	2	0.47	40.19	11.13	back left	net break	0.20	0.01
4	10	caddis +	40	3	0.67	49.69	83.37	right	net break	1.40	0.14
4	10	caddis +	40	3	0.67	49.69	19.74	front			
4	10	caddis +	40	4	0.39	40.82	17.08	right	net break	2.70	0.04
4	10	caddis +	40	5	1.24	48.08	30.20	back	net break	0.40	0.04
4	10	caddis +	40	5	1.24	48.08	38.99	left	net break	2.00	0.13
4	10	caddis +	40	5	1.24	48.08	18.56	back			
4	10	caddis +	40	6	0.54	37.87	49.41	right	net break	9.30	0.08
4	10	caddis +	40	7	2.08	49.16	69.53	right	net break	4.60	0.39
4	10	caddis +	40	7	2.08	49.16	62.88	back	net tear	2.70	0.45
4	10	caddis +	40	7	2.08	49.16	62.88	back	net tear	0.70	1.01
4	10	caddis +	40	7	2.08	49.16	62.88	back	net break	1.50	0.16

Block	Flume	Treatment	Grain Size Bin	Rock pull	Buoyant Weight (N)	B-axis (mm)	Net area (mm ²)	Net orientation (looking DS in pull direction)	Type of observation	Distance net stretched (mm)	Force rise during stretching (N)
4	10	caddis +	40	7	2.08	49.16	13.32	right			
4	10	caddis +	40	7	2.08	49.16	26.25	front			
4	10	caddis +	40	7	2.08	49.16	25.61	left			
4	10	caddis +	40	7	2.08	49.16	42.24	back left			
4	10	caddis +	40	8	0.80	46.31	46.05	right	net break	1.60	0.15
4	10	caddis +	40	8	0.80	46.31	32.26	right	net break	4.10	0.13
4	10	caddis +	40	8	0.80	46.31	39.19	left	net break	1.40	0.08
4	10	caddis +	40	8	0.80	46.31	24.02	back right			
4	10	caddis +	40	8	0.80	46.31	17.53	front			
4	10	caddis +	40	8	0.80	46.31	26.66	left			
5	1	caddis +	50	1	0.63	53.33					
5	1	caddis +	50	2	1.16	55.07	28.64	left	net break	1.80	0.14
5	1	caddis +	50	2	1.16	55.07	20.25	left	net break	1.20	0.09
5	1	caddis +	50	2	1.16	55.07	31.91	back			
5	1	caddis +	50	3	2.34	56.55	42.45	back	net break	3.10	0.14
5	1	caddis +	50	3	2.34	56.55	25.60	back	net break	2.10	0.22
5	1	caddis +	50	3	2.34	56.55		bottom	net break	5.50	0.34
5	1	caddis +	50	3	2.34	56.55	36.40	front			
5	1	caddis +	50	4	1.30	47.15	20.77	right	net break	1.50	0.14
5	1	caddis +	50	4	1.30	47.15	14.54	back	net break	0.80	0.04
5	1	caddis +	50	4	1.30	47.15	6.10	left			
5	1	caddis +	50	4	1.30	47.15	35.45	front			
5	1	caddis +	50	5	1.43	52.34	#####	right	net break	4.10	0.77
5	1	caddis +	50	5	1.43	52.34	52.89	left	net break	1.40	0.24
5	1	caddis +	50	5	1.43	52.34	16.00	back right	net break	8.80	0.10
5	1	caddis +	50	5	1.43	52.34	43.71	front			
5	1	caddis +	50	6	1.42	52.09	34.49	left	net break	0.70	0.04

Block	Flume	Treatment	Grain Size Bin	Rock pull	Buoyant Weight (N)	B-axis (mm)	Net area (mm ²)	Net orientation (looking DS in pull direction)	Type of observation	Distance net stretched (mm)	Force rise during stretching (N)
5	1	caddis +	50	6	1.42	52.09	39.10	right	net break	0.30	0.05
5	1	caddis +	50	6	1.42	52.09	29.13	left	thread break	1.70	0.05
5	1	caddis +	50	6	1.42	52.09	65.08	right			
5	1	caddis +	50	6	1.42	52.09	5.09	back			
5	1	caddis +	50	6	1.42	52.09	8.54	front			
5	1	caddis +	50	7	1.29	55.42	29.01	back	net break	4.70	0.18
5	1	caddis +	50	7	1.29	55.42	28.68	back	thread break	0.60	0.09
5	1	caddis +	50	7	1.29	55.42	28.68	back	thread break	4.70	0.15
5	1	caddis +	50	7	1.29	55.42		bottom	net break	0.80	0.17
5	1	caddis +	50	7	1.29	55.42	28.68	back	net break	2.40	0.18
5	1	caddis +	50	7	1.29	55.42	61.08	right	net break	1.30	0.13
5	1	caddis +	50	7	1.29	55.42	58.32	left			
5	1	caddis +	50	7	1.29	55.42	57.57	front			
5	1	caddis +	50	8	0.71	47.40	35.65	back	net break	2.70	0.17
5	1	caddis +	50	8	0.71	47.40	26.51	right			
5	1	caddis +	50	8	0.71	47.40	8.41	right			
5	2	control	50	1	0.82	54.50					
5	2	control	50	2	1.67	55.23					
5	2	control	50	3	1.39	59.80					
5	2	control	50	4	1.18	54.35					
5	2	control	50	5	0.85	56.04					
5	2	control	50	6	1.77	66.56					
5	2	control	50	7	1.30	50.52					
5	2	control	50	8	1.13	52.40					
5	3	control	40	1	0.65	40.54					

Block	Flume	Treatment	Grain Size Bin	Rock pull	Buoyant Weight (N)	B-axis (mm)	Net area (mm ²)	Net orientation (looking DS in pull direction)	Type of observation	Distance net stretched (mm)	Force rise during stretching (N)
5	3	control	40	2	0.90	49.76					
5	3	control	40	3	0.99	46.38					
5	3	control	40	4	0.65	46.47					
5	3	control	40	5	0.54	43.49					
5	3	control	40	6	0.71	42.81					
5	3	control	40	7	0.93	52.71					
5	3	control	40	8	0.58	45.22					
5	4	caddis +	40	1	0.64	35.45	32.87	right			
5	4	caddis +	40	1	0.64	35.45	12.47	left	net break	3.80	0.09
5	4	caddis +	40	2	0.64	41.41	35.13	right	net break	1.40	0.03
5	4	caddis +	40	2	0.64	41.41	10.29	right			
5	4	caddis +	40	2	0.64	41.41	4.95	front			
5	4	caddis +	40	3	0.37	46.72					
5	4	caddis +	40	4	0.72	39.32					
5	4	caddis +	40	5	0.46	41.51	29.73	back	net break	1.00	0.02
5	4	caddis +	40	6	0.58	51.21	3.92	back			
5	4	caddis +	40	7	0.64	42.04	36.31	back	net tear	1.60	0.11
5	4	caddis +	40	7	0.64	42.04	36.31	back	net tear	2.10	0.11
5	4	caddis +	40	7	0.64	42.04	5.08	left	net break	1.70	0.11
5	4	caddis +	40	7	0.64	42.04	5.08	left	net break	4.30	0.08
5	4	caddis +	40	7	0.64	42.04	9.96	right			
5	4	caddis +	40	7	0.64	42.04	2.59	left	thread break	1.30	0.04
5	4	caddis +	40	8	0.48	43.55	14.53	back	net tear	0.40	0.09
5	4	caddis +	40	8	0.48	43.55	3.50	back left	net tear	1.00	0.03
5	4	caddis +	40	8	0.48	43.55	68.26	back	net break	2.20	0.03
5	4	caddis +	40	8	0.48	43.55	5.30	back left	thread break	3.20	0.02

Block	Flume	Treatment	Grain Size Bin	Rock pull	Buoyant Weight (N)	B-axis (mm)	Net area (mm ²)	Net orientation (looking DS in pull direction)	Type of observation	Distance net stretched (mm)	Force rise during stretching (N)
5	4	caddis +	40	8	0.48	43.55	5.82	back left	thread break	0.80	0.03
5	4	caddis +	40	8	0.48	43.55	68.26	back	thread break	2.00	0.03
5	4	caddis +	40	8	0.48	43.55	28.35	front			
5	4	caddis +	40	9	0.66	38.65	56.83	back	net break	3.00	0.50
5	4	caddis +	40	9	0.66	38.65	7.34	right	net break	0.40	0.08
5	4	caddis +	40	9	0.66	38.65	8.48	back	net break	1.70	0.17
5	4	caddis +	40	9	0.66	38.65	58.23	left	net break	2.90	0.10
5	4	caddis +	40	9	0.66	38.65	18.60	front			
5	4	caddis +	40	9	0.66	38.65	55.19	front			
5	4	caddis +	40	9	0.66	38.65	15.90	front			